WASTEWATER RECYCLING USING A HYGROSCOPIC COOLING SYSTEM

Final Report

Prepared for:

AAD Document Control

National Energy Technology Laboratory
U.S. Department of Energy
626 Cochrans Mill Road
PO Box 10940, MS 921-107
Pittsburgh, PA 15236-0940

Cooperative Agreement No. DE-FE0031810
DUNS No. 102280781

Prepared by:

Christopher L. Martin
Bradley G. Stevens
Jace D. Anderson
Joshua M. Sanford

Energy & Environmental Research Center
University of North Dakota
15 North 23rd Street, Stop 9018
Grand Forks, ND 58202-9018

Yohann Rousselet

Baltimore Aircoil Company (BAC)
7600 Dorsey Run Road
Jessup, MD 20794

2022-EERC-09-01

September 2022

EERC DISCLAIMER

LEGAL NOTICE This research report was prepared by the Energy & Environmental Research Center (EERC), an agency of the University of North Dakota, as an account of work sponsored by the U.S. Department of Energy (DOE) National Energy Technology Laboratory and the North Dakota Industrial Commission. Because of the research nature of the work performed, neither the EERC nor any of its employees makes any warranty, express or implied, or assumes any legal liability or responsibility for the accuracy, completeness, or usefulness of any information, apparatus, product, or process disclosed or represents that its use would not infringe privately owned rights. Reference herein to any specific commercial product, process, or service by trade name, trademark, manufacturer, or otherwise does not necessarily constitute or imply its endorsement or recommendation by the EERC.

DOE DISCLAIMER

This report was prepared as an account of work sponsored by an agency of the United States Government. Neither the United States Government, nor any agency thereof, nor any of their employees, makes any warranty, express or implied, or assumes any legal liability or responsibility for the accuracy, completeness, or usefulness of any information, apparatus, product, or process disclosed, or represents that its use would not infringe privately owned rights. Reference herein to any specific commercial product, process, or service by trade name, trademark, manufacturer, or otherwise does not necessarily constitute or imply its endorsement, recommendation, or favoring by the United States Government or any agency thereof. The views and opinions of authors expressed herein do not necessarily state or reflect those of the United States Government or any agency thereof.

NORTH DAKOTA INDUSTRIAL COMMISSION DISCLAIMER

This report was prepared by the EERC pursuant to an agreement partially funded by the Industrial Commission of North Dakota, and neither the EERC nor any of its subcontractors nor the North Dakota Industrial Commission nor any person acting on behalf of either:

(A) Makes any warranty or representation, express or implied, with respect to the accuracy, completeness, or usefulness of the information contained in this report or that the use of any information, apparatus, method, or process disclosed in this report may not infringe privately owned rights; or
(B) Assumes any liabilities with respect to the use of, or for damages resulting from the use of, any information, apparatus, method, or process disclosed in this report.

Reference herein to any specific commercial product, process, or service by trade name, trademark, manufacturer, or otherwise does not necessarily constitute or imply its endorsement, recommendation, or favoring by the North Dakota Industrial Commission. The views and opinions of authors expressed herein do not necessarily state or reflect those of the North Dakota Industrial Commission.

WASTEWATER RECYCLING USING A HYGROSCOPIC COOLING SYSTEM

ABSTRACT

This project by the Energy & Environmental Research Center (EERC), Baltimore Aircoil Company (BAC), and Great River Energy (GRE) evaluated the concept of recycling wastewater at a coal-fired power plant using a hygroscopic cooling system, which is an evaporative cooling technology analogous to conventional cooling towers, except that sparingly soluble dissolved solids are precipitated and removed as waste solids instead of purging them with a liquid blowdown stream. This technology can maximize the use of plant makeup water by obtaining useful evaporative cooling from wastewater while minimizing the volume of wastes needing disposal. Experimental activities were conducted in two phases, a laboratory-based evaluation of the properties of wastewater from the host site, GRE's Coal Creek Station near Underwood, North Dakota, and a field test of a small pilot hygroscopic cooling system at the host site power plant. Findings from the laboratory study informed the design of the pilot system and the system's field test performance served as the basis for a techno-economic analysis (TEA) of the hygroscopic recycling concept. At the preferred operating conditions identified during the TEA, the wet-bulb approach temperature of the tower was 7.3°C (13°F) and the volume of blowdown produced by the plant was reduced to 5.4% of its incoming volume. Waste solids produced during field testing were classified as nonhazardous waste based on the measured hazardous element content and evaluation of their leaching potential. However, to qualify as a solid for landfill disposal i.e., as determined by the U.S. Environmental Protection Agency's paint filter test, it appears that a dewatering step beyond hydrocyclone separation is needed. The baseline levelized cost of wastewater disposal (LCWD) for hygroscopic wastewater recycling was estimated to be $3.69–$3.72 per m^3 of plant blowdown. Capital cost was estimated to contribute over 54% to the LCWD, and parameters that impact capital cost such as the heat exchange coil material of construction and the tower's wet-bulb approach temperature were identified as having the greatest impact on overall LCWD. A LCWD estimate prepared for the same application but using thermomechanical brine evaporation was almost 40% higher than that calculated for hygroscopic cooling, despite recovering distilled-quality water for reuse, while the LCWD for disposal-only, deep well injection was estimated to be 30% lower compared to hygroscopic wastewater recycling.

TABLE OF CONTENTS

Continued . . .

TABLE OF CONTENTS (continued)

LIST OF FIGURES

Continued . . .

LIST OF FIGURES (continued)

LIST OF TABLES

Continued . . .

LIST OF TABLES (continued)

WASTEWATER RECYCLING USING A HYGROSCOPIC COOLING SYSTEM

EXECUTIVE SUMMARY

Coal-fired power plants typically require tens of millions of gallons of water per day to sustain their operation. Most of this water use is for cooling, but these plants also require it for emission control and material transport purposes. During use, much of the water is evaporated, but the remaining blowdown becomes concentrated with dissolved solids and contaminated with coal combustion residuals that must be cleansed and properly disposed of. The current best available technology (BAT) for wastewater discharge treatment does meet effluent guidelines set by the U.S. Environmental Protection Agency (EPA); however, it does not increase the water-use efficiency of the power plant. Wastewater recycling with hygroscopic cooling is an evaporative cooling approach that aims to recycle the wastewater that would otherwise be disposed of and put it to productive use providing cooling. This process will reduce the freshwater supplied to the primary cooling tower while also allowing for effluent discharges to be eliminated or significantly minimized.

This project by the Energy & Environmental Research Center (EERC), Baltimore Aircoil Company (BAC), and Great River Energy (GRE) was broken into five tasks: project management, laboratory evaluation, development of a pilot unit, pilot-scale testing, and a summary techno-economic analysis (TEA). The combined technical team of the EERC and BAC, with utility application support provided by GRE, performed field testing at a full-scale power plant, GRE's Coal Creek Station, to evaluate the concept. The pilot system was set up to collect wastewater from Coal Creek's cooling tower blowdown (CTB) and ash pond water (APW). Brine was added into the working fluid to accelerate the hygroscopic system's approach to a steady-state composition.

Daily operating data were processed to compute the key performance values of heat load, approach temperature, and wastewater throughput. As the hygroscopic working fluid became more concentrated, its water activity decreased, and the tower's ambient wet-bulb approach temperature increased for the same cooling load. At the preferred operating conditions identified in the TEA, the wet-bulb approach temperature of the hygroscopic tower was 7.3°C (13°F), which was sufficiently low to provide useful cooling at Coal Creek. The purpose of hygroscopic wastewater recycling is not only to provide usable cooling for the power plant, but also to minimize the volume of waste liquid needing disposal. It was determined that zero-liquid discharge (ZLD) may not be feasible with hygroscopic cooling since the working fluid concentration necessary for ZLD resulted in the formation of stable foam that interfered with the pumping and distribution of liquid over the tower's heat exchanger. However, under the preferred operating conditions where the working fluid concentration was limited to a sustainable level that avoided foaming, the incoming wastewater volume was still reduced by over 94%.

The TEA was based on a streamlined version of the pilot unit with the performance model based on field test results to estimate cooling capacity, wastewater consumption, and waste solids production. During operation, the solid waste was classified as nonhazardous; however, to qualify as a solid for landfill disposal, a dewatering step beyond hydrocyclone separation was needed.

Two solids dewatering options were included in the TEA for hygroscopic cooling along with a conventional brine minimization technology, mechanical vapor recompression (MVR), and disposal-only ZLD using direct deep well injection. The TEA suggests that the levelized cost of wastewater disposal (LCWD) for MVR would be nearly 40% higher than hygroscopic recycling, despite recovering distilled-quality water as shown in Figure ES-1.

Hygroscopic wastewater recycling may be a more cost-effective approach to improve the water-use efficiency at coal-fired power plants by indirectly displacing makeup cooling water instead of recovering high-quality distillate. While field test results suggest that this process can substantially minimize the blowdown stream, true ZLD may not be achievable; instead, hygroscopic recycling's primary mode of operation would be as a wastewater concentrator. The TEA estimated hygroscopic recycling to have a 30% higher LCWD compared to direct disposal with an injection well. However, for applications where the volume of disposed fluid is a concern, e.g., when done in conjunction with carbon dioxide sequestration, hygroscopic wastewater recycling could reduce the volume of the disposed liquid to 5.4% of its incoming volume.

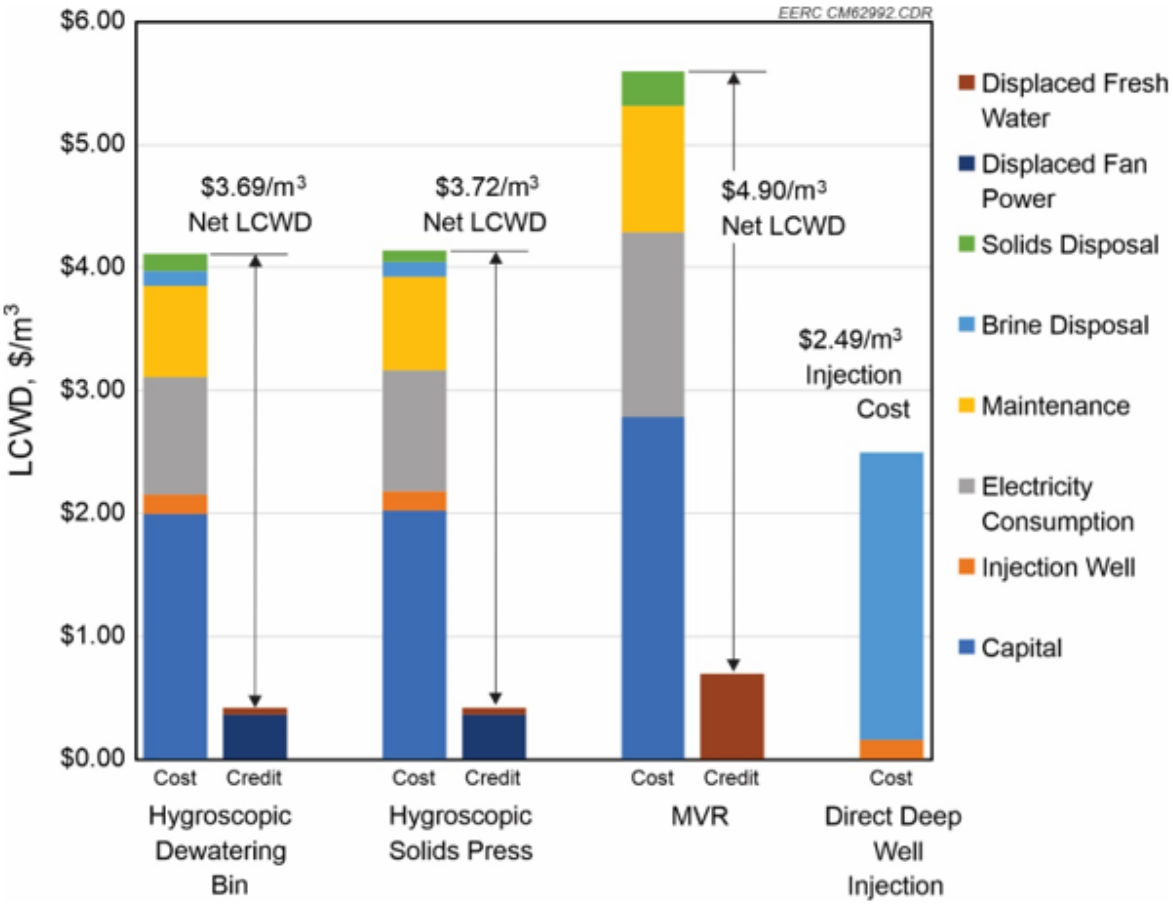

Figure ES-1. Baseline LCWD breakdowns for the two solids dewatering options of hygroscopic wastewater recycling and two conventional alternatives.

WASTEWATER RECYCLING USING A HYGROSCOPIC COOLING SYSTEM

INTRODUCTION

This project by the Energy & Environmental Research Center (EERC), Baltimore Aircoil Company (BAC), and Great River Energy (GRE) evaluated the use of hygroscopic cooling as a complementary wastewater recycling technology for coal-fired power plants. Hygroscopic cooling is an evaporative cooling approach that uses concentrated brine as a cooling tower working fluid to increase the proportion of dry, sensible, cooling capacity of the tower and to virtually eliminate the tower's blowdown stream by precipitating dissolved solids in the makeup water and removing them as a solid waste. Applied at a power plant, hygroscopic cooling could increase the plant's water use efficiency by using plant blowdown to provide useful evaporative cooling. The concept is diagrammed in Figure 1, which shows a hygroscopic cooling system operating on a slipstream of the condenser cooling water circuit at a power plant. By cooling the slipstream, the hygroscopic system augments the plant's existing cooling system and displaces some of the fresh makeup water to the plant's main cooling tower by evaporating wastewater from various waste streams at the plant, potentially including blowdown from the existing cooling tower or aggregated plantwide blowdown. The net result of this scheme is that freshwater makeup to the plant's primary cooling tower would be reduced, and liquid effluent discharges would be either eliminated or significantly reduced in volume while producing a stream of solid precipitates that can be disposed of in the plant's ash disposal landfill.

From a plantwide perspective, the concept in Figure 1 matches the worst-quality water with what should be the least quality-demanding use: evaporative cooling. While this project focused on wastewater recycling within the power plant, the concept might be expanded beyond the plant's boundaries, where poor-quality wastewater from external activities, e.g., reject brine from inland desalination, might be used on-site. Potential benefits of such an arrangement would include increasing source water availability for the plant by seeking water with fewer competing uses or providing a complementary disposal service to the surrounding community as the demand for wastewater disposal grows.

The project's technical team consisted of the EERC and BAC, with utility application support provided by GRE.

BACKGROUND

Fossil power plants face increasing regulation of wastewater discharges as environmental quality standards continue to evolve. In 2015, the U.S. Environmental Protection Agency (EPA) revised the effluent limitation guidelines and standards for coal-fired power plants to specifically address the effluent from flue gas desulfurization systems (Code of Federal Regulations, 2015). While the final rule has been challenged and its implementation delayed, the regulatory limits set by it are expected to eventually become mandated.

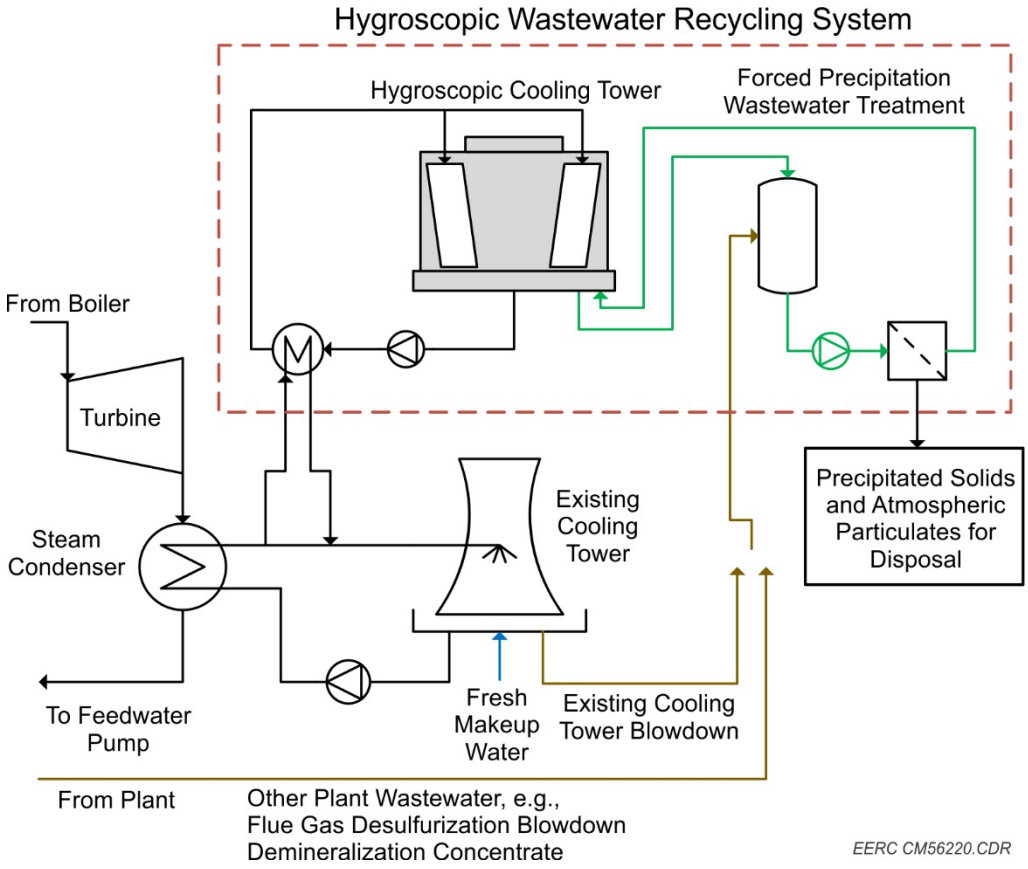

Figure 1. Integration schematic of a hygroscopic wastewater recycling system at a thermal power plant.

As part of its rulemaking process, EPA conducted a thorough evaluation of power plant wastewater treatment technologies that could comply with the final rule (EPA, 2015). This evaluation included approaches currently in full-scale use, those that have been evaluated with power plant wastewater but not demonstrated at full-scale, and state-of-the-art ideas currently at the bench-scale stage. Based on technical and economic considerations, EPA selected the combination of chemical precipitation for metal control with biological treatment for soluble contaminate control as the best available technology economically achievable (BAT) for disposing of flue gas desulfurization (FGD) wastewater. The average costs for EPA's BAT have been determined to be approximately $65,000 per gpm of wastewater throughput for capital costs and $8/kgal for operating costs.

While sufficient to meet effluent guidelines, the BAT selected by EPA for FGD wastewater disposal does not result in recycled water to the plant, nor does it eliminate effluent discharge that could be challenged under future regulations. Zero-liquid discharge (ZLD) with water recycling was identified as a preferred approach since it offers these benefits, but it was judged to be too costly for widespread implementation by EPA. In general, low-cost, disposal-only ZLD options require significant land area to site evaporation ponds or need suitable geology for subsurface injection, which greatly limits their applicability. Alternatively, less site-restrictive ZLD options

such as using a brine concentrator can be costly to operate since the plant must provide the energy needed for treatment. A high-level comparison between the proposed hygroscopic wastewater recycling concept and existing ZLD options is presented in Table 1.

When compared to the other ZLD options shown in Table 1, the hygroscopic cooling concept offers a unique combination of features. Thermomechanical ZLD can use many different configurations, but in general, either high-quality thermal and/or mechanical energy inputs are needed to recover high-purity water by evaporating wastewater. At the other end of the ZLD spectrum are disposal-only options such as evaporation ponds and injection wells. Ponds require virtually no input energy to operate since they rely on solar and wind energy to concentrate the wastewater. However, as a result of being a passive process, no recyclable water is recovered. Likewise, injection wells can use relatively little energy after well development, but no usable water is recovered.

Table 1. Comparison of Hygroscopic Cooling Wastewater Recycling with Other ZLD Options

	Disposal-Only ZLD	**Hygroscopic Wastewater Recycling (this project)**	**Thermomechanical ZLD**
Description	Includes options such as evaporation ponds and subsurface injection wells where wastewater is sent for on-site, long-term disposal.	Steam condenser waste heat is dissipated by a hygroscopic cooling system using wastewater for makeup; the water fraction is completely evaporated, leaving a solid by-product.	Input energy powers a series of concentration stages that culminate with a brine crystallizer or equivalent process to recover a solid by-product.
Water Recovery	No	Indirectly, by displacing water otherwise needed for cooling.	Yes, typically high quality suitable for many purposes.
Indicative Operating Cost	Potentially low but limited to suitable climates and/or subsurface geology.	$7.40/kgal[a]	$10.70[b] to $32.82/kgal[c]
Indicative Installed Capital Cost	Highly variable depending on land availability and/or subsurface conditions.	$65,000/gpm[a]	$89,000[b] to $110,000/gpm[c]

[a] Summary techno-economic analysis (TEA) values for the baseline condition of treating plant blowdown from Coal Creek Station.
[b] Comparative TEA estimates prepared for mechanical vapor recompression at Coal Creek Station.
[c] Reported general costs for ZLD treatment resulting in a solid for disposal (Marlett, 2018).

The hygroscopic wastewater recycling concept has characteristics that fall between these conventional options and was hypothesized to be a beneficial option for existing power plants by competing with EPA's selected BAT. Hygroscopic cooling does require thermal energy input to drive wastewater evaporation, but the temperatures needed are entirely compatible with those of the steam condenser cooling circuit, and useful heat rejection or cooling is performed in the process. The trade-off for using low-grade energy with the hygroscopic process is that purified

water is not directly recovered; instead, the water component of the wastewater is put to productive cooling use, thereby displacing higher-quality makeup water for use elsewhere.

An advantage of hygroscopic wastewater recycling is its lower estimated operating and capital costs compared to thermomechanical ZLD in Table 1. With the thermomechanical approach, energy needed to drive the process includes high-quality steam and/or vapor compressor power, all of which is included in the operating cost. With the hygroscopic approach, waste heat taken from the plant's condenser cooling circuit has virtually no cost aside from any up-front piping additions to the condenser cooling circuit. Even the pumping energy required to circulate the condenser cooling water would likely be provided as part of the plant's normal operation if the hygroscopic cooling tower can operate within the same pressure drop needed for the plant's main towers.

Hygroscopic cooling was previously evaluated for building air conditioner cooling under a project sponsored by the Environmental Security Technology Certification Program (ESTCP). However, municipal tap water was used as tower makeup for that evaluation and had much lower dissolved solids content, typically less than 500 mg/L. For context, the dissolved solids content of the power plant waste streams at Coal Creek Station were 10–30 times more concentrated, and the exploratory task of this project was to determine if such poor-quality water could be used effectively with hygroscopic cooling.

APPROACH

The project was divided into the five tasks detailed below to collect the data necessary for evaluation and to conduct the analysis. Aside from Task 1.0, Project Management and Planning, the remaining scientific tasks were structured in a progression from blowdown water analysis to laboratory evaluation of fundamental interactions, to the development and testing of a small pilot system, and concluding with the TEA.

Task 1.0 – Project Management and Planning. This task was dedicated to project management and maintaining an active dialogue with the U.S. Department of Energy (DOE) regarding project activities.

Task 2.0 – Evaluation of Wastewater–Working Fluid Interactions. The objective of this task was to review the makeup water mixing process and identify optimal conditions to achieve the desired precipitation and separation of wastewater contaminants. Key outcomes were to collect and analyze wastewater samples from the host site power plant and conduct laboratory-scale experiments to evaluate the interactions between the wastewater and the hygroscopic working fluid. A significant challenge with using hygroscopic cooling to evaporate wastewater was to prevent equipment fouling from the precipitation of solids in the wastewater, which, if not controlled, would limit the practicality of hygroscopic recycling. Task 2.0 experiments generated saturation data specific to mixtures of the host site wastewater and the hygroscopic working fluid; from them, the conditions needed for homogeneous nucleation and the rate of precipitation were identified. All of these data were used to inform the design of the small pilot cooling system under Task 3.0.

Task 3.0 – Small Pilot Cooling System Design and Fabrication. The design parameters generated under Task 2.0 were used to inform the design of a small pilot system capable of the following functions: evaporation of the water fraction of a real wastewater feed, sustainable forced precipitation of dissolved contaminants in the wastewater, and recovery of the solid by-products. The pilot system consisted of two subsystems: the makeup water subsystem and the cooling tower subsystem, with the EERC having primary responsibility for the former and BAC the latter. After delivery of the cooling tower by BAC, the EERC integrated the two subsystems and performed shakedown testing.

Task 4.0 – Wastewater Testing. The small pilot system was temporarily installed at a host site power plant and used to evaluate combined wastewater evaporation and condenser cooling using a hygroscopic cooling tower. The pilot system was set up to receive a slipstream of the plant's hot condenser cooling water as the heat source and consumed various plant blowdown streams for evaporative makeup. Field testing generated cooling performance data and stream samples that were used to create a performance model of wastewater recycling with hygroscopic cooling for the TEA under Task 5.0. Testing the small pilot system with a real plant wastewater stream under actual outdoor ambient conditions raised the technology readiness level (TRL) of the concept from 3 to 5.

Task 5.0 – Techno-Economic Analysis. A TEA of wastewater recycling with hygroscopic cooling was conducted that incorporated findings from all prior tasks. The TEA included the development of capital and operating costs for hygroscopic cooling and determination of a levelized cost of water disposal (LCWD). Various sensitivities were evaluated for their impact on LCWD and comparisons were made to disposal-only ZLD and a conventional approach for thermomechanical ZLD.

Task 2.0 – Evaluation of Wastewater–Working Fluid Interactions

The goal of this task was to review the makeup mixing process and identify optimal conditions to achieve the desired precipitation and separation of wastewater contaminants. Data generated under this task were necessary to inform the design of the pilot system fabricated under Task 3.0 since prior to this project, hygroscopic cooling had only been tested using potable-quality makeup water with a dissolved solids content less than 500 mg/L (ESTCP). For context, the dissolved solids content of the power plant waste streams tested at Coal Creek Station were 10–30 times more concentrated, and as a result, the rate of precipitate formation would be higher than previously experienced.

The task began with collecting samples of key wastewater streams at the host site and characterizing their composition. Sample collection points are indicated in simplified water flow diagram in Figure 2 for Coal Creek Station. The three samples were cooling tower blowdown (CTB), FGD slurry, and ash pond water (APW). Each liquid sample was characterized by the analyses listed in Table 2 and included Resource Conservation and Recovery Act (RCRA) elements As, Ba, Cd, Cr, Pb, Hg, Se, and Ag. The concentration of these elements provided an early indication whether the resulting solid precipitates might be considered hazardous for disposal purposes.

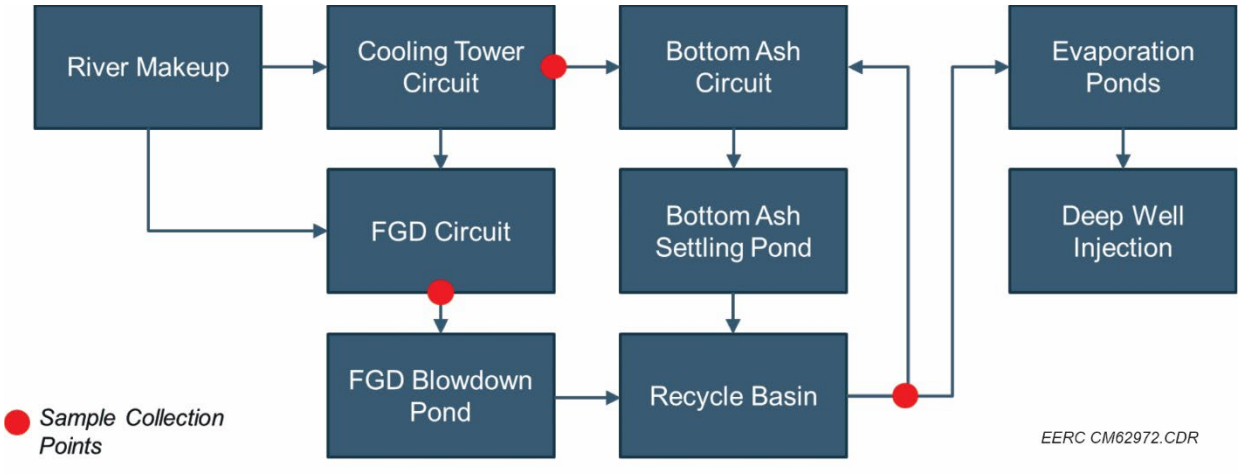

Figure 2. Simplified process flow diagram for water at Coal Creek Station.

Table 2. Analysis Used to Characterize Liquid Samples

Parameter	Measurement Technique
pH	Calibrated electrode and meter
Alkalinity	Titration with standardized HCl solution
Ca, Mg, Sr, Na, K, Li, Si, P, B, As, Ba, Cd, Cr, Pb, Se, and Ag	Inductively coupled plasma optical emission spectrometry (ICP–OES) and mass spectrometry (ICP–MS)
Hg	Cold-vapor atomic absorption spectrometry (CVAA)
F, Cl, Br, NO_3, NO_2, and SO_4	Ion chromatography
Total Organic Carbon (TOC)	Combustion with nondispersive infrared detection
Total Dissolved Solids (TDS)	Gravimetric after 180°C drying

Using the composition data measured for the wastewater samples, the geochemical modeling program PHREEQC (Version 3.310.12220 from the U.S. Geological Survey) was used to predict the saturation characteristics of the fluids as they are concentrated and to guide the design of laboratory-scale precipitation experiments to determine the boundaries of precipitate formation with these specific fluids. The laboratory tests were designed to determine the expected saturation index range for the initiation of solids precipitation and the effective steady-state saturation index with active precipitation.

Testing was based on generating supersaturated solutions from mixing samples of the plant wastewater with a concentrated brine that was selected to result in saturated working fluid mixtures representative of the interactions in the hygroscopic cooling tower. Exposure times varied from nearly instantaneous after mixing up to 24 hours which was used as a relatively long-term approach to equilibrium. During exposure, the samples were kept well mixed using a laboratory rotator. Exposure time was ended by filtering the samples to remove precipitates and any seeds, if present. Follow-up analysis consisted of analyzing the liquids for select major ions in order to calculate an

ending saturation index value. Seeding with calcium sulfate particles was an additional parameter for these tests and was used to reduce the induction time required to initiate precipitation. Table 3 presents the test matrix for initial mixing tests, and Table 4 covers the tests to evaluate the equilibrium approach saturation value.

Table 3. Test Matrix for Determining Saturation Properties of Plant Blowdown Streams

No.	Sample	Exposure Time
1	Starting CTB liquid	NA
2	Starting APW	NA
3	1:1 volume mixture of 30% $CaCl_2$ solution and CTB	0.5 hours
4	1:1 volume mixture of 30% $CaCl_2$ solution and APW	0.5 hours
5	1:1 volume mixture of 30% $CaCl_2$ solution and CTB	24 hours
6	1:1 volume mixture of 30% $CaCl_2$ solution and APW	24 hours

Table 4. Test Matrix for Determining Equilibrium Saturation Index Approach for APW

Test	APW and $CaCl_2$ Mixture Target Saturation Index	Seed Condition	Desiccant-Ash Pond Mixture Equilibration Time
1	0.3	Unseeded	24 hr
2	0.45	Unseeded	24 hr
3	0.6	Unseeded	24 hr
4	0.3	Seeded	24 hr
5	0.45	Seeded	24 hr
6	0.6	Seeded	24 hr

In addition to evaluating the precipitation characteristics of the wastewater and hygroscopic tower working fluid, the composition data along with modeling were used to estimate the steady-state composition of the hygroscopic working fluid and its engineering properties to size pumps and other equipment for the pilot system design under Task 3.0.

Task 3.0 – Small Pilot Cooling System Design and Fabrication

Task 3.0 activities included the design, fabrication, and shakedown testing of the small pilot cooling system that was used for field testing. The pilot system consisted of two subsystems: the makeup water subsystem and the cooling tower subsystem, with the EERC having primary responsibility for the former and BAC the latter.

Because of business interruptions caused by the COVID 19 pandemic, plans for the cooling tower subsystem changed during the course of the project. Instead of developing a custom-designed tower, the team worked with a stock cooling tower with a nominal thermal load rating of 296 kW_{th}. The tower did not have some of the originally planned features like a higher-power, sealless pump or stainless steel basin construction. A higher-power pump was required to circulate

the hygroscopic working fluid, which takes more pumping energy because of its higher density and viscosity relative to water, and stainless steel construction was preferred to stand up to the concentrated brine working fluid. After receipt of the stock tower, the EERC fit a larger (5 hp versus the original 3 hp), sealless pump during integration of the two subsystems.

The originally planned tower was also to be constructed from stainless steel since the hygroscopic working fluid can accelerate metal corrosion, but the substitute tower's mostly galvanized-coated steel construction was judged to be serviceable in light of the relatively short testing duration under Task 4.0. To provide an added degree of protection for the galvanized coating, submerged portions of the tower were coated with an off-the-shelf cooling tower basin sealer that the EERC has found to be compatible with the hygroscopic working fluid under previous projects.

The piping and instrumentation diagram (P&ID) for the pilot cooling system is shown in Figure 3. The cooling tower was a closed-circuit design where condenser cooling water from the plant remained isolated from the evaporative spray water, which in this case was concentrated working fluid undergoing evaporation for disposal. The saturated wastewater was circulated from the basin and sprayed over the heat-transfer coil, while the fan provided a countercurrent flow of air for the wastewater to evaporate into. The figure shows the configuration using cooling tower blowdown as the makeup water source, which was metered directly from the condenser feed. During testing with APW, makeup water was pumped from a tank trailer supplied by the host site.

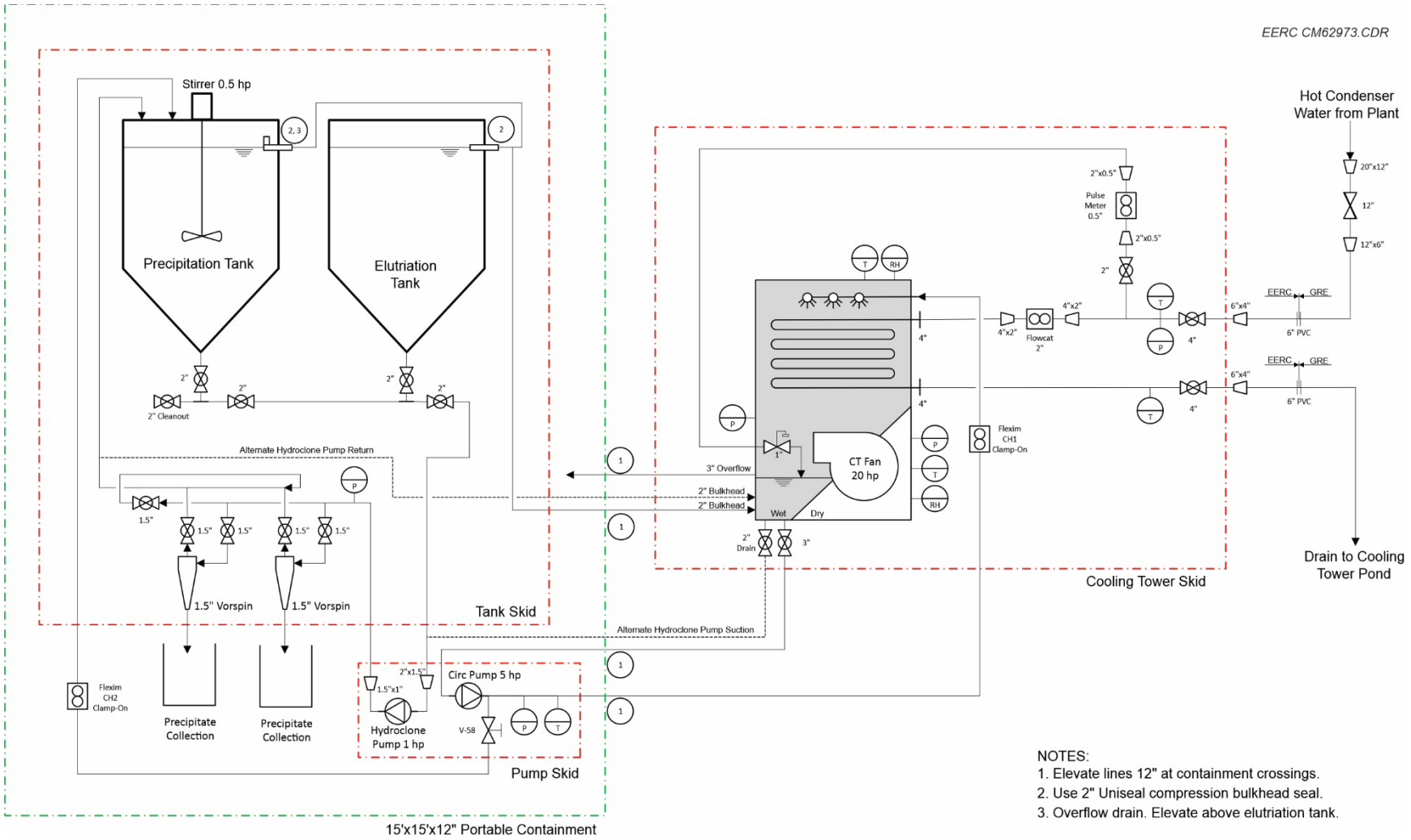

Figure 3. P&ID for the pilot wastewater recycling system.

The pilot system was designed to allow several circulation configurations for precipitated solids separation. In the configuration shown in Figure 3, a slipstream of working fluid was bled from the circulating spray pump and injected into the first of two equilibration vessels. The first vessel was actively mixed while the second was still to allow gravity separation between the larger precipitates and the working fluid. A dedicated slipstream pump could pull fluid from either tank and pass it through the manifold of hydrocyclones for solids separation. There was also a provision to have this pump draw from the basin of the cooling tower directly.

Equipment was mounted to one of three skids for structural support as shown by the skid groupings indicated in Figure 3. Photographs of the various skids are shown in Figures 4 and 5.

Figure 4. Hygroscopic cooling tower skid during field testing.

Figure 5. Pump skid, center, and hydrocyclone manifold mounted to the tank skid, left.

Task 4.0 – Wastewater Testing

Field testing was conducted at Coal Creek Station to have ample access to wastewater and waste heat to drive evaporation. Coal Creek Station is located near Underwood, North Dakota, and has two 550-MWe units. Lignite coal is mined adjacent to the plant and undergoes a beneficiation process developed at the plant called DryFining™ to reduce moisture content. Makeup water for Coal Creek is collected via pipeline from an intake on the Missouri River. The pilot system installed at Coal Creek is shown in Figure 6.

Figure 6. Pilot hygroscopic cooling system installed at Coal Creek Station.

The plant is a ZLD facility, and water is recycled within the plant to minimize makeup and reduce the volume of wastewater for disposal. As one example of water optimization at Coal Creek, the plant's cooling towers operate with 15 cycles of concentration. The site's ZLD management consists of evaporation ponds, and ultimate disposal is with deep well injection as shown in the simplified water flow diagram of Figure 2.

Host Site Integration

Coal Creek Station had unique existing condenser water access that was leveraged for field testing. The plant at one time provided sales of bulk hot water to the oil and gas industry where the water was heated using a slipstream of hot condenser cooling water passing through one side of a plate and frame heat exchanger. The heat exchangers and condenser circuit access points were located in a small shed, Figure 7. No longer in use, the shed and condenser water access points were made available by GRE for field testing.

Figure 7. Heat exchanger shed at Coal Creek Station where the plant's condenser cooling water circuit was accessed.

Hot condenser water supply was extended to the pilot cooling system using lay-flat piping from inside the heat exchanger shed, Figure 8. Since the site was adjacent to the plant's cooling water basin, cooled condenser water from the pilot system drained directly into the basin through an extension made from polyethylene pipe. Flow through the pilot system's heat exchange coil was driven by the existing pressure of the condenser water supply, which was nominally 18 psig. This pressure alone was sufficient to supply the 200-gpm design target through the heat exchange coil of the pilot unit. Flow was controlled manually by a throttle valve in the condenser water circuit shown in Figure 3. The nominal temperature set points across Coal Creek's full-scale cooling tower were 46°C in and 29°C out (115° to 85°F). During field testing, temperature of the hot condenser water at the test location was typically 44°C (112°F).

Figure 8. Plant condenser water supply, center, and return pipe to the basin, right.

Two plant wastewater sources were tested on-site: CTB from the plant's main cooling towers and APW taken from the deep well transfer pump. Since the plant continually bled blowdown water from the cooling tower basin to maintain its composition, the circulating condenser water was equivalent to the blowdown stream composition. This makeup water was accessed by extracting it from the condenser water supply line at a point upstream of the flow measurement used to determine flow rate through the pilot cooling tower's heat exchange coil.

The second makeup water source was collected from the deep well injection circuit, which itself was drawn from the plant's ash settling pond. It was not feasible to extend a supply line for APW to the pilot cooling system, instead the plant provided an 800-gal trailer-mounted tank, Figure 9, that GRE personnel would fill and bring to the test unit one or two times per day depending on usage. A small transfer pump was then used to pump from the tank through a metering valve on the tower.

Figure 9. Portable tank, at left, used to bring APW to the test unit.

Precipitated solids from testing were collected and disposed of into drums placed at the test unit by GRE. After characterization of the waste solids, the bins were emptied into the on-site landfill by plant personnel.

A field safety plan was prepared by the EERC in advance of on-site activities. The plan identified potential hazards during testing and outlined the mitigation strategies that were employed. The plan was reviewed by GRE personnel and approved after their comments were addressed. Copies were kept at the test unit and at the plant's security desk.

Pilot system installation and testing at Coal Creek Station began in June 2021 shortly after the plant's annual maintenance outage. Because of technical and contractual reasons, on-site testing was completed by September 2021. The technical reason for this end date was that the pilot system was not designed to function in freezing temperatures, and in North Dakota, overnight freezes typically begin by mid-September. The contractual reason was that, during the course of this project, GRE elected to sell Coal Creek Station and one of the target sale dates was October 2021. Since GRE made the original commitment to participate in this project, it was desired to complete on-site work under GRE ownership.

Testing Approach

Field testing was structured to generate the necessary range of operating data to evaluate wastewater recycling with the hygroscopic cooling pilot unit. Testing began with CTB based on the premise that it would be easier to process than APW given its lower dissolved solids concentration. APW was tested during the second phase of field testing when the dissolved solids content of the working fluid was higher.

During operation of the hygroscopic cooling system, sparingly soluble species in the wastewater, such as gypsum, were predicted to reach saturation and begin precipitating relatively soon into testing. However, the more soluble sulfate and chloride species were unlikely to reach equilibrium within the time frame of the field test. In order to evaluate operation across the entire range of expected working fluid concentrations, the working fluid concentration was increased by mixing in $CaCl_2$ brine, and then $MgCl_2$ brine, in stepwise increments. After each addition of brine, the system was operated to collect performance data and precipitate samples for analysis. The final, and highest, working fluid concentration was predicted to correspond to a condition where even highly soluble chloride compounds began to precipitate.

Data collection focused on supporting TEA modeling assumptions regarding cooling performance, wastewater throughput, waste solids characterization, and operations and design recommendations. These data were ultimately used to inform a techno-economic model of the process under Task 5.0. Details of the methodology for each data set are described below. As for the mechanics of data collection, raw data from each day's testing underwent a cursory check to look for anomalies and to verify that the targeted test conditions were being reached. However, significant data analysis was not performed until after the completion of field testing.

Cooling Performance

This data set addressed the quantity and quality of cooling provided by the hygroscopic cooling tower while evaporating plant wastewater. Cooling quantity was a straightforward determination from the log of condenser water flow and temperature change across the pilot system's heat exchange coil. Cooling quality was characterized by determining the hygroscopic tower's approach to the ambient wet-bulb temperature under a range of heat load conditions and working fluid concentrations.

Conventional cooling tower performance can be described by a single performance curve that can be used to correlate cooling capacity and wet-bulb temperature approach given constant ambient wet-bulb temperature and fan power. However, with hygroscopic cooling, properties of the working fluid also impact cooling performance and a second criteria is needed to define a performance curve. Water activity of the working fluid was selected as the second property, and it is defined as the water vapor pressure of the working fluid relative to the vapor pressure of pure water at the same temperature and pressure conditions. The hygroscopic working fluid will have a water activity value less than one, which indicates restricted evaporation compared to pure water. In a cooling tower, the effect of decreased water activity is an increase in the wet-bulb temperature approach to maintain the same cooling load. For the same reason, the proportion of sensible heat

transfer is slightly higher with a hygroscopic tower compared to the same tower operating with pure water, and the throughput of makeup water will be slightly less.

To evaluate cooling performance of the pilot unit, periods of steady-state heat transfer were identified during the stepwise increases in working fluid concentration. Water activity was calculated by modeling the measured composition of working fluid samples using PHREEQC. Between each adjustment of the working fluid concentration, water activity was calculated to be relatively constant, and cooling data for each step were categorized under a single average activity value. Only conditions with full-load fan operation were chosen to develop the performance curves so that the trends could be compared to factory data of the tower with water working fluid.

Wastewater Throughput

Related to cooling performance was the quantity of makeup water the pilot system consumed during operation, or in terms of recycling, the wastewater throughput rate. This rate is also impacted by the working fluid properties since a lowered water activity slightly increases the proportion of sensible heat transfer in the tower compared to latent heat transfer. The heat of vaporization also slightly increases for a hygroscopic working fluid compared to water. Since these effects impact the consumption rate of wastewater by the system, direct measurements of wastewater throughput were made using a flow totalizer, and the data were correlated to the same steady-state performance evaluation periods.

Waste Solids Characterization

Wastewater recycling with hygroscopic cooling reduces the wastewater stream to precipitated waste solids for disposal. Analysis of the solids sampled at key points during testing were performed to determine what applicable disposal options would be and whether secondary processing would be required. Solids analyses are summarized in Table 5.

Table 5. Analysis Used to Characterize Waste Solids

Parameter	Method
Bulk Chemical Composition	X-ray fluorescence (Ca, Mg, Na, K, Si, and Sr) Ion chromatography (chloride, nitrate, and nitrite) Combustion with thermal conductivity detection (C, H, and S)
RCRA Element Concentration	ICP–MS (As, Ba, Cd, Cr, Pb, Se, and Ag) CVAA (Hg)
Leaching Potential	EPA Method 1311 (EPA, 1992)
Bulk Density	Gravimetric with graduated cylinder volume determination
Liquid Content	Gravimetric after 105°C drying
Landfill Evaluation	EPA Method 9095B (EPA, 2004)

Operations and Design

Additional data sets were collected during field testing and, in some cases, after field testing using samples returned to the EERC. These data generally document operation of the hygroscopic cooling tower and include particle-size distribution measurements of the precipitated solids, microbial activity within the working fluid, corrosion screening of candidate materials of construction, and foaming tendencies of the working fluid. Conclusions from these data were used to guide development of the TEA performance model and to inform specific sensitivity studies.

The particle-size distribution of precipitates in the working fluid was routinely measured to provide guidance for effective nucleation seed size and concentration. Data were collected using a portable, laser diffraction-based particle sizer (LISST-Portable XR by Sequoia Scientific Incorporated) that was taken to Coal Creek Station. Most working fluid samples were too concentrated for direct reading by the instrument and required dilution, which was recorded at the time of analysis and used to scale the results during data reduction.

Microbial activity of the hygroscopic system and the makeup water sources was periodically monitored using common industrial dip slides. These slides are coated with sterile growing media and were inoculated by immersing them directly in the cooling tower basin or makeup water source under evaluation. After a prescribed incubation period, growing colonies of bacteria or fungi caused a color change on the slide, and a semiquantitative assessment of microbial activity was made by comparing the incubated slide to reference images provided by the manufacturer. Photographs of each slide were taken to record their condition and are included in Appendix A.

Corrosion coupons were installed in the pilot unit to perform a quantitative screening of candidate materials of construction for a hygroscopic cooling system since corrosion is a concern with the increased dissolved-solids content of the working fluid. To evaluate at least the short-term effects of corrosion, coupons were installed in the cooling tower at two locations. One location was in the cooling tower basin where the coupons were submerged, and the other was on a rack placed near the heat-transfer coil that experienced a regular combination of liquid spray and air exposure. Coupon materials included:

- 316 stainless steel
- 2205 duplex stainless steel
- TI-5 titanium
- CDA651 silicon bronze
- 2024 aluminum

Coupons were installed prior to the start of testing and remained in place until testing was complete. A total of five coupons were installed for each metal: two of each were submerged in the basin and three of each were installed in the spray zone. Analysis of the recovered coupons was conducted by the coupon provider and consisted of cleaning, determining the loss in weight during exposure, and calculating a normalized corrosion rate. All materials were selected on recommendations for chloride corrosion resistance and/or seawater service.

During operation of the hygroscopic cooling tower, the working fluid displayed some tendency for foam formation, and the phenomena increased in severity during the later stages of testing when the foam began to stabilize and persist for extended periods of time. As a stable foam developed, it prevented the normal operation of the cooling tower's level control valve and led to excessive pass-through of foam to the drift eliminator. In order to identify the key factors affecting foam formation, a series of foaming tendency tests were conducted on samples of collected working fluid. The test procedure was based on an established standard for evaluating foaming with lubricating oil (American Society for Testing and Materials D892-18) and is fully described in Appendix B. In summary, the procedure involved sparging nitrogen into a fixed volume of working fluid held at a constant temperature for a prescribed length of time. The volume of foam produced was then recorded immediately at the conclusion of gas sparging and again after a subsequent 10-minute stilling interval. These data provided relative indicators of foaming tendency and foam stability that were correlated to changes in working fluid composition over the duration of field testing.

Task 5.0 – Techno-Economic Analysis

The TEA was based on a performance model of hygroscopic cooling developed from field test results that estimated cooling capacity, wastewater consumption, and waste solids production. Wastewater properties and other site-specific parameters, including the throughput sizing, were based on conditions at Coal Creek Station. Capital costs were developed using the pilot unit as a known data point and scaled using standard chemical engineering plant estimating procedures (Woods, 2007). Similar estimates were prepared for disposal-only ZLD and thermomechanical ZLD for comparison. Results for all approaches were standardized by encompassing the entire lifetime of system operation with the LCWD computation in Equation 1:

$$LCWD = \frac{System\ Capital\ Cost + Present\ Value(Annualized\ Operations\ and\ Maintenance\ Costs - Savings)}{Lifetime\ Wastewater\ Treatment\ Capacity} \quad \text{[Eq. 1]}$$

RESULTS

Wastewater–Working Fluid Interactions

Composition data for the three wastewater streams sampled at Coal Creek Station are presented in Table 6. At the plant, APW represented the plantwide blowdown stream being sent for ZLD disposal, and it was selected as the primary stream of interest for this study, although initial testing with the pilot system was conducted using CTB. After being used elsewhere in the plant, both the CTB and FGD slurry ultimately ended up as components of APW. Sulfate was the dominant anion in APW, likely due to the use of H_2SO_4 during treatment of the makeup river water and from accumulating additional sulfates in the FGD scrubber. Significant cations were Na and Mg which form higher solubility sulfate species compared to Ca, the concentration of which was effectively capped by the lower solubility of calcium sulfate compounds.

Table 6. Composition Data for Wastewater Streams at Coal Creek Station

		Cooling Tower Blowdown	FGD Slurry	Ash Pond Water
pH		7.29	5.33	7.79
Alkalinity, as HCO_3	mg/L	75	26.5	239
Alkalinity, as $CaCO_3$	mg/L	61.5	21.7	196
Ca	mg/L	712	391	734
Mg	mg/L	313	8030	1190
Sr	mg/L	6.43	1.02	13.6
Na	mg/L	898	4280	1680
K	mg/L	59.6	492	176
Li	mg/L	0.9	3.4	1.3
Si, as SiO_2	mg/L	92.0	102.7	55.6
Cl	mg/L	227	1240	440
F	mg/L	5.8	150	6.5
Br	mg/L	<1	420	130
SO_4	mg/L	4200	34900	8800
NO_3	mg/L	<5	<5	<5
NO_2	mg/L	<5	<5	9.8
P, as PO_4	mg/L	<6.1	16	<6.1
B, as BO_3	mg/L	12	278	81
TOC	mg/L	42.2	63.6	26.9
TDS	mg/L	6920	57600	14800
RCRA Elements				
As	mg/L	0.0346	0.0285	0.108
Ba	mg/L	0.5	0.17	0.31
Cd	mg/L	<0.01	<0.01	<0.01
Cr	mg/L	<0.05	<0.05	<0.05
Pb	mg/L	<0.005	<0.005	<0.005
Hg	mg/L	<0.0001	0.00473	<0.0001
Se	mg/L	0.014	0.45	0.017
Ag	mg/L	<0.05	<0.05	<0.05

A totals analysis for hazardous waste determination was performed using the RCRA element concentrations and the corresponding TDS values in Table 6 that assumed all of the RCRA content would precipitate and become incorporated into the total mass of dissolved solids. For the totals analysis, it was further assumed that all of the RCRA content would then leach from these solids into 20 L of water per kg of solid to yield a maximum theoretical leachate concentration. Table 7 shows these maximum leachate concentrations relative to the regulation limits. The totals analysis indicates that steady-state solids produced from any of the wastewater streams would not exceed the toxicity characteristics limit.

Table 7. Maximum RCRA Element Leachate Concentration Based on Liquid Analysis

		Cooling Tower Blowdown	FGD Slurry	Ash Pond Water	EPA Toxicity Characteristic Limit
As	mg/L	0.250	0.0247	0.365	5
Ba	mg/L	3.61	0.147	1.05	100
Cd	mg/L	<0.07	<0.009	<0.03	1
Cr	mg/L	<0.4	<0.04	<0.2	5
Pb	mg/L	<0.04	<0.004	<0.02	5
Hg	mg/L	<0.0007	0.004	<0.0003	0.2
Se	mg/L	0.101	0.391	0.0574	1
Ag	mg/L	<0.4	<0.04	<0.2	5

The geochemical modeling program PHREEQC was used to model the saturation index values for simplified wastewater compositions consisting of only the major ionic species: HCO_3, Cl, SO_4, Ca, Mg, and Na. Table 8 presents the calculated saturation index values for common precipitants, where a negative value indicates a subsaturated, nonprecipitating condition for the associated species and a positive value indicates supersaturation and the possibility of precipitation. Whether precipitation actually occurs is determined by a number of factors and is not solely dependent on the saturation index. For example, according to Table 8, carbonate species and gypsum in APW were predicted to be in a supersaturated, metastable condition in their as-collected condition.

Table 8. PHREEQC Saturation Index Results for the Wastewater Samples

Precipitant	Composition	CTB	FGD	APW
Anhydrite	$CaSO_4$	−0.1	−0.16	−0.03
Aragonite	$CaCO_3$	−0.09	−3.18	0.76
Calcite	$CaCO_3$	0.06	−3.04	0.9
Dolomite	$CaMg(CO_3)_2$	0.06	−4.46	2.32
Gypsum	$CaSO_4 \cdot 2H_2O$	0.21	0.14	0.27
Halite	NaCl	−5.42	−4.13	−4.91

The working fluid mixing tests outlined in Tables 3 and 4 generated data that were used to probe the boundaries of this metastable condition and refine the conditions where precipitation might actually start and stop. Two sets of data were collected: one was used to estimate the limit of spontaneous nucleation and the other to determine the saturation index that a system at equilibrium would likely approach. Given the composition of APW and predictions by PHREEQC, gypsum was the focus of these tests.

Figure 10 plots the gypsum saturation index as a function of equilibration time for two wastewater–working fluid solutions. The initially higher-concentration mixture initiated homogeneous nucleation and precipitated, while the lower-concentration solution remained supersaturated for an extended time. These results were used to bound the saturation index range of 0.9–1.2 as the likely point where spontaneous nucleation could be expected for the conditions of this project. Similarly, Figure 11 is a plot of the ending gypsum saturation index versus the initial value after a 24-hour equilibration period. The data show that, without seeds, the threshold of spontaneous nucleation is not exceeded, at least up to a saturation index of approximately 0.45, which is consistent with the data of Figure 10. However, with seeds present, precipitation does begin at a saturation value between approximately 0.1 and 0.25. Further increasing the starting saturation index with seeds present results in added precipitation to maintain an effective equilibrium saturation index near 0.28, which again appears consistent with the long-term equilibration trend of the spontaneous nucleation case in Figure 10.

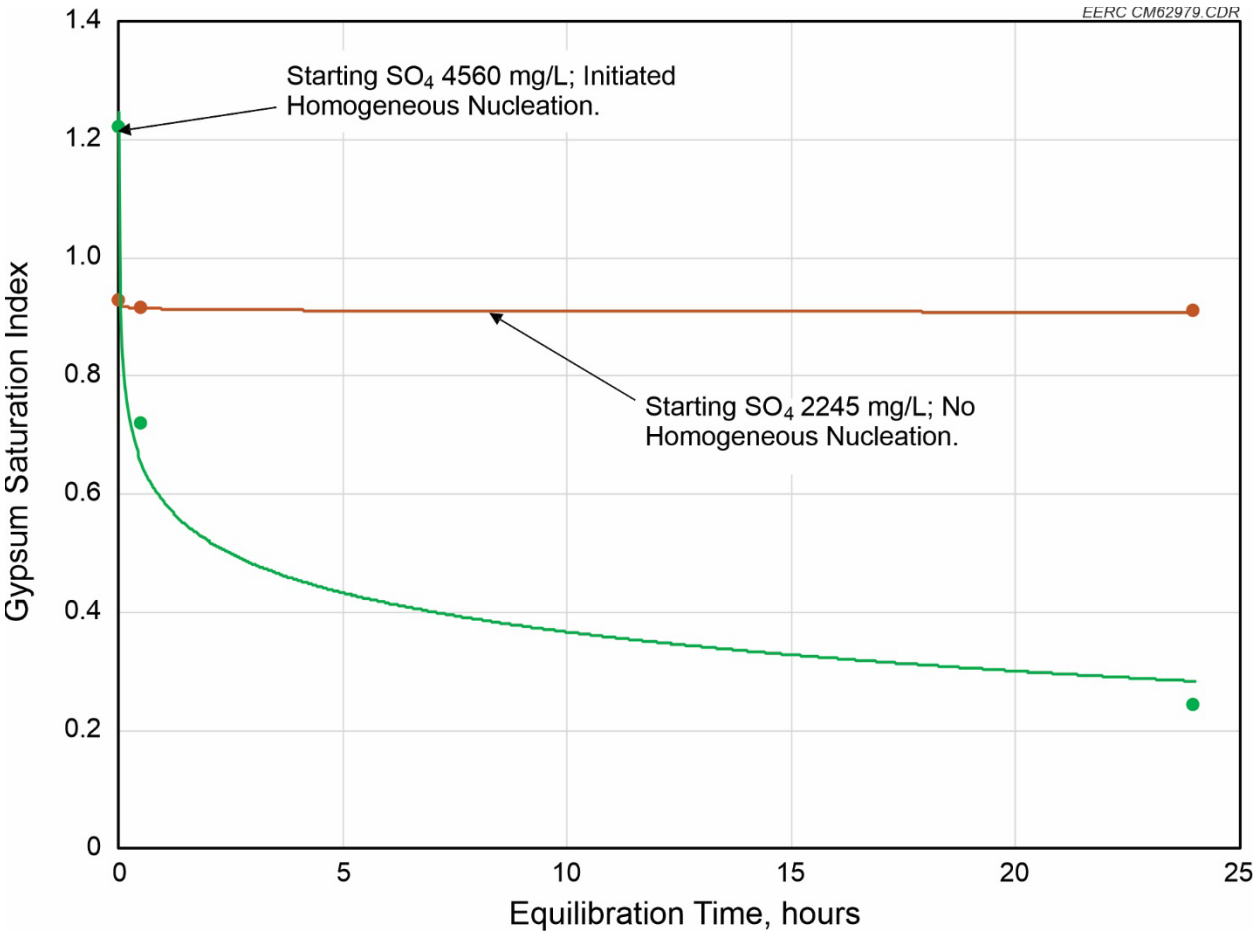

Figure 10. End of test saturation index data for metastable and unstable precipitation conditions in concentrated APW.

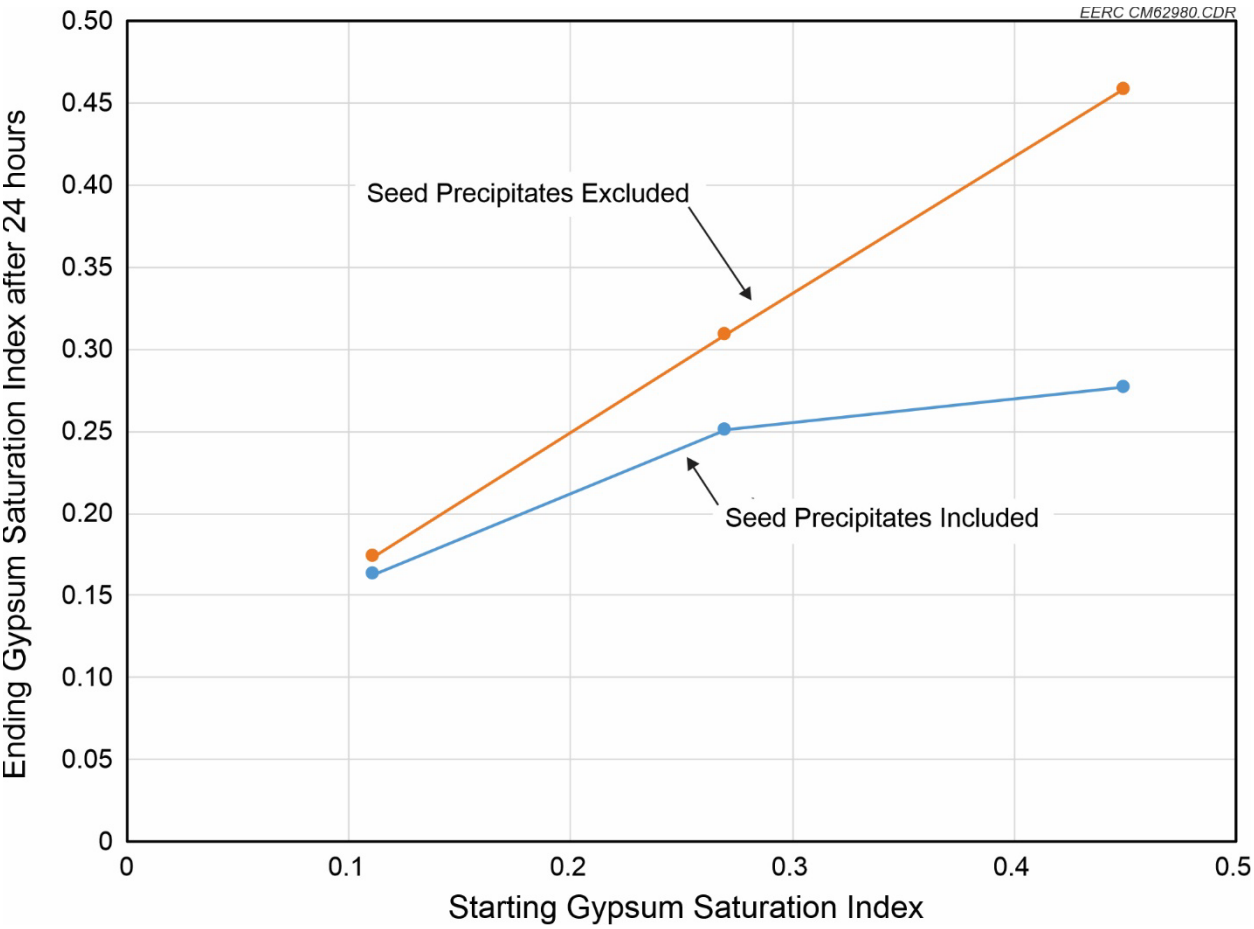

Figure 11. End of test saturation index values highlighting the effective equilibrium saturation index for concentrated APW.

Field Test Results

Field testing took place June to September 2021, and the key metrics for individual test days are summarized in Table 9. Test conditions were categorized by the source of makeup water and the working fluid concentration. This information is also plotted in Figure 12 using chloride concentration to quantify the working fluid concentration.

Table 9. Summary of Field Test Days

	High-Level Parameters			Wastewater Consumption	
Test Date	Wastewater Source	Desiccant Concentration	Waste Heat Coil Flow, gpm	Daily, gal	Cumulative, gal
6/18/2021	CTB[1]	None	Varied	304	304
6/21/2021	CTB	None	Varied	68	372
6/22/2021	CTB	Low	219	979	1351
6/23/2021	CTB	Low	115	828	2179
7/13/2021	CTB	Low	120	895	3074
7/14/2021	CTB	Low	165	1060	4134
7/15/2021	CTB	Low	220	812	4946
7/21/2021	CTB	Low	110	801	5747
7/22/2021	CTB	Low	110	479	6226
7/23/2021	CTB	Low	110	406	6632
8/2/2021	CTB	Low	155	612	7244
8/3/2021	CTB	Medium	120	180	7424
8/4/2021	CTB	Medium	120	318	7742
8/5/2021	CTB	Medium	160	993	8735
8/16/2021	CTB	Medium	165	686	9421
8/17/2021	CTB	Medium	220	1151	10,572
8/18/2021	CTB	Medium	220	973	11,545
8/20/2021	CTB	Medium	220	967	12,512
8/30/2021	CTB	Medium	72	772	13,284
8/31/2021	CTB	Medium	72	1091	14,375
9/1/2021	APW[2]	Medium	55	536	536
9/2/2021	APW	Medium	80	684	1220
9/7/2021	APW	Medium	80	874	2094
9/8/2021	APW	Medium	50	693	2787
9/9/2021	APW	Medium	160	1295	4082
9/10/2021	APW	High	50	100	4182
9/13/2021	APW	High	80	685	4867
9/14/2021	APW	High	160	1591	6458
9/15/2021	APW	High	50	842	7300
9/16/2021	APW	High	215	920	8220
				Project Total	**22,595**

[1] Cooling tower blowdown from Coal Creek's main cooling towers.
[2] Ash pond water extracted from Coal Creek's deep well injection circuit.

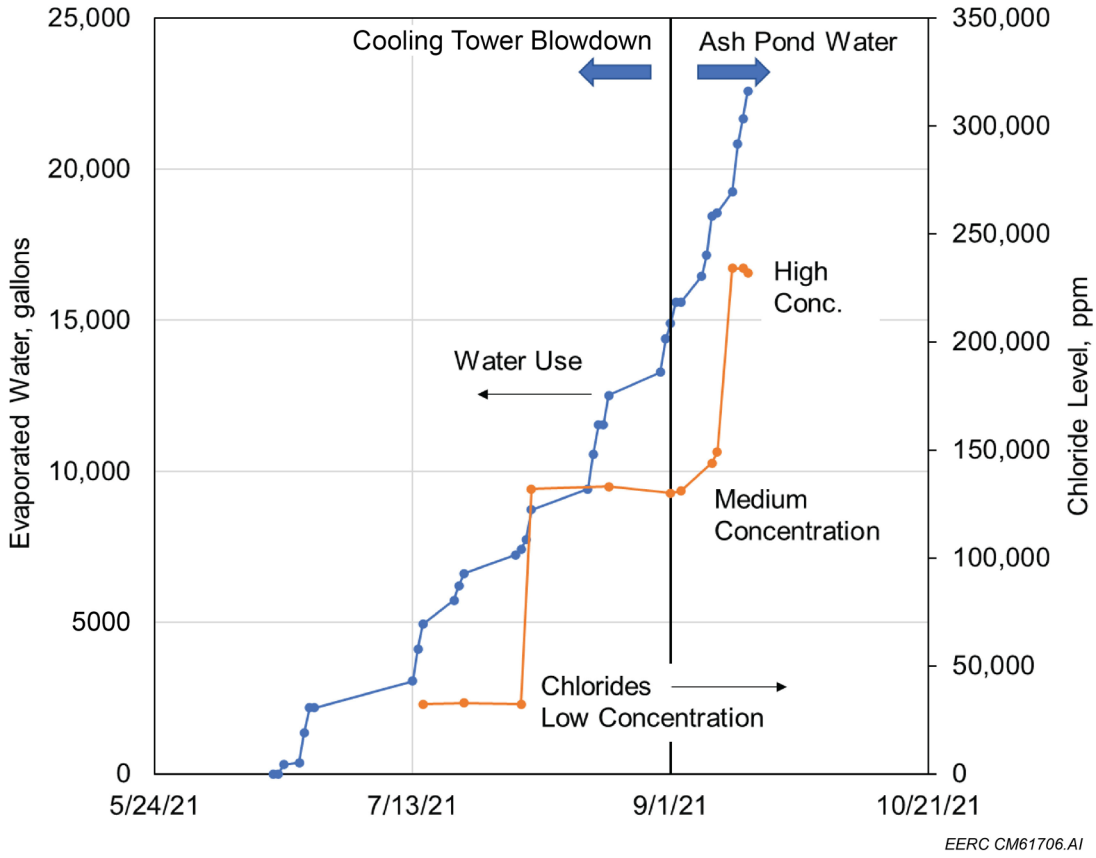

Figure 12. Division of test data by makeup water source and working fluid chloride level.

Working Fluid Composition

Virtually all of the evaluation criteria for hygroscopic wastewater recycling are impacted by the composition of the working fluid, the exact composition of which is determined by the dynamic balance between the incoming dissolved constituents in the makeup water and those outgoing as either a precipitated solid or as a dissolved constituent of the concentrated working fluid. The distinct concentration levels in Figure 12 were intended to span the entire range of precipitating species, from the sparingly soluble constituents up to the most soluble chloride salt species. Figure 13 is a similar plot showing the concentration history of the other major ions in the working fluid.

After approximately 15,000 gal of CTB wastewater was consumed by the pilot unit, testing switched to using APW for makeup, which resulted in an accelerated accumulation of most constituents. With the final concentration adjustment near 18,000 gal, the system appeared to be approaching its limiting concentration with potential leveling or reductions in most constituents.

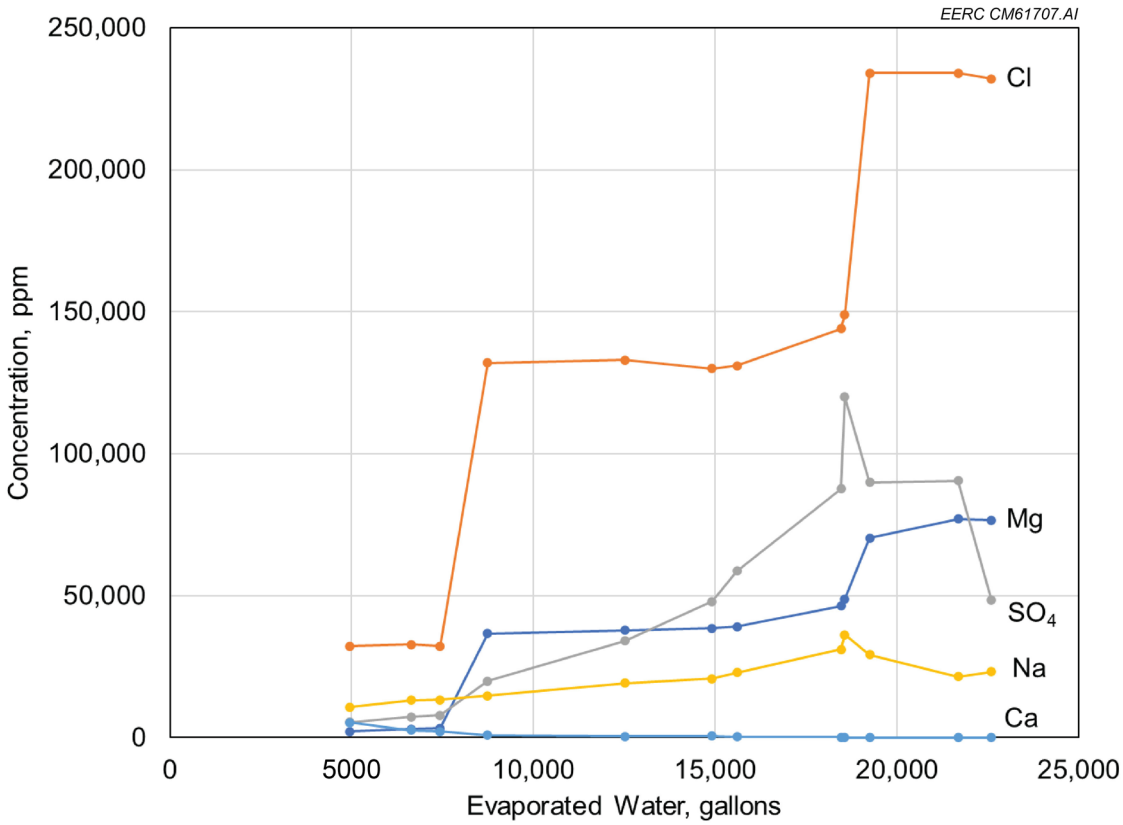

Figure 13. Measured major ion concentration in the working fluid over the course of field testing.

A subset of the working fluid samples was analyzed for RCRA elements, which are used in part to classify whether solid wastes are considered hazardous. These data are summarized in Table 10. Results for the eight elements can be grouped into categories of not significantly present in the wastewaters (Cd and Ag), those that concentrated over time but possibly reached steady state (Ba and Se), and those that concentrated without reaching steady state during the test period (As, Cr, Pb, and Hg). Given the small concentrations of these elements in the incoming wastewater streams, it is possible that this last category of RCRA elements would continue to concentrate in the working fluid before being removed on a steady-state basis as either a precipitate or entrained in the working fluid.

Cooling Tower Performance

Daily operating data were processed to develop summary performance relationships for hygroscopic operation. These relationships were ultimately used in the TEA to predict system performance for a variety of scenarios. Daily operating data were processed to compute the key performance values of heat load, approach temperature, and wastewater throughput. Steady-state periods were identified where these values, along with constant fan power and working fluid water activity, were consistent and an average could be calculated. Water activity is defined as the ratio

Table 10. Working Fluid RCRA Element Concentrations

Makeup Water Source Chloride Concentration Level Sample Date		CTB Low 8/3/2021	CTB Medium 9/1/2021	APW Medium 9/10/2021	APW High 9/16/2021
Arsenic	µg/L	118	1490	2130	3290
Barium	µg/L	506	220	<50	<50
Cadmium	µg/L	<5	<5	<5	<5
Chromium	µg/L	<10	<10	13	22
Lead	µg/L	13	21	23	43
Mercury	µg/L	<0.2	<0.2	<0.2	0.49
Selenium	µg/L	85.2	156	255	220
Silver	µg/L	<10	<10	<10	<10

of the equilibrium water vapor pressure of the working fluid relative to that of pure water at the same temperature and pressure conditions. It was selected as the proxy for working fluid concentration since it is a fundamental measure of the key impact that high levels of dissolved solids have on evaporative cooling performance. Water activity also provides a way to estimate hygroscopic performance with differing wastewater types in the future that may have differing chemical composition from the wastewater at Coal Creek Station.

Averages from the steady-state periods identified during testing with APW are shown in Table 11. These data are also plotted in Figure 14 that highlights summary relationships between approach temperature, cooling load, and working fluid water activity. The water activity groupings of 0.8 and 0.4 correspond to the medium- and high-chloride concentration working fluid conditions, respectively. Factory data in Figure 14 used tap water during testing, and these were assigned to a 1.0 water activity category. The linear data fits in Figure 14 were used during the TEA to estimate hygroscopic approach temperature over a continuous range of cooling loads by interpolating values that fell between the tested water activity groupings.

Table 11. Steady-State Averages from Field Testing with APW

Test Day	Ambient Wet-Bulb Temperature, °F	Coil Leaving Temperature, °F	Coil Entering Temperature, °F	Cooling Load, kW_{th}	Coil Flow, gpm	Wastewater Makeup, gpm
0.8 Average Water Activity (Medium Chloride Concentration)						
8/30/2021	64.2	80.0	112	339	71.9	2.01
8/31/2021	66.6	81.6	113	318	69.9	2.15
9/1/2021	67.1	79.0	113	267	54.2	1.33
9/2/2021	65.4	81.8	112	355	79.7	1.69
0.4 Average Water Activity (High Chloride Concentration)						
9/13/2021	59.4	86.4	112	327	85.6	1.49
9/14/2021	54.6	94.8	116	491	160	2.56
9/15/2021	64.2	83.8	115	226	49.7	1.64
9/16/2021	52.3	96.3	112	499	215	2.20

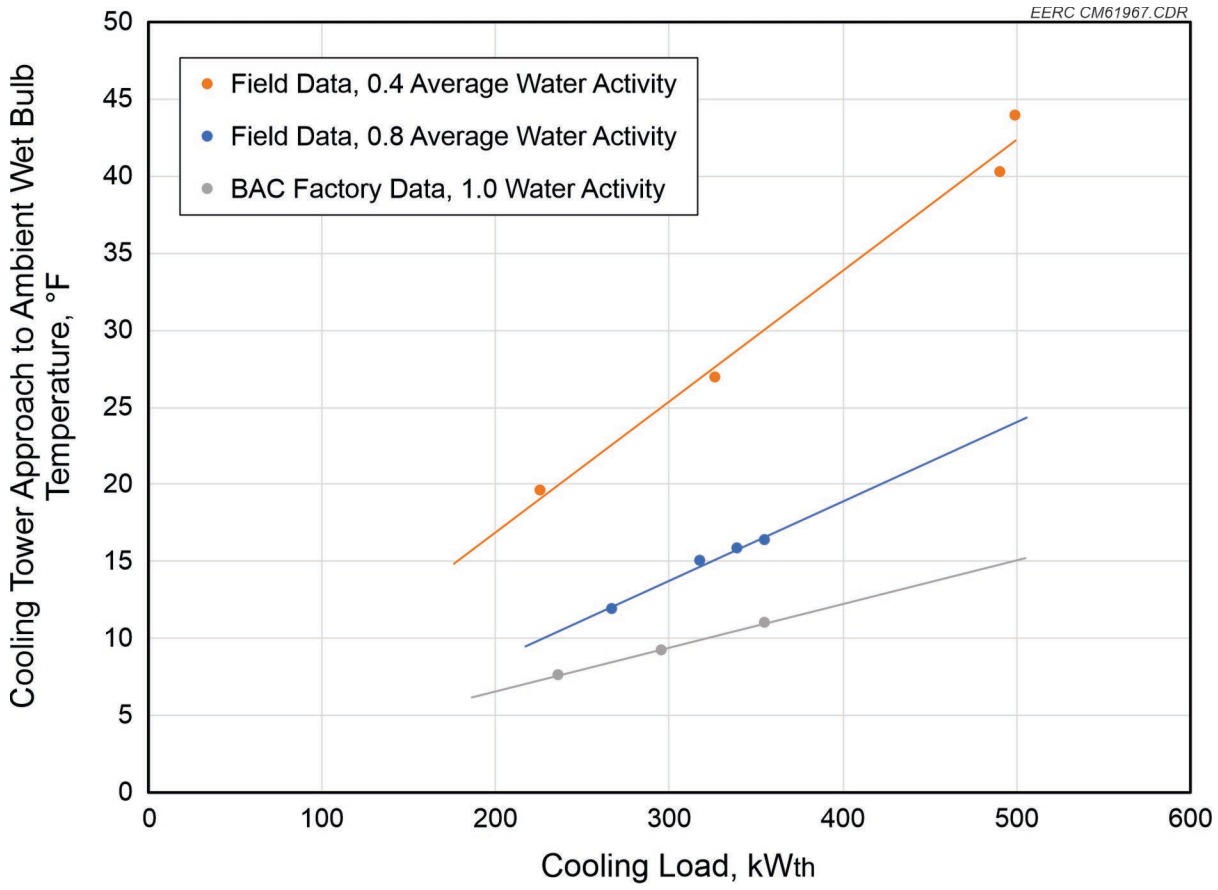

Figure 14. Correlations developed from operating data with the pilot unit.

Figure 14 clearly shows the impact of concentrated hygroscopic working fluid relative to conventional, pure water operation. Specifically, as the working fluid becomes more concentrated and water activity decreases, the tower's approach to the ambient wet-bulb temperature increases for the same cooling load. For example, at a cooling load of 350 kWth, the hygroscopic tower's approach to the ambient wet bulb would nearly triple from 6.1°C (11°F) with pure water to 17°C (30°F) with the highest concentration working fluid that was tested.

Since the hygroscopic tower's operating range is fixed by the ambient wet-bulb temperature and the plant's hot condenser water temperature, excessively large wet-bulb approach values could constrain its cooling capacity and wastewater throughput. This effect was not a concern at Coal Creek Station but will need to be evaluated for differing conditions at other sites. One strategy to manage the negative impact on wet-bulb approach is to limit working fluid concentration by having a blowdown of the working fluid in addition to the waste solids stream. This action would reduce the working fluid's dissolved solids content and raise its water activity value. For example, with a water activity of 0.8, the wet-bulb approach at 350 kWth is approximately 8.9°C (16°F), only 2.8°C (5°F) above the value with pure water.

Wastewater Throughput

The purpose of hygroscopic wastewater recycling was to not only provide usable cooling for the power plant, but to also minimize the quantity of waste liquid needing disposal. Steady-state wastewater consumption values were included in Table 11 and are plotted in Figure 15 as a function of total cooling load. These data do not appear to result in a clear trend, probably due to other key parameters not being kept constant. For interpretation, trend lines of the theoretical water evaporation rate have been added by assuming the proportion of the total heat load that is dissipated evaporatively. Since the trends assuming 100% and 75% evaporative cooling load appear to bound the recorded data, an average trend assuming 85% evaporative heat transfer was selected for TEA modeling. This imperfect but reasonable fit of experimental APW consumption was used to estimate wastewater throughput for the TEA performance model. Specifically, at a cooling load of 350 kWth, the average wastewater consumption was determined to be 2.0 gpm, resulting in a specific cooling capacity of 2.78 GJ/m^3 of APW.

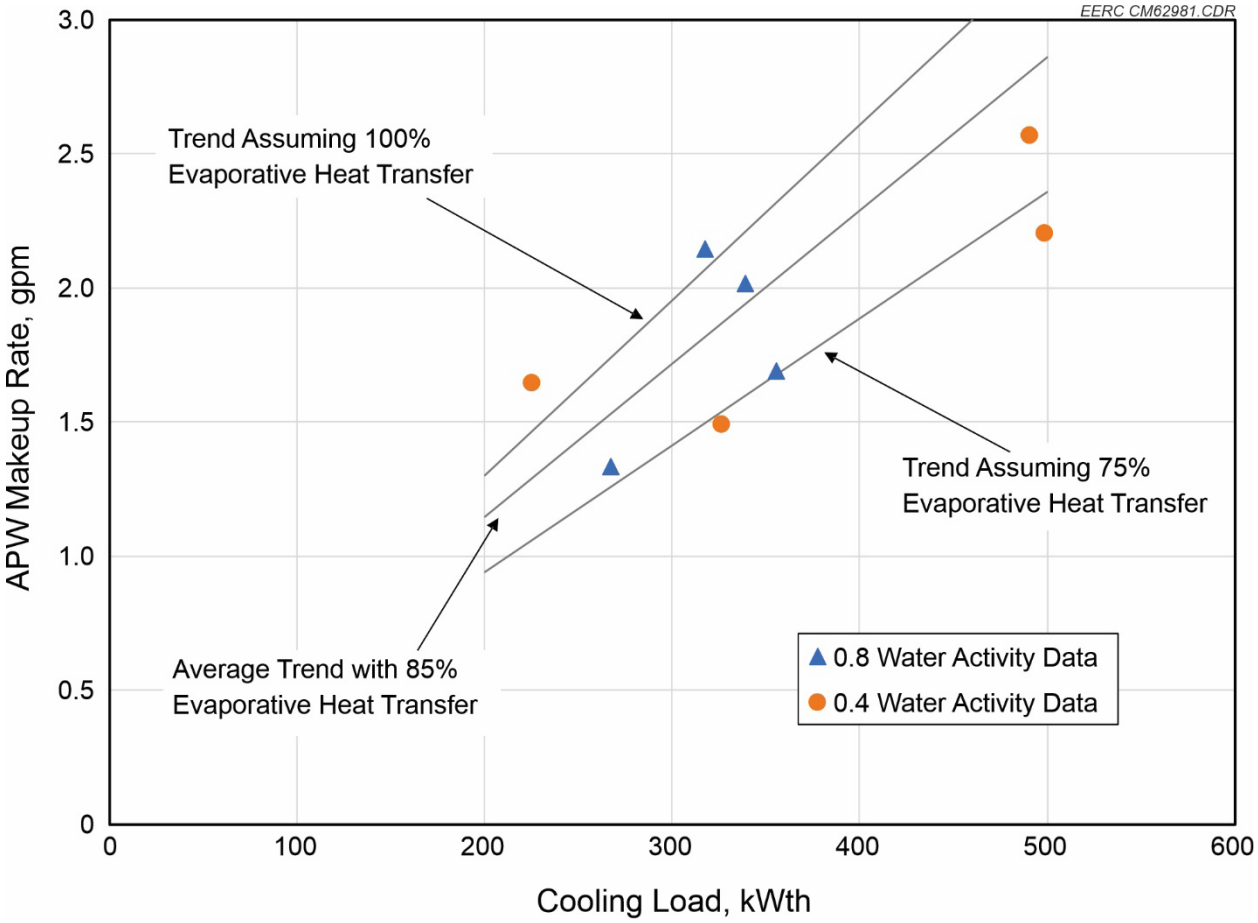

Figure 15. Fit of wastewater consumption data from steady-state average periods.

Precipitate Characterization

During field testing of the hygroscopic wastewater recycling concept, precipitates that formed in the working fluid were separated for disposal using hydrocyclones operating with a slipstream of working fluid from the cooling tower basin, Figure 16. To evaluate solids disposal options and provide a basis for disposal cost, samples of the precipitates were analyzed for composition and physical characteristics. Figure 17 summarizes the chemical composition of the precipitates at each phase of field testing. As shown, the solids were generally dominated by sulfates, specifically calcium sulfate in the earlier samples from June 23, 2021, and July 23, 2021. Later samples corresponding to the medium and high chloride concentration working fluid show increased magnesium, sodium, and chloride content. Virtually all of the chloride content with the medium samples and most with the high sample was from the brine extracted with the precipitates as interstitial fluid since only under the most concentrated conditions at the highest chloride level was sodium chloride (i.e., halite) expected to precipitate.

Figure 16. Example solids collection stream during field testing.

The composition breakdowns in Figure 17 were reported on a dry basis, after drying to constant weight at 105°C (221°F). However, the figure shows increased water content with working fluid concentration. This persistent water after drying suggests that the water molecules were likely chemically bound, hydration water associated with the various solid phases present.

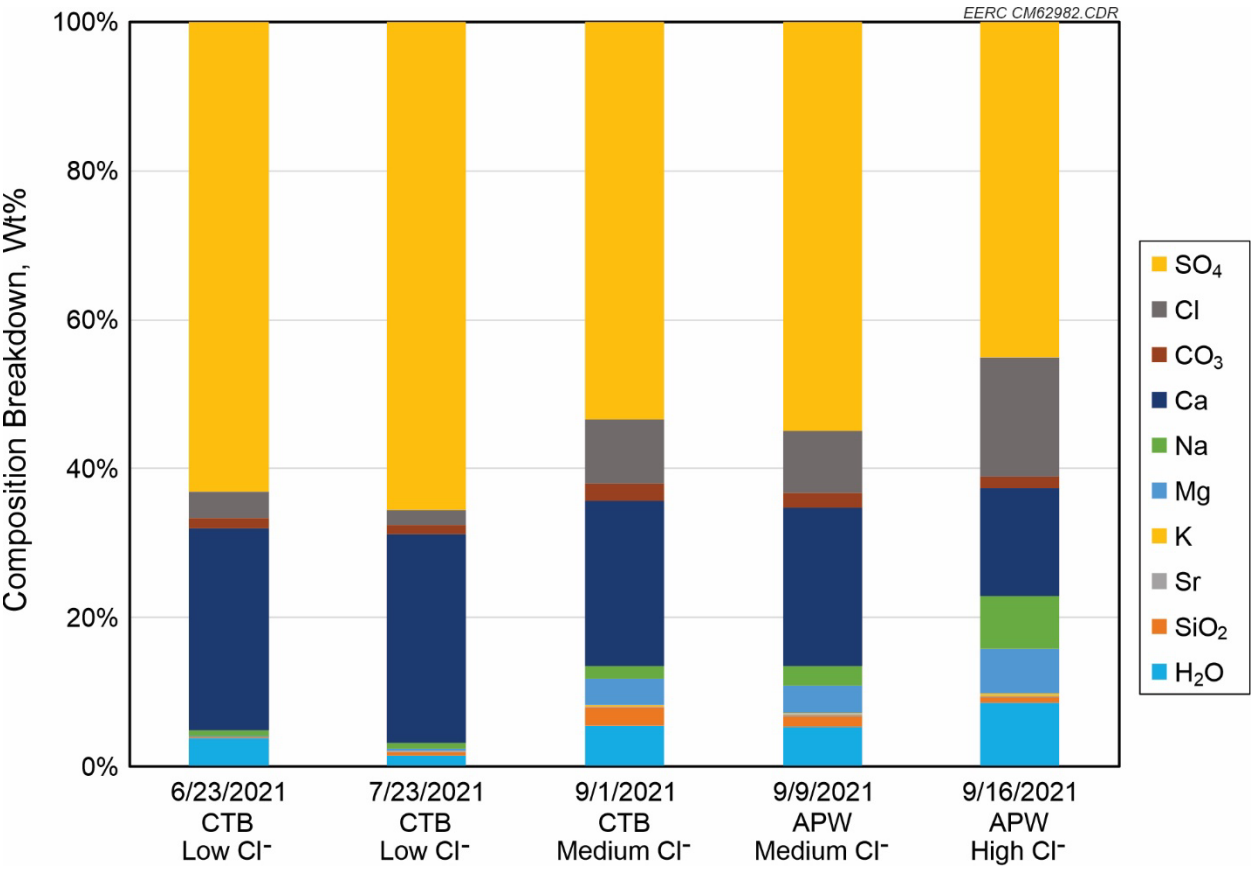

Figure 17. Composition breakdown for solid precipitates.

The precipitates were also analyzed for RCRA element content and evaluated for their toxicity characteristics with respect to hazardous waste determination. RCRA element concentrations for the five precipitate samples in Figure 17 are provided in Table 12. As the results show, most of the elements were below detection limits, and only As and Ba were consistently detected in the samples. The concern with RCRA elements during long-term disposal is that they may leach from the solid and be released to the environment. Leaching potential was evaluated two ways. First, a total analysis was conducted assuming that the entire RCRA content of the precipitates would leach into 20 L/kg of water. These worst-case values are presented in Table 13, and all elements appear to be well below levels of concern with respect to displaying toxicity characteristics.

Table 12. RCRA Element Concentrations in the Precipitate Samples, mg/kg

Wastewater Chloride Level	CTB Low	CTB Low	CTB Medium	APW Medium	APW High
Date	6/23/2021	7/23/2021	9/1/2021	9/9/2021	9/16/2021
As	1.8	1.8	4	3.5	3.8
Ba	7.4	37.2	107	81.3	44.8
Cd	<0.25	<0.25	<0.25	<0.25	<0.25
Cr	1.2	<0.5	3.4	1.5	<0.5
Pb	<0.5	<0.5	0.59	<0.5	<0.5
Hg	<0.002	<0.002	<0.002	<0.002	<0.002
Se	0.52	<0.5	<0.5	<0.5	<0.5
Ag	<0.5	<0.5	<0.5	<0.5	<0.5

Table 13. Maximum RCRA Leachate Concentrations Assuming a 20:1 Dilution in Water, mg/L

Wastewater Chloride Level	CTB Low	CTB Low	CTB Medium	APW Medium	APW High	
Date	6/23/2021	7/23/2021	9/1/2021	9/9/2021	9/16/2021	Regulatory Limit
As	0.090	0.090	0.20	0.17	0.19	5
Ba	0.37	1.86	5.35	4.06	2.24	100
Cd	<0.012	<0.012	<0.012	<0.012	<0.012	1
Cr	0.060	<0.02	0.17	0.075	<0.02	5
Pb	<0.02	<0.02	0.029	<0.02	<0.02	5
Hg	<0.0001	<0.0001	<0.0001	<0.0001	<0.0001	0.2
Se	0.026	<0.02	<0.02	<0.02	<0.02	1
Ag	<0.02	<0.02	<0.02	<0.02	<0.02	5

The second evaluation of leaching characteristics was provided by GRE and included synthetic leaching measurements according to EPA Method 1311 for precipitate samples generated during APW testing. These results are summarized in Table 14, and the laboratory report is included in Appendix C. As with the maximum leachate estimates in Table 13, none of the regulated elements approach levels of concern, suggesting that these solids would be classified as nonhazardous for disposal purposes.

In addition to hazardous waste determination, another criterion for evaluating landfill disposal is free liquid content, which is commonly evaluated by the paint filter test, EPA Method 9095B. This test provides a binary indication of the presence of free liquid based on whether any liquid is released from the sample under evaluation and drips through a coarse filter within a 5-minute observation period. Figure 18 shows a waste solids sample being loaded for paint filter evaluation at the EERC.

Table 14. TCLP Results for Precipitate Samples from Field Testing, mg/L

Wastewater Chloride Level Date	APW High 9/28/2021	Regulatory Limit
As	<0.2	5
Ba	<1	100
Cd	<0.1	1
Cr	<0.5	5
Pb	<0.1	5
Hg	<0.01	0.2
Se	<0.2	1
Ag	<0.2	5

Figure 18. Paint filter test set up at the EERC.

Several precipitate samples collected across the time frame of field testing were evaluated using the paint filter test under both as-collected and decanted conditions. As-collected conditions meant that, prior to paint filter testing, the sample was stirred to incorporate any free liquid that separated during storage while the decanted measurements separated any free liquid and evaluated only the settled solids. During field testing, precipitate samples were generally collected soon after they were separated from the working fluid before much settling could occur. These samples, therefore, represent the solids concentration achieved solely by the hydrocyclone whereas the decanted conditions represent hydrocyclone separation followed by a step of gravity settling.

The paint filter test results are summarized in Table 15, where the key observation was that the as-collected samples universally contained enough free liquid to fail the paint filter test while the same samples passed if they were allowed to settle overnight and had the free liquid decanted. Quantitative measurements of the solids content for these passing and failing conditions are also included in Table 15. While there is overlap in the range of solids content between failing and passing samples, the average failing sample had 51.7% solids, and the average passing sample had 58.2% solids content.

Table 15. Waste Solids Paint Filter Test and Solids Content Results

Makeup Water	Chlorides	Date	As-Collected Conditions		Decanted Conditions	
			Paint Filter	Solids, wt%	Paint Filter	Solids, wt%
CTB	Low	6/24/2021	Fail	45.60	Pass	52.86
CTB	Low	7/14/2021	Fail	54.50	Pass	61.83
CTB	Medium	8/17/2021	Fail	50.68	Pass	59.38
CTB	Medium	8/31/2021	Fail	48.64	Pass	53.75
APW	Medium	9/7/2021	Fail	50.39	Pass	57.95
APW	Medium	9/9/2021	Fail	54.04	Pass	60.06
APW	High	9/15/2021	Fail	58.18	Pass	61.35
			Average	**51.7**	**Average**	**58.2**

The measured bulk density for several as-collected precipitate samples averaged 1.5 g/cm^3. The bulk density of the decanted passing waste solids was estimated to be about 3% higher using the average solids content of the failing and passing wastes, 51.7% and 58.2%, respectively.

Precipitate Particle-Size Distribution

Particle-size distribution measurements for the suspended and separated solids were made on-site during field testing. These measurements documented a change in the precipitated solids over time, which is illustrated by the daily average measurements in Figure 19 for two indicative field test days. Data from August 17, 2021, correspond to medium chloride concentration with CTB makeup, while September 9, 2021, was also at a medium chloride concentration but with APW makeup. Both suspended solids profiles show peaks centered near 2.7 and 4.5 μm, but the September 9 distribution had also developed a concentration centered near 23 μm. The difference is believed to be related to the loading of dissolved solids into the hygroscopic tower, which was roughly doubled after switching from CTB to APW. This hypothesis was based on differences between the daily averages for all CTB samples in Figure 20 and all APW samples in Figure 21.

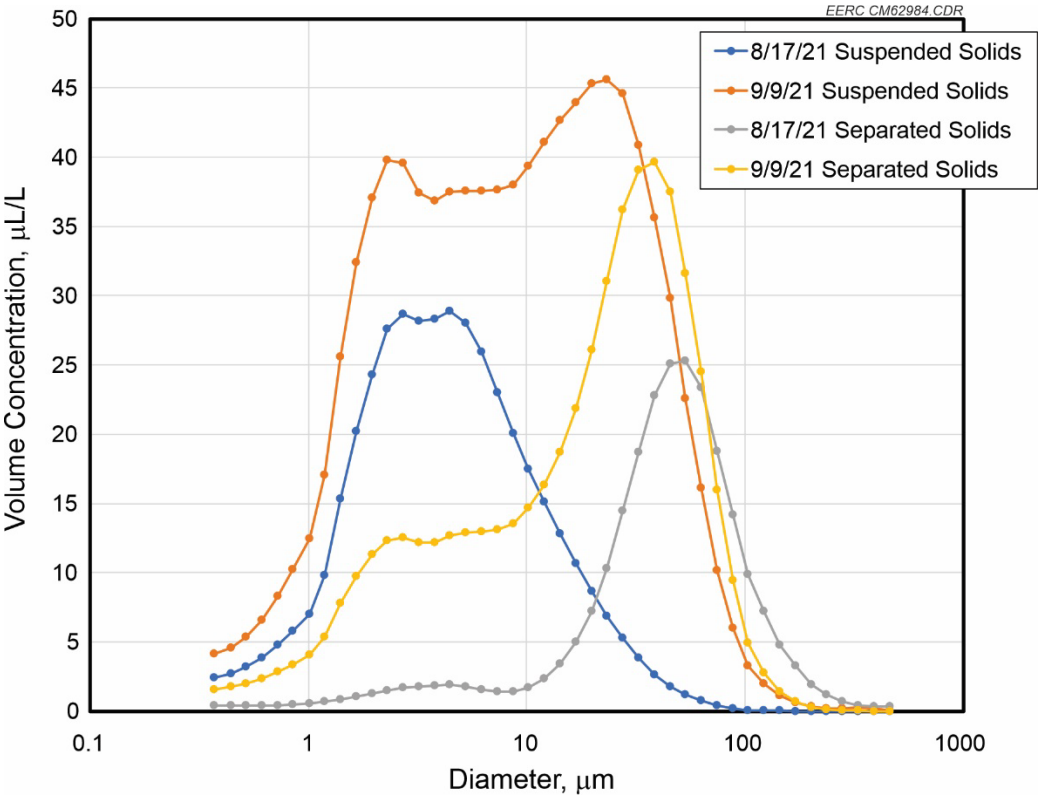

Figure 19. Representative particle-size distributions for working fluid precipitates.

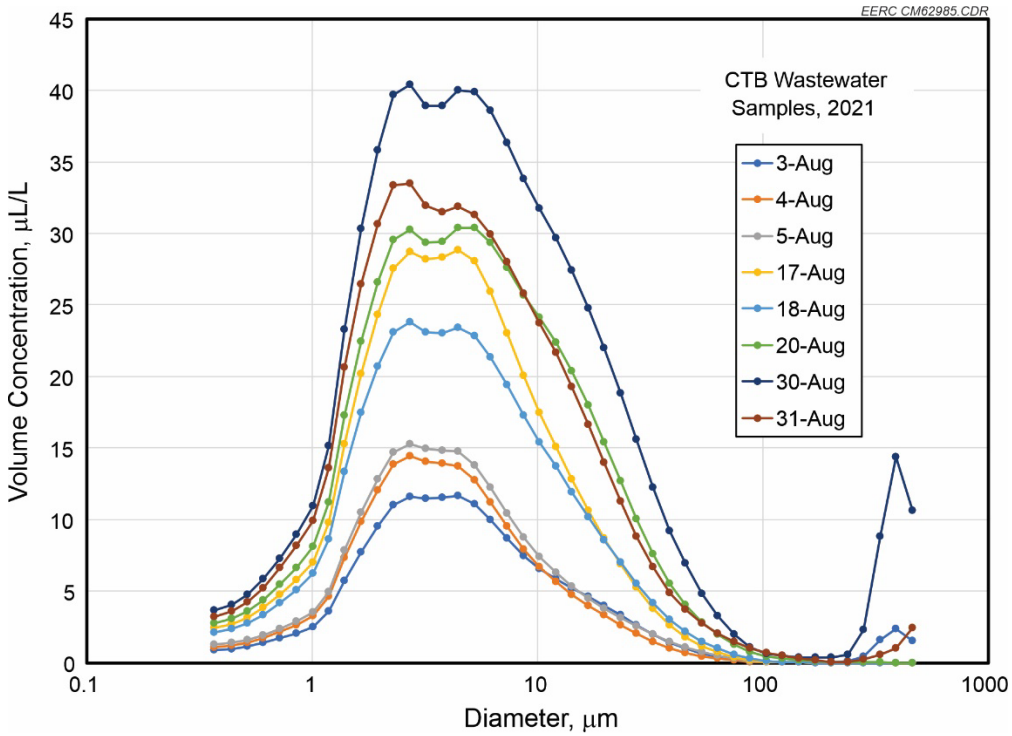

Figure 20. Daily-averaged suspended solids size distributions with CTB wastewater.

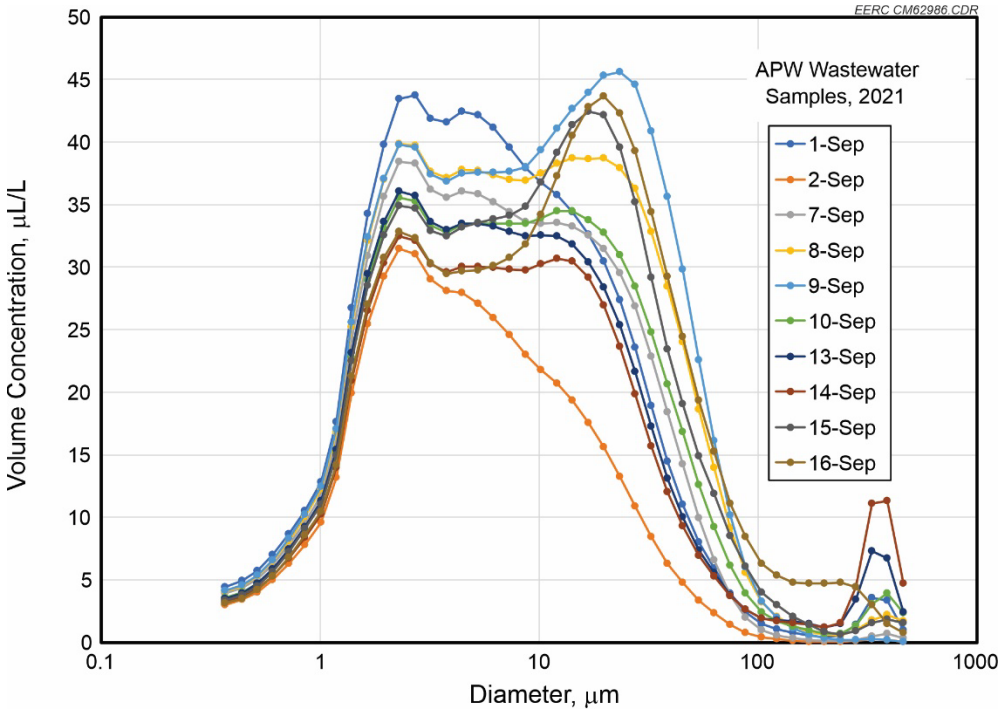

Figure 21. Daily-averaged suspended solids size distributions with APW wastewater.

Figures 19, 20, and 21 were interpreted as showing the effect of dissolved solids loading from the two different wastewater sources. During the lower TDS loading with CTB, the separated solids appear as a distinct population from the bulk suspended solids in Figure 19, while for the APW samples, the suspended particle sizes have grown to fully encompass the size of the separated solids. This observation suggests that the rate of particulate separation with CTB may have been adequate to control the size distribution of circulating particulates, but the rate was perhaps too slow with APW since it is likely that particles larger than those captured in the suspended solids sample simply settled out of the fluid before passing through the hydrocyclone. Indeed, it was noted during field testing that the hydrocyclones appeared less effective, i.e., extracted fewer solids, with APW than they did with CTB, despite the approximate doubling of TDS input. Furthermore, cleanup of the cooling tower after testing revealed an accumulation of solids in the cooling tower basin, suggesting that the majority of precipitation with APW took place in the cooling tower and that after growing in mass in the tower, the largest of the particulates could no longer stay entrained and were separated by settling in the basin.

Microbiological Activity

Limited samples of microbiological activity were conducted to confirm previous observations that the reduced water activity of the hygroscopic working fluid can restrict the proliferation of microbes. Samples were collected while processing APW under medium and high working fluid concentrations and the results are summarized in Table 16. Slide images are provided in Appendix A. Overall, the results for bacteria colonization show that the hygroscopic working fluid had either the same or fewer active colony forming units (cfu). However, the fungi results show that only the hygroscopic fluid had active growth, albeit at a low concentration of 10 cfu/mL, which is categorized as under control.

Table 16. Dip Slide Microbiological Results with APW, cfu/mL

	48-hr Bacteria			96-hr Fungi
Sample Date	9/7/21	9/13/21	9/14/21	9/13/21
Chloride Concentration	Medium	High	High	High
Hygroscopic Working Fluid	1000	<100	1000	10
Coal Creek Cooling Water	1000	10,000	1000	<10
Coal Creek Ash Pond Water	10,000	100,000	10,000	<10

Corrosion Coupons

The corrosion coupons were recovered after field testing and returned to the vendor for cleaning and loss in weight determination. Averaged results are shown in Table 17 and are color-coded based on the severity of mass loss indicated (individual coupon results are included in Appendix D). Recommended alloys appear to be standard 316 stainless steel, the higher performing duplex stainless steel alloy 2205, and titanium. Silicon bronze is a common fastener upgrade material with cooling towers; however, its corrosion rate was marginal under the test conditions. The aluminum alloy was severely affected by constant immersion in the working fluid.

Table 17. Averaged Corrosion Coupon Results, mil/yr

	Location		
Material	**Spray Zone**	**Immersed**	
316L (stainless steel)	0.0434	0.0497	
2205 (duplex SS)	0.0250	0.0236	
TI-5 (titanium)	0.0212	0.0513	
CDA651 (silicon bronze)	0.2314	0.3401	
AL2024 (aluminum)	0.1093	0.6768	

Corrosion Rate Categorization	
<0.1	Excellent
>0.1 to 0.2	Good
>0.2 to 0.3	Fair
>0.3 to 0.5	Poor
>0.5	Unacceptable

These corrosion coupon results are only the first step in a complete material selection evaluation and are useful primarily as a way to eliminate potential candidates from subsequent screenings. For this project, these results are used to base TEA sensitivity studies for the materials that passed this initial screening.

Foaming Evaluation

Working fluid samples collected from field testing were evaluated for their foam-forming tendencies using a test protocol adapted from ASTM D892. The full procedure is described in Appendix B. Example images from testing minimum and maximum foaming samples are shown in Figure 22. The foaming evaluation took place several months after the conclusion of field testing, yet the samples still showed clear differences in foaming potential after the extended equilibration time. This behavior suggests that the root cause(s) are inherent to the working fluid composition and not from a transient of operation.

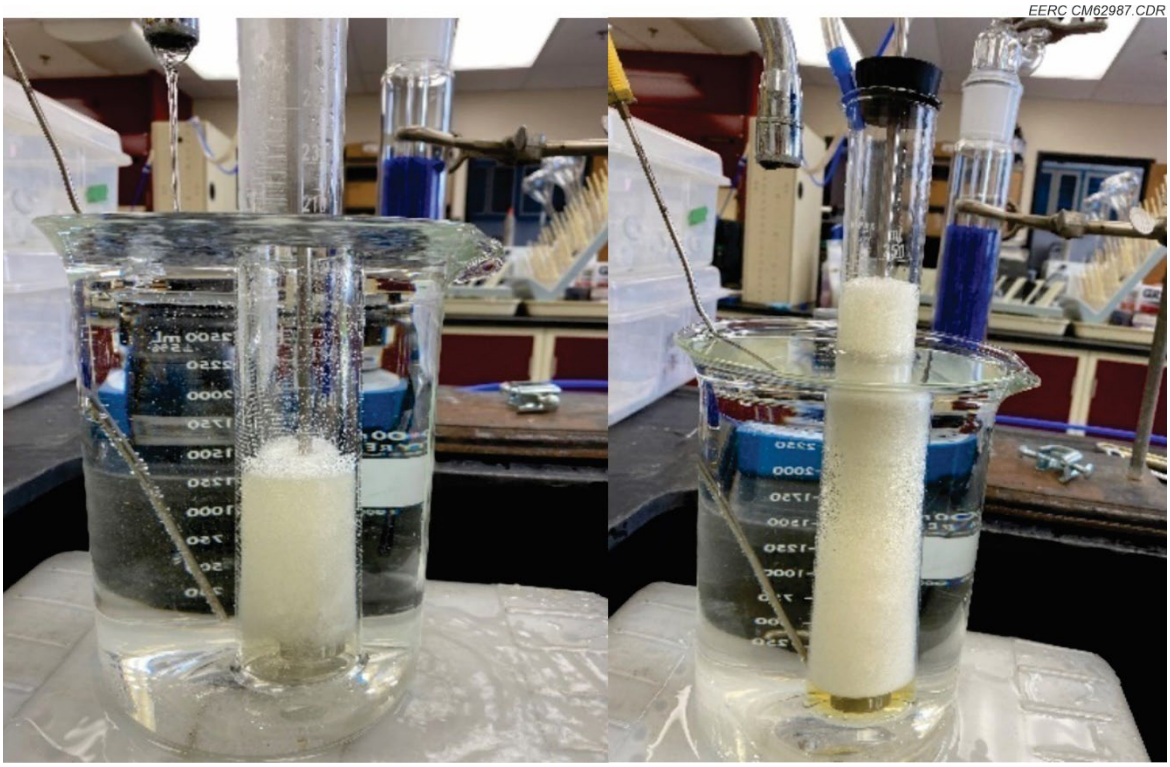

Figure 22. Left: working fluid from July 14, 2021, showing a minimal foaming tendency and right: September 14, 2021, sample reaching the maximum measurable foam production.

Measured foaming test volumes are summarized in Figure 23 as a function of the measured TDS value for each working fluid sample. The data appear to show a strong, albeit discontinuous, correlation of foaming tendency with increasing TDS content. The step change in foam at the end of nitrogen flow around 250,000 mg/L TDS corresponds to the transition between CTB and APW while the step change in stable foam after 10 minutes at approximately 400,000 mg/L TDS corresponds to the final adjustment of the working fluid concentration between medium and high chloride concentrations. While TDS content is certainly an indicator of foaming tendency, the fact that step changes were observed over relatively small changes in TDS indicates a possible species-specific driver, but none has been clearly identified that would apply to both instances.

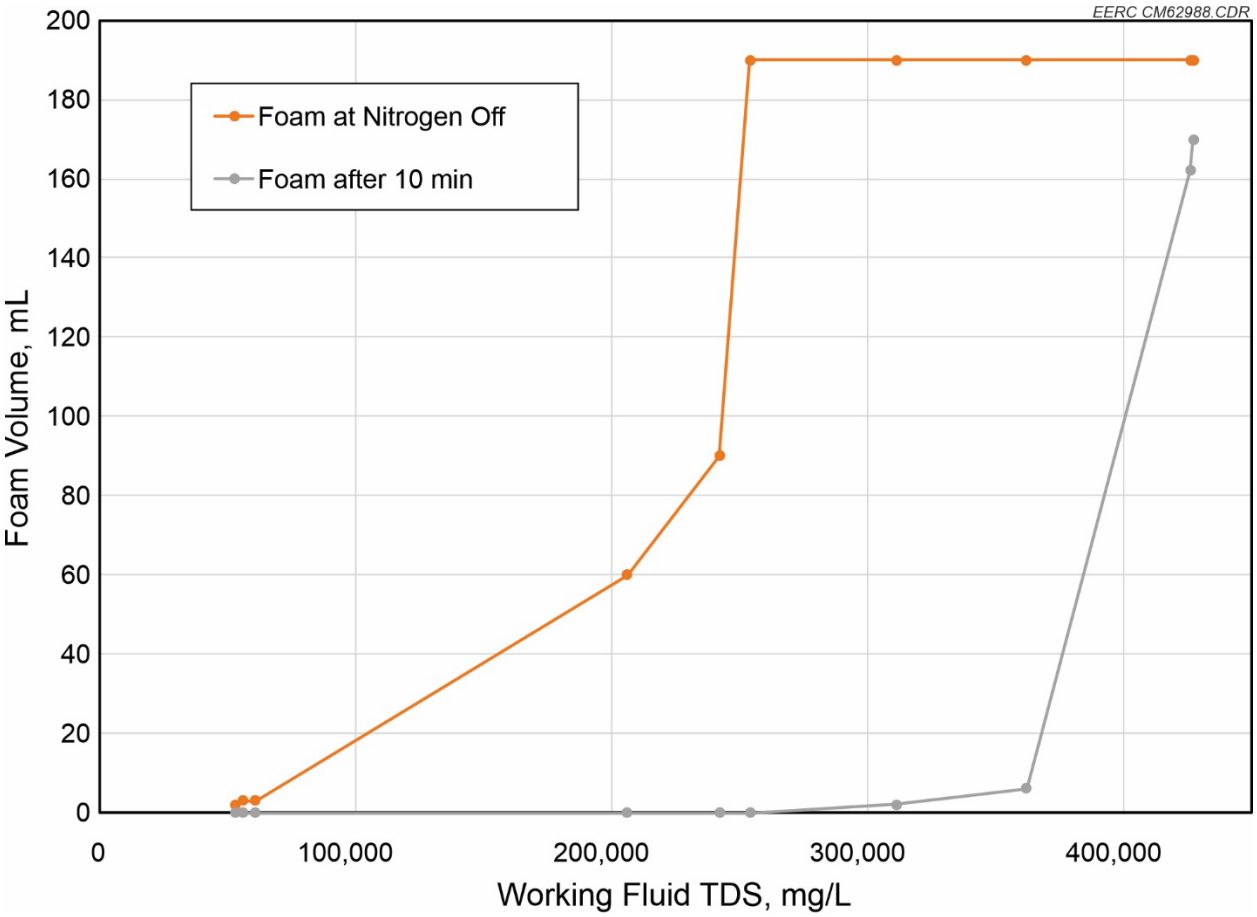

Figure 23. Foaming test results with samples of the working fluid.

Observed consequences of excessive and stable foam formation included difficulty managing liquid level in the cooling tower and having excessive carryover of foam into the drift eliminators. As a stable layer of foam built up in the cooling tower basin, it altered the buoyancy of the level valve float to the point that it no longer rested on the liquid surface, which reduced the liquid depth in the basin and the suction head pressure of the main circulation pump. A temporary solution to complete testing was to begin regulating liquid level using a level sight tube instead of relying on the float valve.

Another key impediment with foam formation was that the foam would become entrained in the air stream and be carried into the drift eliminator at the tower exhaust. Unstable foam appeared to decompose and allow the liquid to drain back, but stable foams would eventually fill air channels in the drift eliminators and could be pushed out of the tower entirely into the exhaust air stream. Aside from being a potential source of air emissions, the foam also appeared to be a transport mechanism for depositing solids on the drift eliminators.

Tested antifoam compounds discussed in Appendix B were effective but had a high consumption rate. The preferred alternative for low-cost, sustainable operation appears to be limiting working fluid concentration to avoid stable foam formation.

Another observation that could also have been foaming-related was the cavitation tendency of the main circulation pump, the frequency of which increased further into the field testing in an analogous manner to the foaming trend in Figure 23. During testing, these issues were attributed to precipitates accumulating in the basin and periodically blocking the pump suction port. However, in hindsight, it is possible that flow interruptions from cavitation may have increased the likelihood of particulates settling in the basin, creating negative performance feedback. Regardless of whether foaming led to cavitation and/or particulate settling, the best correction appears to be placing a limit on working fluid concentration since operations were much more predictable earlier in the field testing.

Heat-Transfer Surface Fouling Potential

The measured inventory of seed particulates in Figures 19, 20, and 21 appeared sufficient to prevent fouling of the heat exchange coil during any individual segment of operating time, which was always limited to a single day. The daily averaged values of the coil heat-transfer coefficient during APW testing are shown in Figure 24, along with uncertainty bars showing one standard deviation in the measured data. According to the figure, the day-to-day variations in the heat-transfer coefficient generally exceeded the standard deviation observed during each day, which suggest the heat-transfer coefficient was more impacted by starting and stopping operation rather than continuous run time. While most of these impacts were recognized by the time of APW testing, fouling and heat-transfer reduction were observed to worsen overnight during CTB shakedown. After shutdown procedures were reviewed, it was noted that hot condenser water flow through the hygroscopic tower's coil either continued after the circulation of hygroscopic working fluid or both flows were shut off at nearly the same time. It is believed that this practice allowed particulates to be "baked on" the coil as its surface dried out. After these observations, shutdown was changed so that the coil flow was stopped well in advance of the working fluid spray and that the entire mass of the coil and tube water was cooled down. A further step was sometimes employed where the cooled coil was then manually rinsed with CTB.

Since the shutdown procedures were modified prior to APW testing, the suggestion of heat-transfer coefficient degradation in Figure 24 was more likely due to the deteriorating spray flow as the working fluid became more concentrated rather than from fouling of the coil's exterior surface. Based on visual observation of the coil, surfaces that were cleaned after the initial shakedown fouling and that received adequate spray flow remained clean during the remainder of field testing.

TECHNO-ECONOMIC ANALYSIS

Performance Model

The performance model used for the TEA is based on a streamlined version of the pilot unit used for field testing and is diagrammed in Figure 25. Compared to the P&ID in Figure 3, the TEA performance model omits the mixing and settling vessels since field testing showed that precipitate growth occurred rapidly and that many of the solids appeared to settle in the cooling tower basin before being transported to the tanks.

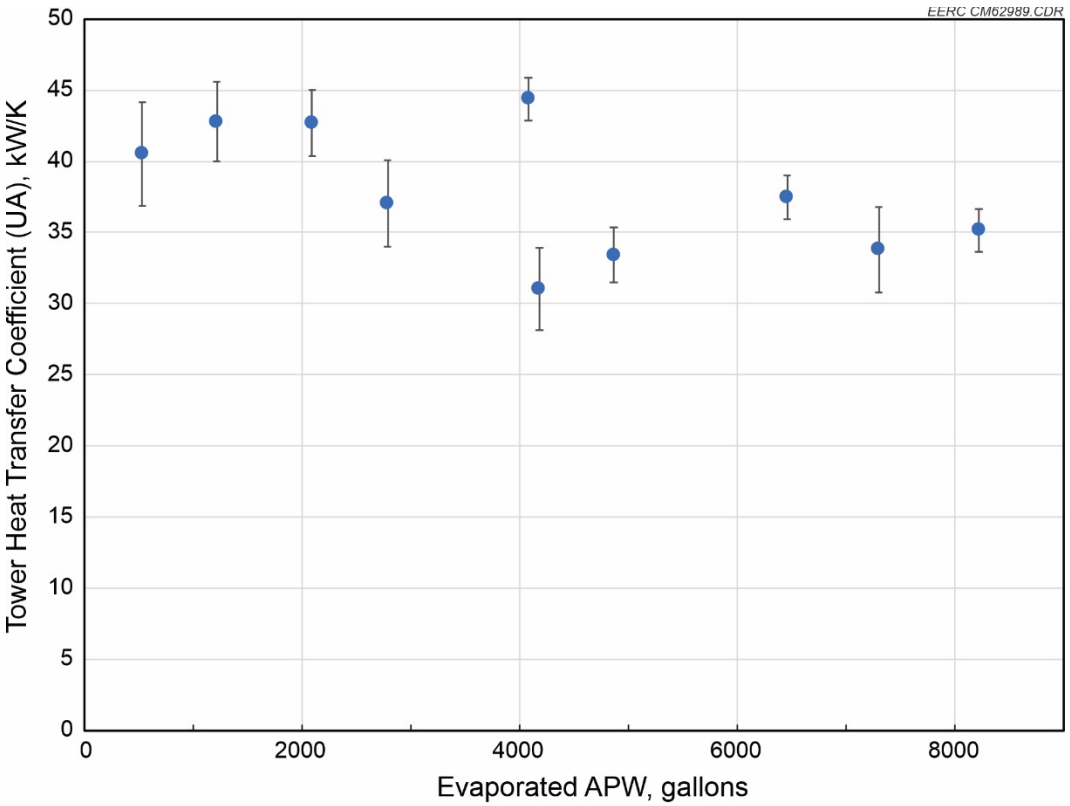

Figure 24. Measured daily average heat-transfer coefficient for the hygroscopic cooling tower during APW testing. Error bars indicate the standard deviation for each day.

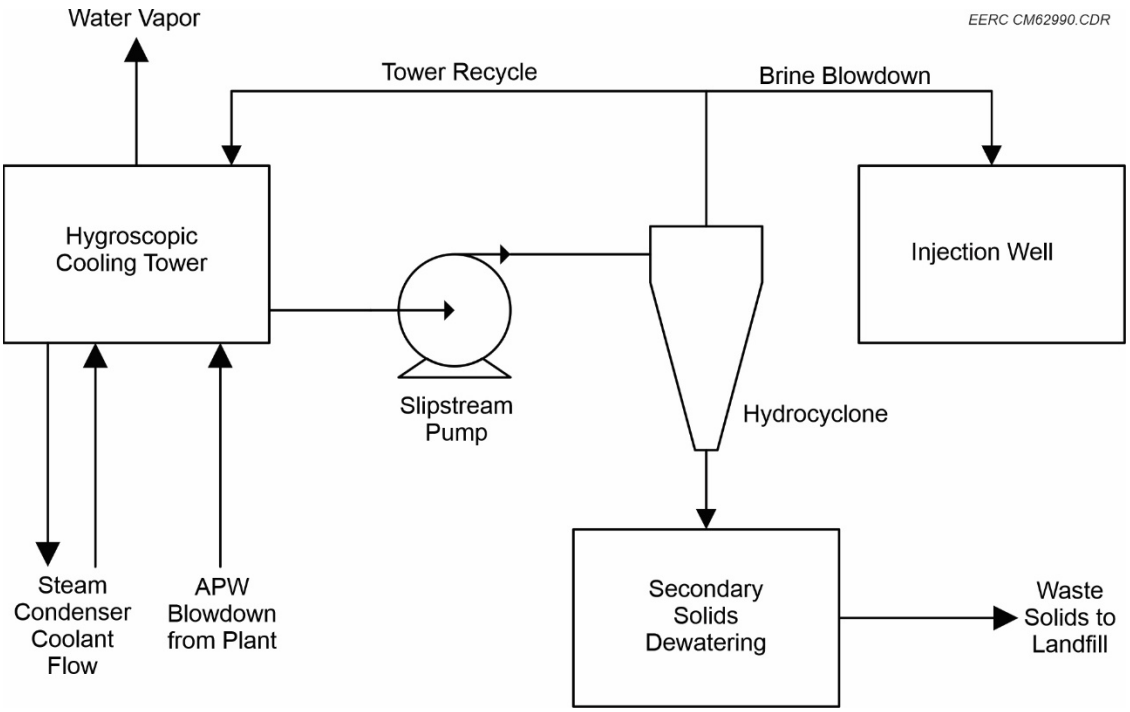

Figure 25. Included model components for the TEA.

The other key difference from the P&ID is that the performance model in Figure 25 includes a dewatering step beyond the hydrocyclone separator. This addition is based directly on the solids characterization testing that showed additional dewatering was necessary beyond the as-collected conditions for the waste solids to pass paint filter testing. In the TEA, two alternatives for final dewatering of the solid waste were considered: a gravity dewatering bin based on letting the separated precipitates gravity-settle for 24 hours followed by decanting free liquid and a solids screw press that speeds dewatering by using mechanical force to compress the precipitate and force out a higher fraction of the interstitial liquid. The dewatering bin is analogous to the arrangement used during field testing; it is simple with low-power requirements but is inherently an intermittent, batch process. The solids press concept was not tested during the project but was added to the TEA to evaluate the trade-offs of a continuous, but powered, dewatering process.

Steady-state operation of the hygroscopic cooling tower is reached when the inflow of dissolved solids with the makeup wastewater is balanced by their outflow in the waste solids stream, either as solid precipitates or as a dissolved component in the concentrated working fluid. Field testing explored three levels of working fluid concentration, with the highest selected to correspond to a ZLD scenario where no liquid blowdown was allowed and all dissolved species were forced to precipitate. However, as discussed with the field test results, operation at this concentration level introduced several complications including severe foaming of the working fluid.

Since the field test results suggest that true ZLD operation might not be practical with hygroscopic wastewater recycling, a working fluid concentration limit was assumed when conducting the TEA. This limit meant that the hygroscopic system would produce both a solids waste stream and a blowdown of concentrated working fluid as a necessary compromise for sustainable operation. PHREEQC modeling results shown in Figure 26 were used to estimate the steady-state working fluid concentration over a range of solids content in the combined hygroscopic tower waste stream, i.e., including both the separated solids and a liquid blowdown to limit TDS. As the solids content of the waste increases, so does the dissolved solids content of the working fluid in order to maintain a steady-state mass balance. The inflection peak near 50% solids is the point at which more soluble sodium sulfate and magnesium sulfate species begin to precipitate, according to the PHREEQC model.

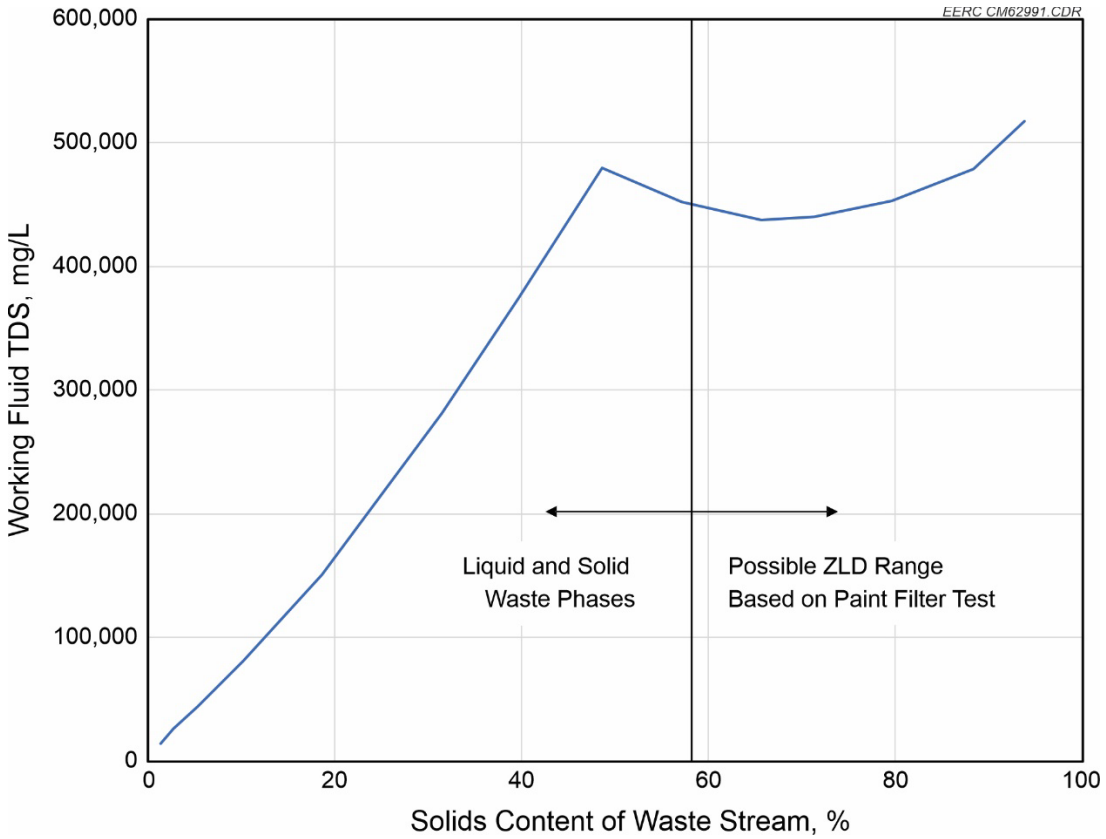

Figure 26. Calculated steady-state values of working fluid TDS level as a function of the solids content of the combined brine and solids waste stream.

The vertical dividing boundary shown in Figure 26 between having both liquid and solid waste phases and solid-only ZLD has been placed at the average solids content (58.2%) for field samples that passed the EPA paint filter test. At this solids concentration and greater, the resulting waste would be expected to pass the paint filter test and leave only solid material for disposal. However, below this threshold solids content, the material is likely to fail the paint filter test, resulting in disposal of a liquid phase in addition to the solid. According to the modeling, and as generally confirmed by the working fluid analysis, to achieve ZLD requires highly concentrated working fluid with a TDS of approximately 450,000 mg/L.

Since the hygroscopic cooling tower avoided many of the observed operational issues while using a lower concentration working fluid, a working fluid TDS cap of 200,000 mg/L was assumed for the TEA. This assumption meant that the hygroscopic recycling system would act as a wastewater concentrator rather than a complete ZLD system. Working fluid properties at the 200,000 mg/L cap needed for the TEA were derived from PHREEQC modeling; these included a density of 1150 kg/m^3 and a water activity of 0.92. With that activity, the wet-bulb approach temperature trend of the hygroscopic tower falls between the factory data trend and that measured for the 0.8 water activity grouping in Figure 14. For a nominal cooling load of 350 kWth with the pilot unit, the interpolated wet-bulb approach temperature of the hygroscopic tower was estimated at 7.3°C (13.1°F), only 1.3°C (2.3°F) above the approach with pure water.

Field-based performance data were used to derive operating metrics for wastewater recycling with hygroscopic cooling. The metrics and notes about how they were derived are provided in Table 18. All values have been normalized on a unit volume (m^3) of APW feed basis. While both CTB and APW were tested during field testing, APW was the focus of the TEA because of its relevance as Coal Creek Station's ultimate disposal stream.

The recycled wastewater cooling capacity in Table 18 represents the quantity of heat dissipated by the hygroscopic system from the plant's condenser cooling circuit, and it is based on the experimental average ratio of evaporative heat transfer in the hygroscopic tower relative to the total heat load dissipated by the tower. While a constant value has been assumed for the TEA, in reality, the evaporative heat-transfer fraction will vary over a limited range with variations in working fluid concentration and ambient air conditions.

Table 18. Operating Metrics for the Techno-Economic Model of Hygroscopic Cooling

	Values per m^3 of APW	
Metric	**Input**	**Basis**
Recycled Wastewater Cooling Capacity	2.78 GJ	Based on the measured average ratio of 0.85 evaporative to total heat transfer in the hygroscopic tower
Working Fluid Blowdown to Maintain 200,000 mg/L TDS	0.0540 m^3	Mass balance assuming
Waste Solids, Gravity Dewatering Bin	6.59 kg	Assumes APW composition and a settled solids content of 58%
Waste Solids, Screw Press	4.56 kg	Assumes APW composition and a pressed solids content of 84%
Specific Electrical Energy Consumption, Gravity Dewatering Bin	42.8 kWh	Pilot unit electrical rating normalized by the average throughput
Specific Electrical Energy Consumption, Screw Press	44.2 kWh	Pilot unit electrical rating plus screw press allowance
Fresh Makeup Water Displaced by Recycling	0.97 m^3	Heat of vaporization ratio for the concentrated working fluid to fresh makeup water

All TEA scenarios assumed a liquid blowdown stream to regulate the working fluid's dissolved solids at a concentration of 200,000 mg/L, which was judged to avoid the formation of a stable foam that was observed during field testing and confirmed with follow-up laboratory testing. Since TDS was not regulated during field testing, the magnitude of the blowdown stream for the TEA was estimated from a mass balance of incoming dissolved material in the wastewater balanced by the liquid blowdown and solid streams.

Two waste solids production values are provided in Table 18, one for each dewatering approach included in the TEA. The mass difference between the two rates represents the additional liquid removed by the screw press relative to simple gravity settling. The screw press was not tested for its actual dewatering effectiveness; instead, the assumption regarding liquid removal from the pressed solids was based on an estimate provided by an equipment vendor. Both solid waste streams were assumed to be sufficiently dry to pass the EPA paint filter test and were assumed to go to a landfill for disposal. Similar to solids mass flow, two electrical ratings are provided with one corresponding to gravity dewatering and the other that includes screw press power consumption.

The remainder of electrical power consumption by the hygroscopic tower was the same for both solids dewatering options and primarily consisted of fan and pump power. Both values were based on the specific power consumption of the pilot unit, for which fan power was over 75% of the electrical power consumption. Some decrease in specific fan power would be expected if the system were scaled to larger sizes and the test units forced-draft, centrifugal fan were replaced with an induced-draft, propeller fan typical of large cooling towers.

Costing Model

The costing model is based on a component-level estimate of the capital costs for a hygroscopic wastewater recycling system shown in Figure 25. Table 19 outlines the capital cost methodology for each major component. The hygroscopic cooling tower cost was estimated as the combination of two subcomponents: the heat exchange coil and the chassis that contains the basin, fan, air ducting, spray piping, spray pump, drift eliminator, and level control system. Total tower cost was corroborated with costs prepared for the pilot unit and scaled to a maximum single module size using a scaling exponent recommended for cooling towers (Woods, 2007). Larger hygroscopic tower sizes were based on modular units having an individual cooling capacity up to 8.8-MW$_{th}$ cooling capacity (roughly a 2000-ton conventional cooling tower rating). The other system components were costed in a similar manner, typically referencing either the cost paid for pilot equipment or a vendor quotation.

Values in Table 19 provided estimates for the equipment cost along with the associated instrumentation, installation labor, and installation materials. In order to calculate a more inclusive total module cost that included typical construction allowances but that excluded contingencies, the factors in Table 20 were used to compute a bare module cost by adding estimated costs for taxes, freight, and insurance and home office and field expenses. Contractor fees were estimated based on the bare module cost, and finally, the total module cost was scaled to a Chemical Engineering Plant Cost Index (CEPCI) value of 600 from the basis of 1000 that the values in Table 19 assumed.

Costing model assumptions regarding operational costs and the time value of money are presented in Table 21. Values for electricity, water treatment, and solids disposal were based on charges at Coal Creek Station. The assumed deep well injection fee of \$3.14/m^3 is equivalent to \$0.50/bbl and was based on regional, non-transportation costs for produced water disposal in western North Dakota (EERC, 2020).

Table 19. Capital Cost Inputs

Item	Equipment Costing Metric	Equipment Scaling Exponent	Alloy Factor	Installation Labor and Materials Factor	Instrumentation per Unit
Hygroscopic Cooling Tower: Heat Exchange Coil	$400/m2 of coil area	0.71	2.4 for 316SS 2.9 for 2205 9.0 for TI-5	2.2	Included with chassis
Hygroscopic Cooling Tower: Chassis	$1200/(L/s) of coil flow	0.64	1	1.22	$27,000
Slipstream Pump	$760/(L/s) of flow	0.59	1	1.47	$7000
Hydrocyclone	$240/cm of body diameter	1.07	1	1.8	$7000
Dewatering Bins	$11,300/$m^3$ of storage volume	0.93	1	2.3	$7000
Solids Press	$4210/(kg/hr) of waste solids	0.67	1	1.32	$7000

Table 20. Costing Factors Used to Derive Total Module Costs

Category	Value
Taxes, Freight, and Insurance	15% of installed equipment
Offsite and Indirect Costs for Home Office and Field Expenses	15% of installation labor and materials
Contractors Fees	3% of bare module cost
CEPCI Basis	600

Table 21. Economic Evaluation Parameters

Parameter	Units	Baseline Value
Plant Electricity Rate	$/MWh	30.0
Makeup Water Treatment	$/$m^3$	0.0765
Liquid Blowdown Deep Well Injection	$/$m^3$	3.14
Landfill Solids Disposal	$/metric ton	27.5
Maintenance Costs	% of capital	2.5
Annual Capacity Factor	–	0.8
Operating Life	yr	20
Investment Rate	%	3.0

Analysis

Baseline Scenario – Coal Creek Station

The baseline scenario assumed the hygroscopic system received APW and hot condenser water from Coal Creek Station. The site has a nominal need for 114 m^3/hr (500 gpm) of plant blowdown disposal and has nominal condenser cooling water range of 46°–29°C (115°–85°F). The volume flow requirement was used with the operating metrics in Table 18 to calculate the mass and energy flows shown in Table 22. Using the 2.78 GJ/m^3 metric in Table 18 leads to a total cooling capacity estimate of 314 GJ/hr or 73.9 MW_{th}, and given the 8.8 MW_{th} module size limit, means that nine hygroscopic cooling tower modules would be required.

Table 22. Sizing Results for Coal Creek Baseline Scenario

Parameter	Dewatering Bin Configuration	Solids Press Configuration
Wastewater Consumption Rate, gpm (m^3/hr)	500 114	
Cooling Capacity, MW_{th}	87.7	
Displaced Freshwater, gpm (m^3/hr)	484 110	
Displaced Fan Power, MW_e	1.87	
Waste Streams Concentrated Brine, m^3/hr (gpm) Landfilled Solids, metric ton/hr (ton/hr)	6.14 (27.0) 0.75 (0.82)	6.14 (27.0) 0.52 (0.57)
Energy Consumption, MW_e	4.87	5.02

Slipstream flow was assumed to be handled in aggregate for all towers, with each contributing 5% of its circulation rate for a total flow of 160 L/s (2500 gpm). Hydrocyclones were based on multiple units with a 5-cm body diameter to achieve the desired separation. According to manufacturer-provided data, this separation task would require 100 individual units for costing purposes. In an actual system design, alternatives would be evaluated that could meet the particle separation and total flow requirements but with a more optimal (i.e., fewer) number of units. The screw press dewatering option was straightforward to size based on the calculated throughput of waste solids while the dewatering bin option required determining the whole number of 25 yd^3 (19 m^3) settling bins required to continuously provide 24 hours of settling time. A rotation of five dewatering bins was determined for the baseline Coal Creek scenario. A breakout of the capital costs for the baseline scenario is shown in Table 23. Operating cost inputs to determine the LCWD for the baseline scenario are summarized in Table 24.

Table 23. Hygroscopic System Capital Cost Estimates for the Baseline Scenario

Total Module Costs	Costing Basis	Dewatering Bin Configuration	Solids Press Configuration
Hygroscopic Cooling Tower	Nine 8.8 MW_{th} units	$29,600,000	
Slipstream Circulation Pump	158 L/s total flow	$59,300	
Precipitate Hydrocyclones	100 5-cm body hydrocyclones	$644,000	
Solids Dewatering Approach	5 19.1-m^3 dewatering bins	$1,540,000	2,020,000
Total System Capital		$31,800,000	$32,300,000
Normalized Capital Cost for 500 gpm APW		$63,600/gpm	$64,600/gpm
Injection Well Development	$1,500,000 for Bakken-area disposal well and $1,000,000 for surface facilities	$2,500,000	

Table 24. Hygroscopic System Operating Costs for the Baseline Scenario, $/yr

O&M* Cost or Credit	Dewatering Bin Configuration	Solids Press Configuration
Hygroscopic Power Consumption	$1,020,000	$1,060,000
Brine Disposal	$135,000	$135,000
Solids Disposal	$144,000	$100,000
Displaced Plant Fan Power	($394,000)	($394,000)
Displaced Fresh Water	($59,000)	($59,000)
Maintenance	$795,000	$807,000
O&M Total	**$1,640,000**	**$1,650,000**

* Operating and maintenance.

Table 24 includes operational cost reductions at the power plant from hygroscopic wastewater recycling. These included a reduction in the quantity of makeup water required and the estimated fan power reduction from lowering the cooling duty on the plant's main cooling tower. The Coal Creek scenario was modeled as a retrofit addition of hygroscopic recycling, which meant the plant would end up with a net increase in cooling capacity and, assuming the same cooling load, the load applied to the plant's existing towers would be reduced. However, the power displacement was not assumed as one-to-one; instead, it was assumed that the plant's cooling tower fans only required half the power per unit of cooling load as the hygroscopic system to reflect the performance of a higher efficiency fan typical of the full-scale cooling towers at Coal Creek Station.

Baseline LCWD values were calculated to be $3.69/m^3 with dewatering bins and $3.72/m^3 for the solids press; breakdowns for both options are provided in Figure 27 with the underlying values provided in Table 25. As indicated, capital equipment and the maintenance expenses derived from it dominated the LCWD. Electricity cost was also a significant contributor, especially given the relatively low cost for power available at Coal Creek. As for credits, hygroscopic cooling can displace nearly one-for-one fresh water makeup on a volume basis; however, given the low cost of makeup water treatment at Coal Creek, total credit value was dominated by the potential savings in the plant's cooling tower fan power. The comparison further shows that the additional capital cost and operating power for the screw press appear to be largely offset by savings associated with the reduced mass of solids for disposal. As such, the decision to use dewatering bins or a screw press would likely be driven by site-specific factors and operational preference rather than being an opportunity for significant cost optimization.

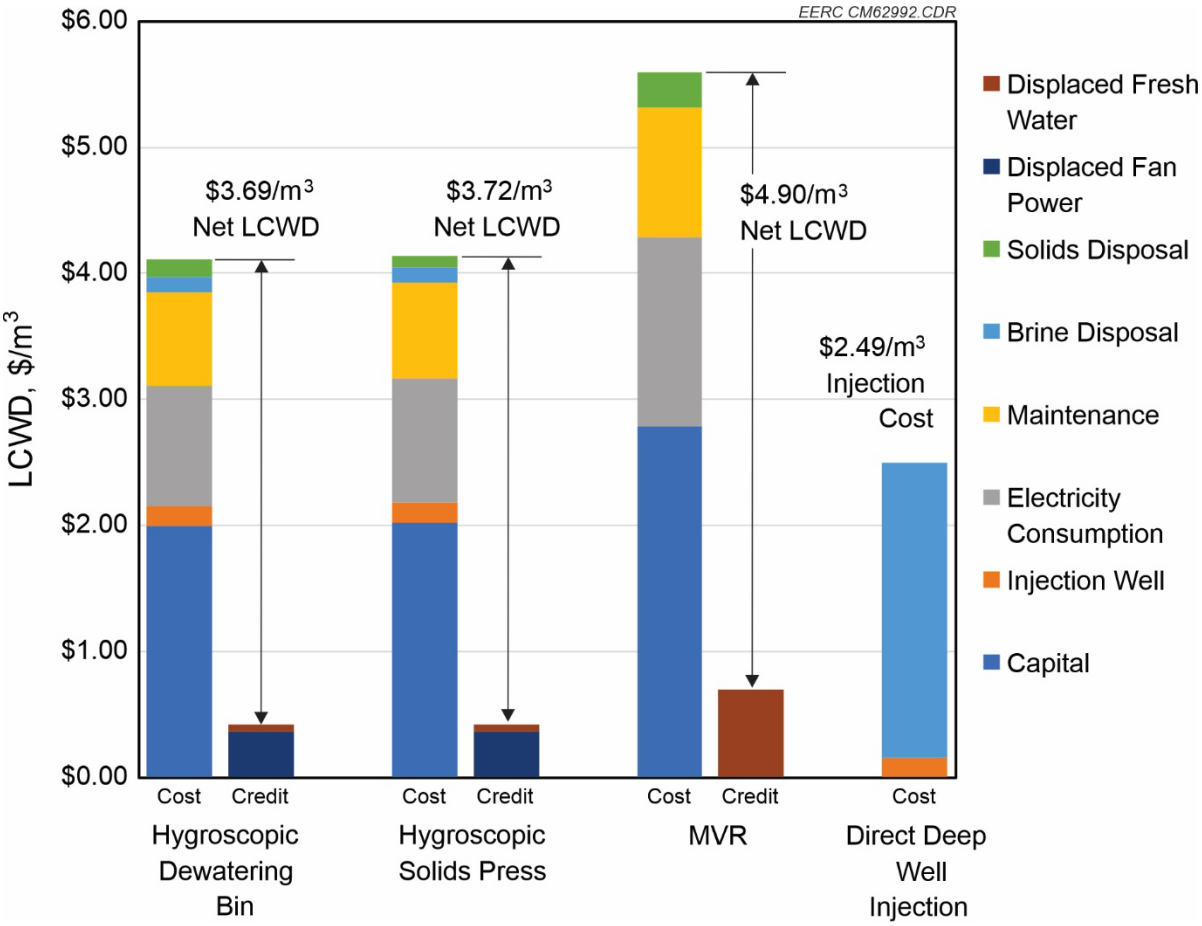

Figure 27. Baseline LCWD breakdowns for the two solids dewatering options.

Table 25. Baseline LCWD Contributing Values for the Evaluated Options, $/m^3 ($/kgal)

Cost/Credit	Hygroscopic Recycling with Gravity Dewatering Bin	Hygroscopic Recycling with Solids Press	Mechanical Vapor Recompression Evaporator	Direct Deep Well Injection
Capital	$2.00 ($7.56)	$2.03 ($7.68)	$2.78 ($10.55)	–
Injection Well Development	$0.16 ($0.59)	$0.16 ($0.59)	–	$0.16 ($0.59)
Electricity Consumption	$0.96 ($3.62)	$0.99 ($3.74)	$1.50 ($5.68)	–
Maintenance	$0.74 ($2.81)	$0.75 ($2.86)	$1.04 ($3.92)	–
Brine Disposal	$0.13 ($0.48)	$0.13 ($0.48)	–	$2.34 ($8.86)
Solids Disposal	$0.13 ($0.51)	$0.09 ($0.35)	$0.28 ($1.07)	–
Displaced Fan Power	−$0.37 (−$1.39)	−$0.37 (−$1.39)	–	–
Displaced Fresh Water	−$0.06 (−$0.21)	−$0.06 (−$0.21)	$0.69 ($2.63)	–
Total LCWD	$3.69 ($13.98)	$3.72 ($14.09)	$4.90 ($18.59)	$2.49 ($9.45)

Mechanical Vapor Recompression Comparison

A comparative case based on a falling film evaporator was also computed for the baseline conditions at Coal Creek Station. With the falling film evaporator, it was assumed that the wastewater would be evaporated to the point of precipitating the dissolved solids and dewatering them sufficiently for landfill disposal (84% solids in the solid waste assumed). Evaporation energy would be provided by a mechanical vapor recompression (MVR) cycle where evaporation takes place under a vacuum created on the suction side of a compressor and the water vapor is recompressed and condensed on the discharge side, releasing its latent heat of evaporation to drive further evaporation on the suction side. Input energy is, therefore, electric power, the quantity of which was estimated by assuming a 1–10 leveraging of input compressor power to latent evaporation energy. Unlike hygroscopic wastewater recycling, a falling film evaporator recovers a high-quality water distillate from the wastewater that can be reused for many purposes at the plant. Given the relatively higher quality of this water stream, a higher water displacement value of $1.05/m^3 ($4.00/kgal) was used to calculate makeup savings. Other O&M costs were calculated using the same assumptions used for the hygroscopic system.

Cost modeling details are summarized in Table 26 for the MVR falling film evaporator. Capital costs were estimated using a similar total module cost approach used for the hygroscopic system costing. The resulting capital cost estimate of $88,700/gpm is roughly 20% lower than the estimate of $110,000/gpm provided by Marlett (2018), but the differences were not investigated.

Table 26. Cost Modeling Inputs for an MVR Falling Film Evaporator ZLD System

Parameter	TEA Assumption	Basis
Electrical Energy Intensity	67.2 kWh/m^3 of APW	10:1 leveraging of input electrical power to thermal energy for evaporation
Distilled Water Recovery	0.94 m^3/m^3 of APW	Mass balance of input APW composition and an assumption of 84% solids content of the waste stream
Waste Solids Production	13.8 kg/m^3 of APW	Mass balance assuming 84% solids content of waste
Capital Equipment	$88,700/gpm of APW	Falling film evaporator scaled to 500 gpm APW baseline scenario (Woods, 2007)

Results for LCWD with MVR were also shown in Figure 27. The LCWD for the evaporator was \$4.90/m^3, which was nearly 40% higher than wastewater treatment with the hygroscopic system. Key differences with MVR are its higher capital and energy costs. As for credit values, the higher-quality water produced by MVR is estimated to be more valuable than the combined credits with hygroscopic recycling but still remains a relatively small contributor to the overall LCWD.

Direct Deep Well Injection Comparison

Hygroscopic wastewater recycling was also compared to disposal-only ZLD in the form of directly injecting plant blowdown without evaporation to reduce its volume. Costing assumptions included \$2,500,000 to drill a disposal well and provide the necessary surface facilities, which was based on typical costs noted for produced water disposal wells in western North Dakota. Injection O&M costs were estimated using the same aggregate value of \$3.14/m^3 (\$0.50/bbl) used for hygroscopic system costing.

Deep well injection results were included in Figure 27 and Table 25 and show a LCWD of \$2.49/m^3, which is nearly 30% lower than hygroscopic recycling. While potentially less costly, deep well injection is predicated on adequate subsurface injection capacity. For sites without adequate capacity or where the available capacity is needed for carbon dioxide sequestration, wastewater volume reduction might become important. With hygroscopic recycling, the volume of wastewater needing injection disposal was reduced to 5.4% of the incoming volume. Finally, as Figure 27 shows, the cost of deep well injection is dominated by O&M costs, which are reported to vary across the Bakken shale play in North Dakota (EERC, 2020). This sensitivity was explored by computing the breakeven cost of injection O&M where the LCWD of direct deep well injection would equal that for hygroscopic recycling. The breakeven value was determined to be \$4.84/m^3 (\$0.77/bbl), to result in a LCWD of \$3.76/m^3.

Sensitivity Studies

Sensitivity studies for each of the key model inputs were conducted to evaluate potential uncertainties with costing wastewater recycling using hygroscopic cooling. Ranges of +/- 50% of the baseline values were used for the studies, and the specific values are tabulated in Table 27. Results for the dewatering bin and the screw press configurations are shown in Figures 28 and 29, respectively.

Table 27. Parameter Ranges Used in the Sensitivity Studies

	50%	Baseline	150%
Electricity, $/MWhr	15	30	45
Tipping, $/metric ton	13.7	27.5	41.2
Wastewater Disposal, $/bbl	0.25	0.5	0.75
Maintenance, % of Capital	1.25	2.5	3.75
Makeup Treatment, $/kgal	0.145	0.29	0.435
Capital – Dewatering Bin, $/gpm	$31,793	$63,586	$95,379
Capital – Solids Press, $/gpm	$32,282	$64,563	$96,845
Investment Rate, %	1.5	3.0	4.5
Wet-Bulb Approach, °F	6.53	13.1	19.6

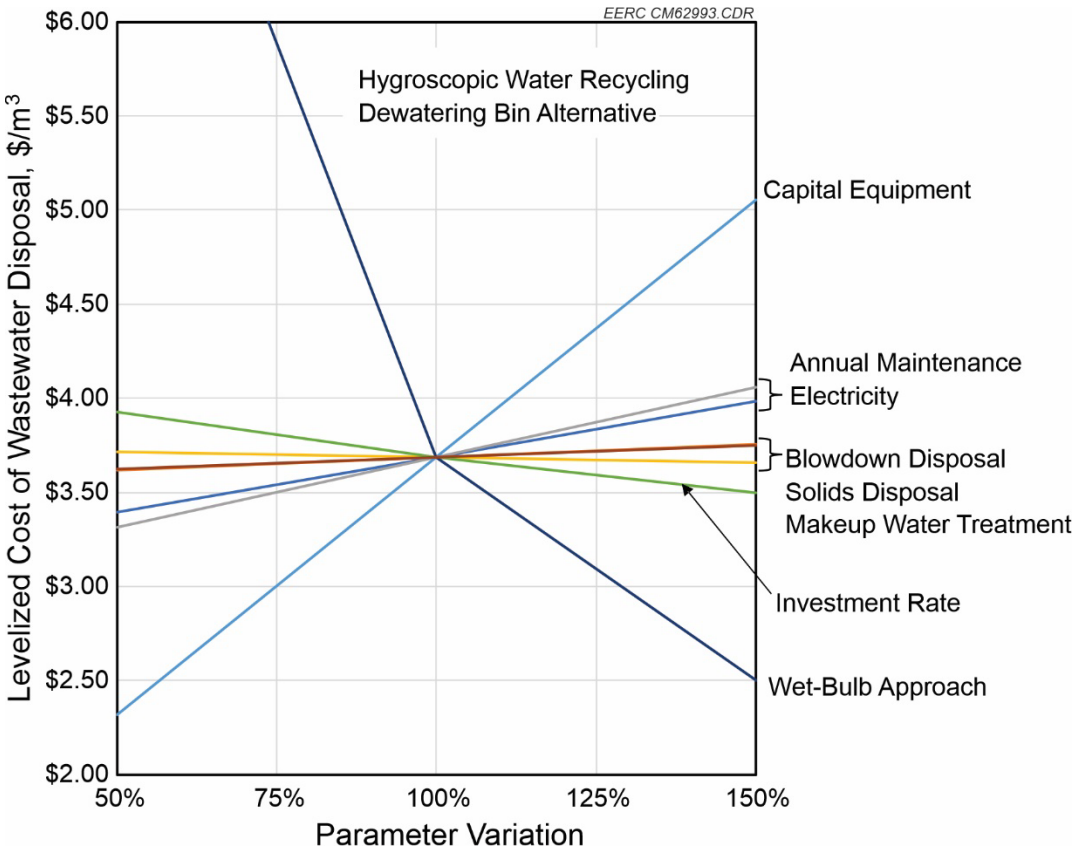

Figure 28. Sensitivity study results for the dewatering bin configuration.

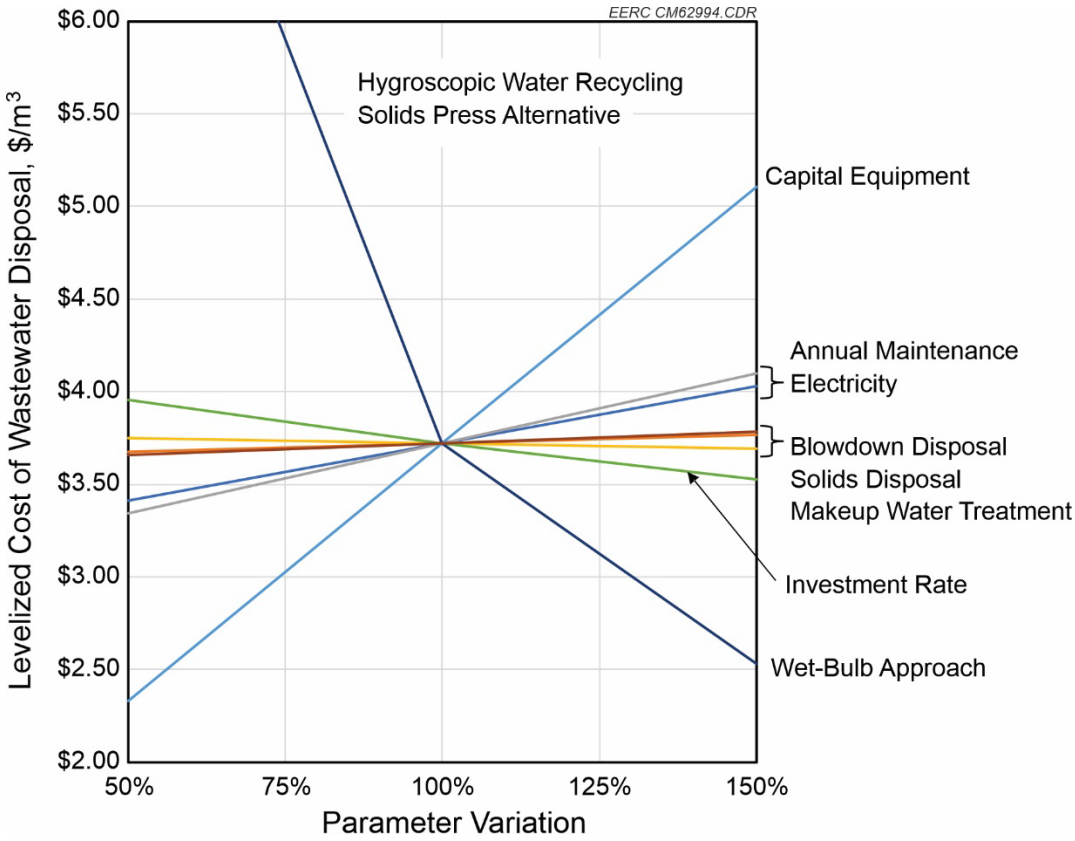

Figure 29. Sensitivity study results for the solids press configuration.

Both studies identify capital cost as the key sensitivity parameter, which is unsurprising given its large contribution to the total cost. Capital expenses could, of course, vary due to changes in design configuration as with any developing technology. However, a key uncertainty with hygroscopic cooling is the choice of compatible materials of construction given the concentrated working fluid's corrosion potential. The bare module method of cost estimation allows for evaluation of the impact of material changes for the cooling tower coil section, which was estimated to represent 57% of the entire cooling tower cost for the baseline material of 316 SS.

Table 19 included alloy costing factors for other materials that might be considered for the coil section, and Table 28 shows the impact to total system capital cost with varying the material of coil construction. The coil in the field test unit was constructed from baseline 316 SS, and as mirrored by the corrosion coupon results of Table 17, it did not suffer from significant surface corrosion during the relatively short duration of field testing. However, the corrosion coupons did not evaluate stress corrosion cracking potential under the test conditions, and this is a key concern for using 316 SS in an elevated chloride environment. The other materials in Table 17 that passed the initial evaluation, 2205 and titanium, were specifically selected for their resistance to stress corrosion cracking. If 316 SS were to prove inadequate over a longer time period, alloy 2205 offers improved chloride resistance at a modest cost increase. However, if a nearly impervious material is required, like titanium, total system cost would escalate significantly and would have a similarly substantial impact on the LCWD, potentially raising it above $\$5.00/m^3$.

Table 28. Impact of Cooling Tower Coil Material on System Capital Cost

	Hygroscopic Tower Coil Material		
Configuration	**316SS**	**2205 Duplex SS**	**TI-5 Titanium**
Dewatering Bin Total System Capital, $/gpm	$63,586	$66,820	$106,273
Relative to Baseline Value	100%	105%	167%
Solids Press Total System Capital, $/gpm	$64,563	$67,797	$107,250
Relative to Baseline Value	100%	105%	166%

The other key sensitivity highlighted in Figures 28 and 29 was the wet-bulb approach temperature, trends for which are shown in Figure 14, versus hygroscopic tower cooling capacity. Essentially, as the wet-bulb approach decreases, so does the potential cooling capacity of the tower and the amount of wastewater it is able to evaporate, effectively raising the normalized capital cost of the hygroscopic system. Since the hygroscopic cooling tower must operate below the upper temperature limit set by the power plant's main cooling tower, the lower bound of its wet-bulb approach will need to be selected to both make the most of the available heat source while optimizing the wastewater throughput capacity of the system. An upper bound on wet-bulb approach also exists since the risk of fouling the heat exchange coil increases as the temperature differential across the coil wall increases.

The LCWD ranges for the remaining sensitivity parameters in Figures 28 and 29 were less impactful than either capital or wet-bulb approach temperature and are similar for the two dewatering design alternatives. The only notable contrast between the two is that the solids press alternative appears insulated somewhat from changes to the landfill disposal fee, which is reflective of the reduced mass flow of waste solids for this design.

SUPPLEMENTARY STUDY OF CDR PRODUCED WATER RECYCLING

With the increasing likelihood that some power plants in North Dakota will be retrofitted with carbon dioxide recovery (CDR) and geologic sequestration, the EERC conducted a supplementary study to estimate how water demand and wastewater production at these plants would be impacted by CDR retrofitting. The study also collected data about related CDR process water streams and evaluated them as alternative sources of cooling water makeup using both conventional cooling towers and the EERC's wastewater-minimizing hygroscopic cooling. By applying configuration-specific factors to the power plants in North Dakota, water demand was estimated to increase 15%–20% for derated CDR and 60%–70% for maintaining the plant's full-power output. Key exceptions to these trends were plants that use once-through cooling. For these plants, CDR water consumption was highly dependent on the continued use of their once-through condensers. It was further estimated that the water demand increase for derated CDR could, in theory, be met by improvements to plant water-use efficiency, specifically by using plant blowdown for cooling within a hygroscopic cooling tower. Full-power CDR water demands could not be met with improved water-use efficiency alone, and a new water supply would be needed.

Produced water from geologic CO_2 sequestration in the Inyan Kara Formation shows promise as a possible source of cooling water makeup, but actual testing for this purpose is needed. If Inyan Kara water could be used for plant makeup, it was estimated that it could provide a substantial fraction of the plant's makeup water needs (50%–70%) at an extraction rate that might be relevant for managing reservoir pressure and CO_2 plume spread.

The supplementary study is included as Appendix E.

CONCLUSIONS

This evaluation of wastewater recycling with hygroscopic cooling demonstrated several key aspects of its operation with real power plant wastewater. Overall, the concept seems feasible as no insurmountable technical challenges were identified. Key conclusions from this work are summarized in this section.

- **Cooling capacity.** The pilot hygroscopic cooling tower was able to provide useful cooling for the host site power plant while consuming blowdown from the plant's existing cooling towers and with ash pond water that was diverted from deep well injection. At the preferred operating conditions identified during the TEA, the wet-bulb approach temperature of the tower was 7.3°C (13°F).

- **Wastewater minimization.** True ZLD operation may not be feasible with hygroscopic wastewater recycling; instead, its sustainable mode of operation will likely be as a wastewater concentrator. Testing at the working fluid concentration needed to precipitate soluble sulfate and chloride species resulted in the formation of a stable foam that interfered with pumping and distribution of liquid over the tower's heat exchange coil. Since this issue was largely avoided at lower working fluid concentrations, the TEA assumed the hygroscopic system would operate with a cap on concentration that would be maintained with the blowdown of a liquid brine in addition to producing waste solids. Under the TEA operating conditions, the incoming wastewater volume was still reduced by over 94% with the hygroscopic blowdown.

- **Waste solids disposal.** Waste solids produced during operation with both CTB and APW appear that they would be classified as nonhazardous waste based on their measured RCRA element content and evaluation of their leaching potential. However, to qualify as a solid for landfill disposal, i.e., as determined by the EPA paint filter test, it appears that a dewatering step beyond hydrocyclone separation is needed. The method of dewatering appeared to have little impact on the LCWD with hygroscopic cooling.

- **Levelized disposal cost.** The baseline LCWD for hygroscopic wastewater recycling was estimated to be \$3.69–\$3.72 per m^3 of APW wastewater. Capital cost contributed over 54% to the LCWD, and parameters that impact capital cost such as the heat exchange coil material of construction and the tower's wet-bulb approach temperature were identified as having the greatest sensitivity for overall LCWD. Under the extreme parameter range for capital, the TEA sensitivity study showed that LCWD values could exceed \$5.00/m^3.

- **Comparison to MVR.** The TEA performed for hygroscopic wastewater recycling suggests that it could have a lower levelized cost of disposal compared to conventional brine minimization technologies that recover distilled-quality water. The LCWD for MVR blowdown treatment was estimated to be almost 40% higher than that calculated for hygroscopic cooling.

- **Comparison to deep well injection.** Disposal-only ZLD using deep well injection was estimated to have a 30% lower LCWD compared to hygroscopic wastewater recycling. The relatively low value of displaced makeup water and fan power does not appear to be sufficient to justify hygroscopic recycling versus direct disposal. However, for instances where the volume of disposed fluid is a concern, perhaps when done in conjunction with carbon dioxide sequestration, hygroscopic wastewater recycling could reduce the volume of disposed liquid to 5.4% of its incoming volume.

REFERENCES

American Society for Testing and Materials, D892-18 Standard Test Method for Foaming Characteristics of Lubricating Oils, 2018

Effluent Limitations Guidelines and Standards for the Steam Electric Power Generating Point Source Category. *Code of Federal Regulations*, Part 423, Title 40, 2015.

Energy & Environmental Research Center. *Produced Water Management and Recycling Options in North Dakota*; Final Report for North Dakota Legislative Management Energy Development and Transmission Committee and North Dakota Industrial Commission, 2020.

Hygroscopic Cooling Tower for Reduced HVAC Water Consumption. Environmental Security Technology Certification Program (ESTCP) Project EW-201723. www.serdp-estcp.org/projects/details/19434960-47d5-4bd4-b336-8c78c505c0db/ew-201723-project-overview (accessed September 2022).

Marlett, M.A. Cost Comparison of ZLD and Biological Treatment for FGD Wastewater. *Power Engineering* **2018**. www.power-eng.com/articles/2018/07/a-cost-comparison-of-zld-and-biological-treatment-for-fgd-wastewater.html (accessed May 2019).

U.S. Environmental Protection Agency, Method 1311 Toxicity Characteristics Leaching Procedure, Revision 0, July 1992.

U.S. Environmental Protection Agency, Method 9095B Paint Filter Liquids Test, Revision 2, November 2004.

U.S. Environmental Protection Agency. *Technical Development Document for the Effluent Limitations Guidelines and Standards for the Steam Electric Power Generating Point Source Category;* Report EPA-821-R-15-007; U.S. Environmental Protection Agency: Washington, DC, September 2015.

Woods, D.R. *Rules of Thumb in Engineering Practice*; Wiley-VCH Verlag GmbH & Co. KGaA, Weinheim, 2007. ISBN: 978-3-527-31220-7.

APPENDIX A

MICROBIOLOGICAL DIP SLIDE RESULTS

24-hour Exposure Results (09/07/21)

System	Sample Date	Exposed Dip Slide Time	24-hour Exposure Time, Bacteria	Results, cfu/mL	24-hour Exposure Time, Fungi	Results, cfu/mL
HCT Basin	09/07/21	07:21		<100		<10
Coal Creek CT	09/07/21	07:21		100		<10
AP Water	09/07/21	07:21		10,000		<10

48-hour Exposure Results (09/07/21)

System	Sample Date	Exposed Dip Slide Time	48-hour Exposure Time, Bacteria	Results, cfu/mL	48-hour Exposure Time, Fungi	Results, cfu/mL
HCT Basin	09/07/21	07:21		1,000		<10
Coal Creek CT	09/07/21	07:21		1,000		<10
AP Water	09/07/21	07:21		10,000		<10

24-hour Exposure Results (09/13/21)

System	Sample Date	Exposed Dip Slide Time	24-hour Exposure Time, Bacteria	Results, cfu/mL	24-hour Exposure Time, Fungi	Results, cfu/mL
HCT Basin	09/13/21	07:33		<100		<10
Coal Creek CT	09/13/21	07:30		1,000		<10
AP Water	09/13/21	07:33		10,000		<10

48-hour Exposure Results (09/13/21)

System	Sample Date	Exposed Dip Slide Time	48-hour Exposure Time, Bacteria	Results, cfu/mL	48-hour Exposure Time, Fungi	Results, cfu/mL
HCT Basin	09/13/21	07:33		<100		<10
Coal Creek CT	09/13/21	07:30		10,000		<10
AP Water	09/13/21	07:33		100,000		<10

72-hour Exposure Results (09/13/21)				
System	**Sample Date**	**Exposed Dip Slide Time**	**72-hour Exposure Time, Fungi**	**Results, cfu/mL**
HCT Basin	09/13/21	07:33		<10[1]
Coal Creek CT	09/13/21	07:30		<10
AP Water	09/13/21	07:33		<10

96-hour Exposure Results (09/13/21)				
System	**Sample Date**	**Exposed Dip Slide Time**	**96-hour Exposure Time, Fungi**	**Results, cfu/mL**
HCT Basin	09/13/21	07:33		10
Coal Creek CT	09/13/21	07:30		<10
AP Water	09/13/21	07:33		<10

24-hour Exposure Results (09/14/21)

System	Sample Date	Exposed Dip Slide Time	24-hour Exposure Time, Bacteria	Results, cfu/mL	24-hour Exposure Time, Fungi	Results, cfu/mL
CT Desiccant	09/14/21	06:49		1,000		<10
Coal Creek Basin	09/14/21	07:17		1,000		<10
AP Water	09/14/21	07:22		10,000		<10
Mix Tank	09/14/21	07:36		100		10

48-hour Exposure Results (09/14/21)

System	Sample Date	Exposed Dip Slide Time	48-hour Exposure Time, Bacteria	Results, cfu/mL	48-hour Exposure Time, Fungi	Results, cfu/mL
CT Desiccant	09/14/21	06:49		1,000		<10
Coal Creek Basin	09/14/21	07:17		1,000		<10[1]
AP Water	09/14/21	07:22		10,000		<10
Mix Tank	09/14/21	07:36		100		10

APPENDIX B

WORKING FLUID FOAMING EVALUATION

FOAMING TESTS FOR HYGROSCOPIC COOLING TOWER

During the course of the testing at Coal Creek Station, samples were taken for different forms of analysis. It was noted throughout the testing that foaming inside the cooling tower increasingly became an issue. To see if the foaming characteristics had any relationship with the run time versus the total dissolved solids, it was decided to make use of a modified version of ASTM D892 (Standard Test Method for Foaming Characteristics of Lubricating Oils). The test setup was similar to the procedure used in Thitakamol and Veawab (2008). The setup is similar to Figure B-1, with a few key differences that will be described.

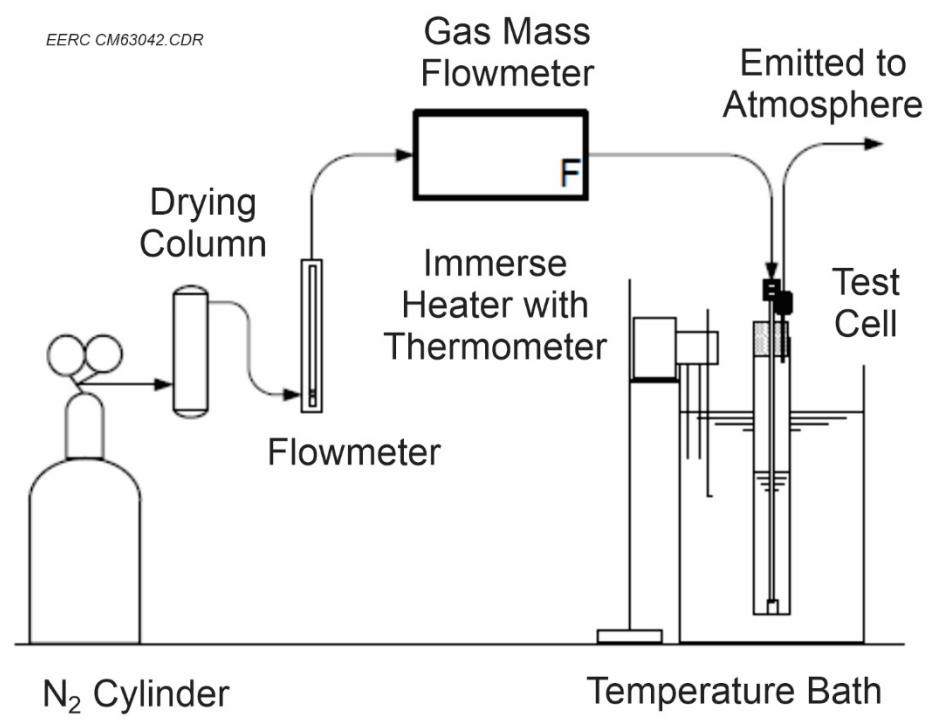

Figure B-1. Foaming test setup.

The key differences are as follows:

- N_2 was supplied by house, not a separate cylinder.
- A Gilibrator was used instead of a mass flowmeter for a secondary flow rate measurement.
- Thermometer was replaced with a handheld thermocouple reader and a Type K thermocouple.

- In order to control the temperature in the bath, hot water was introduced intermittently to keep the water in the desired range since an immersion heater was not available.

Before the foaming tests were started, ten samples were selected, ranging from early in the experiment toward the end, to examine how the length of time affected foaming tendencies. The procedure used to perform the tests is described as follows:

1) Fill the test cell (a graduated cylinder) to the 80-mL mark with the designated sample.

2) Fill up the test bath with hot water, aiming for 40°C ± 5.
   a. This temperature was chosen because it represents the operating temperature of the cooling tower.
   b. Keep the water running, increasing/decreasing the flow as needed to keep the temperature within range.

3) Immerse the test cell in the test bath, and wait at least 10 minutes to ensure the sample reaches the same temperature of the bath.

4) Insert gas diffuser, air inlet tube with air source disconnected, and air outlet tube into the test cell. Let the diffuser saturate in the sample for 5 minutes.

5) Make sure the diffuser is centered and barely touching the bottom of the test cell.

6) While the diffuser saturates, use the Gilibrator to get the nitrogen flow to 94 mL/min ± 5.
   a. The flow rate is recommended from the ASTM D892 test standard.
   b. Use the Gilibrator 10 times to get an average for better accuracy. The Gilibrator is a low-range volume flowmeter that is activated manually by pressing a plunger. Press the plunger, and it calculates the air flow. The screen shows the amount of presses and the average.

7) Once the average flow has been determined to be in the acceptable range, disconnect the air line from the outlet of the rotameter used to control flow from the Gilibrator, and connect the line from the diffuser.

8) Make sure the 5-minute saturation period is up.

9) Flow gas through the diffuser into the sample for 5 min ± 3 seconds from the appearance of first air bubbles.

10) Record the volume of foam, then shut off gas flow at the 5-min mark, and immediately record the volume of foam once again (to see if there is a significant difference between the foam level and the instantaneous shutoff of gas).
    a. Shut off gas by disconnecting at the outlet of the rotameter.
       i. This is to prevent any pressure build up in the air-drying column, as it will explode if pressurized too high.

b. Measure the foam at the point of contact between liquid and foam to the top of the foam itself.
    i. Once you have this measurement, turn off the gas at the source.
    ii. The gas can be shut off at the source if the testing apparatus is in close enough proximity to get a measurement immediately after, which was not the case in this experimental setup because lab space was occupied by other equipment.

11) Let the test cell stand for 10 minutes (while still maintaining the correct temperature range), and record the volume of foam at the end.

12) If the foam completely collapses before the time runs out, the result is zero.

13) Clean the gas inlet tube and diffuser before proceeding to test the next sample.
    a. ASTM-D892 recommends using toluene and heptane to clean the diffuser and air tube.
    b. Clean the air tube first by disassembling it from the diffuser and flushing it with toluene and heptane.
    c. Reconnect the air tube and diffuser and immerse the diffuser in toluene.
    d. Flush a portion of the toluene back and forth through the gas diffuser at least 5 times.
    e. Repeat with the heptane.
    f. Dry the air tube and diffuser by forcing clean air through.
    g. Wipe the outside of the air tube with a dry cloth; do not wipe the diffuser.

Results and Observations

The first test performed was to find the foaming tendencies of the solution versus the operation time. A total of ten samples were used, ranging from June 23, 2021, to September 13, 2021. The tests showed the samples closer to the later date would generate more foam during the 5 minutes of gas flow to the point where the test cylinder would be filled with foam before the time was up. It can be noted that the difference in foam volume from when the gas was flowing versus getting shut off right at the 5-minute mark was negligible. It also showed that the test samples from the later dates typically retained a greater amount of foam after the 10-minute period after gas was shut off. The samples from the later dates also had increasing amounts of total dissolved solids present, showing a strong relationship between that and the foaming tendencies of the solution. Figure B-2 shows the foaming during gas agitation of a sample from July 14, 2021, and Figure B-3 shows foaming of a sample from September 14, 2021, to show the difference in the amount of foam present during gas flow.

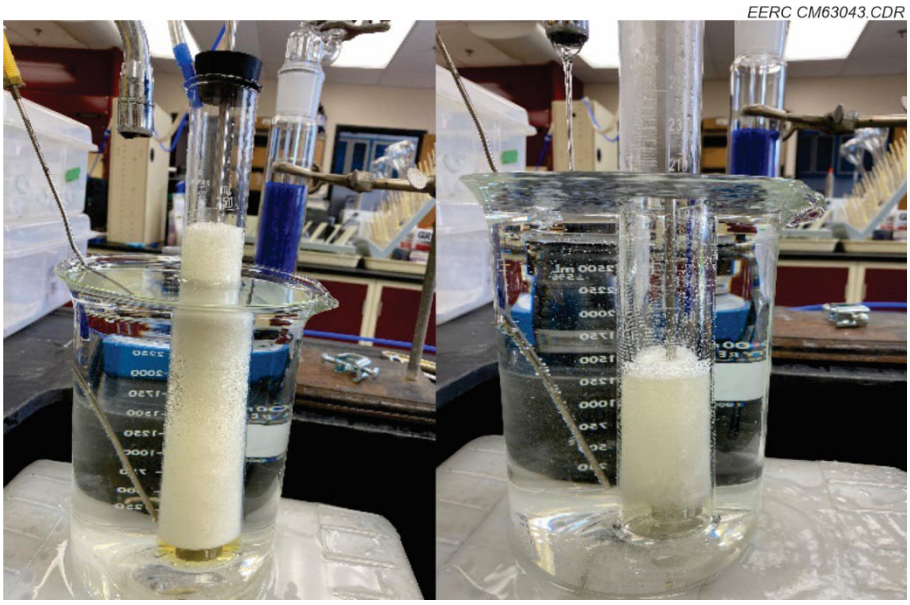

Figure B-2. July 14, 2021, sample.

Figure B-3. September 14, 2021, sample.

A second set of testing was done to investigate the effect different types of antifoam agents would have on the foaming tendencies. Two samples were chosen: one from an earlier date with very minimal foaming and one from later in the experiment with substantial foaming. Three different types of antifoam agents were used:

- Antifoam A (A1302)
- WD-40
- Canola oil

The procedure for these tests followed the same plan listed above, with the extra step of adding in the antifoam. To see how each agent affects the foaming tendencies, five different tests were performed with different amounts of antifoam on each sample. The five different amounts are shown in Table B-1 and were introduced to the sample with an eye dropper. The amount is expressed in volume and total concentration.

Table B-1. Antifoam Amounts

1 Drop	0.05 mL	625 ppmv
5 Drop	0.25 mL	3125 ppmv
10 Drops	0.50 mL	6250 ppmv
20 Drops	1.00 mL	12500 ppmv
30 Drops	1.50 mL	18750 ppmv

Before switching to the next type of antifoam, the diffuser, air inlet tube, and test cell were cleaned thoroughly to avoid any sort of contamination. This process was done with all three antifoams in each sample, and observations were made about how the antifoam affected the foaming tendencies.

With the sample from early in the experiment, Antifoam A seemingly had no effect because of the low foaming tendency of this sample. With each amount, the foam amount right at the 5-minute end was essentially always the same, with the foam collapsing immediately once the gas flow was turned off. With the more WD-40 and canola oil added, the amount of foam seemingly increased, as by the time 30 drops were reached, the foam did not completely disappear after the 10-minute mark. However, it is noted that it looked like the WD-40 and canola oil formed a layer between the sample and the foam itself, which may have caused the foam to no longer completely collapse.

With the sample taken toward the end of the experiment, the addition of Antifoam A caused the foam to collapse quicker once gas was turned off. However, it seemed to have no effect on the foaming itself while gas was flowing through the diffuser. The WD-40 decreased the foaming tendency during the 5-minute gas flow period as well as decreased how quickly the foam collapsed during the 10-minute period after gas flow was turned off. However, at 10 drops and beyond, the amount of foam present during the 5-minute period started increasing, along with the amount of time it took for the foam to collapse. The canola oil also followed a similar pattern; the key differences being the amount of foam was overall less than the amount produced during the 5-minute period with the WD-40 and the amount increased with each addition of canola oil. The time to collapse after the gas was turned off was also significantly lower than the WD-40 and the Antifoam A but followed the pattern of the more that was added, the longer it took to collapse.

Overall, the modified ASTM D892 foaming test revealed the relationship of foaming tendencies between the run time and the total dissolved solids present as well as the effect different antifoam agents had on the solution. It was shown that as time progressed and more total dissolved solids were present in the solution, a greater amount of foaming occurred in the system. For the antifoam agents, each one performed differently from the other. Antifoam did not have an apparent effect on the amount of foam during gas flow but caused the foam to collapse quicker the more that was added. WD-40 initially caused the amount of foam during gas flow to decrease, but the foam began increasing again as more WD-40 was added. The time it took for the foam to collapse followed the same pattern. Canola oil caused the greatest decrease in the foaming amount during the 5-minute period but caused the amount of foam to increase as more canola was introduced. The amount of time for the foam to collapse after gas flow was shut off was the lowest by far compared to the other two, but the time for the collapse increased as more canola oil was added.

APPENDIX C

TCLP RESULTS

MINNESOTA VALLEY TESTING LABORATORIES, INC.

MVTL

1126 N. Front St. ~ New Ulm, MN 56073 ~ 800-782-3557 ~ Fax 507-359-2890
2616 E. Broadway Ave. ~ Bismarck, ND 58501 ~ 800-279-6885 ~ Fax 701-258-9724
51 W. Lincoln Way ~ Nevada, IA 50201 ~ 800-362-0855 ~ Fax 515-382-3885

MEMBER ACIL

FINAL ANALYSIS REPORT

David Christianson
Great River Energy
2875 3rd. Str. SW
Coal Creek Station
Underwood ND 58576-9659

Report Date: 21 Oct 2021
Lab Number: 21-H322
Work Order #: 81-0719

Account #: 021010
PO #: 6163930

Sample Description: EERC Waste

Date Sampled: 28 Sep 2021 10:00
Date Received: 28 Sep 2021 16:32
Temp at Receipt: 12.3C ROI

Sampled By: Client

SW846 Method 1311

TCLP Ext: 29 Sep 2021

Analyte	Result		Dilution Factor	Reporting Limit	Action Level mg/L	Method Reference	Date Analyzed
Metal Digestion	--		--	--	--	EPA 200.2	30 Sep 21
% Solids (dry)	63.3	wt %	N/A	0.50		SW846 1311	29 Sep 21
% Solids (wet)	91.5	wt %	N/A	0.50		SW846 1311	29 Sep 21
Arsenic TCLP	< 0.2	mg/l	100	0.200	5.0	SW846 6020B	1 Oct 21
Barium TCLP	< 1	mg/l	10	1.00	100	SW846 6010D	1 Oct 21
Cadmium TCLP	< 0.1	mg/l	10	0.10	1.0	SW846 6010D	1 Oct 21
Chromium TCLP	< 0.5	mg/l	10	0.50	5.0	SW846 6010D	1 Oct 21
Corrosivity by pH**	7.64	units	N/A	1.00		SW 846 9045D	29 Sep 21
Ignitability Screening**	See comment below		N/A	N/A		40 CFR 261.21	
Lead TCLP	< 1	mg/l	10	1.00	5.0	SW846 6010D	1 Oct 21
Mercury TCLP	< 0.01	mg/l	50	0.0100	0.2	SW846 7470A	6 Oct 21
Selenium TCLP	< 0.2	mg/l	100	0.200	1.0	SW846 6020B	1 Oct 21
Silver TCLP	< 0.2	mg/l	100	0.200	5.0	SW846 6020B	1 Oct 21
TCLP pH	4.66	units	N/A	1.00		SW846 1311	30 Sep 21

**This parameter is not performed by Method 1311.

Approved by: Claudette K. Carroll

Claudette K. Carroll, Laboratory Manager, Bismarck, ND

All TCLP Extractions performed in the Bismarck Laboratory, with the exception of the ZHE Extraction, which is performed in the New Ulm Laboratory.

The reporting limit was elevated for any analyte requiring a dilution as coded below:
@ = Due to sample matrix # = Due to concentration of other analytes
! = Due to sample quantity + = Due to internal standard response

APPENDIX D

CORROSION COUPON RESULTS

CORROSION COUPON RESULTS

Data for individual corrosion coupons are presented in Table D-1. The corrosion rates were calculated based on the exposure during field testing. Coupons were installed on June 16, 2021, and recovered on September 17, 2021, for a total of 93 exposure days.

Table D-1. Corrosion Coupon Data

Material	Serial No.:	Location	Initial Wt., g	Final Wt., g	Difference, g	Corrosion Rate, mils/yr	Comments
316L (stainless steel)	6042	Immersed	10.7991	10.7921	0.0070	0.0632	No visible etching
	6043	Immersed	10.7457	10.7417	0.0040	0.0361	No visible etching
	6044	Sprayed	10.8094	10.8041	0.0053	0.0479	No visible etching
	6045	Sprayed	10.8255	10.8212	0.0043	0.0389	No visible etching
	6046	Sprayed	10.8660	10.8612	0.0048	0.0434	No visible etching
2205 (duplex SS)	1	Sprayed	11.0175	11.0156	0.0019	0.0176	No visible etching
	2	Sprayed	11.0142	11.0110	0.0032	0.0296	No visible etching
	3	Sprayed	10.9996	10.9966	0.0030	0.0277	No visible etching
	4	Immersed	10.9747	10.9725	0.0022	0.0203	No visible etching
	5	Immersed	11.0050	11.0021	0.0029	0.0268	No visible etching
TI-5 (titanium)	1	Immersed	6.6322	6.6286	0.0036	0.0586	No visible etching
	2	Sprayed	6.6676	6.6289	0.0387	0.6299*	Even etching
	3	Sprayed	6.6380	6.6368	0.0012	0.0195	No visible etching
	4	Sprayed	6.6446	6.6432	0.0014	0.0228	No visible etching
	5	Immersed	6.6815	6.6788	0.0027	0.0439	No visible etching
CDA651 (silicon bronze)	1	Immersed	16.3899	16.3468	0.0431	0.3597	Even etching
	2	Immersed	16.3819	16.3435	0.0384	0.3204	Even etching
	3	Sprayed	16.3003	16.2731	0.0272	0.2270	No visible etching
	4	Sprayed	16.0278	15.9991	0.0287	0.2395	No visible etching
	5	Sprayed	16.4136	16.3863	0.0273	0.2278	No visible etching
Al 2024 (aluminum)	1	Immersed	4.1446	4.1204	0.0242	0.6299	Spotty etching
	2	Sprayed	4.1443	4.1404	0.0039	0.1015	No visible etching
	3	Sprayed	4.1417	4.1377	0.0040	0.1041	No visible etching
	4	Sprayed	4.1409	4.1362	0.0047	0.1223	No visible etching
	5	Immersed	4.1404	4.1126	0.0278	0.7236	Spotty etching

* Result appeared anomalous compared to the matching samples and was not used in the calculation of average corrosion rate.

APPENDIX E

LEC COMPANION STUDY

WATER DEMAND AND RECYCLING POTENTIAL AT NORTH DAKOTA POWER PLANTS RETROFITTED WITH CARBON DIOXIDE RECOVERY AND GEOLOGIC SEQUESTRATION

White Paper

Prepared for:

Mr. Michael Holmes

Lignite Energy Council
1016 East Owens Avenue
PO Box 2277
Bismarck, ND 58502

Prepared by:

Christopher L. Martin

Energy & Environmental Research Center
University of North Dakota
15 North 23rd Street, Stop 9018
Grand Forks, ND 58202-9018

December 2021

EERC DISCLAIMER

LEGAL NOTICE This research report was prepared by the Energy & Environmental Research Center (EERC), an agency of the University of North Dakota, as an account of work sponsored by Lignite Energy Council. Because of the research nature of the work performed, neither the EERC nor any of its employees makes any warranty, express or implied, or assumes any legal liability or responsibility for the accuracy, completeness, or usefulness of any information, apparatus, product, or process disclosed or represents that its use would not infringe privately owned rights. Reference herein to any specific commercial product, process, or service by trade name, trademark, manufacturer, or otherwise does not necessarily constitute or imply its endorsement or recommendation by the EERC.

ACKNOWLEDGMENT

This material is based in part upon work supported by the Department of Energy National Energy Technology Laboratory under Award Number DE-FE0031810.

DOE DISCLAIMER

This report was prepared as an account of work sponsored by an agency of the United States Government. Neither the United States Government, nor any agency thereof, nor any of their employees, makes any warranty, express or implied, or assumes any legal liability or responsibility for the accuracy, completeness, or usefulness of any information, apparatus, product, or process disclosed, or represents that its use would not infringe privately owned rights. Reference herein to any specific commercial product, process, or service by trade name, trademark, manufacturer, or otherwise does not necessarily constitute or imply its endorsement, recommendation, or favoring by the United States Government or any agency thereof. The views and opinions of authors expressed herein do not necessarily state or reflect those of the United States Government or any agency thereof.

NDIC DISCLAIMER

This report was prepared by the Energy & Environmental Research Center (EERC) pursuant to an agreement partially funded by the Industrial Commission of North Dakota, and neither the EERC nor any of its subcontractors nor the North Dakota Industrial Commission nor any person acting on behalf of either:

(A) Makes any warranty or representation, express or implied, with respect to the accuracy, completeness, or usefulness of the information contained in this report or that the use of any information, apparatus, method, or process disclosed in this report may not infringe privately owned rights; or

(B) Assumes any liabilities with respect to the use of, or for damages resulting from the use of, any information, apparatus, method, or process disclosed in this report.

Reference herein to any specific commercial product, process, or service by trade name, trademark, manufacturer, or otherwise does not necessarily constitute or imply its endorsement, recommendation, or favoring by the North Dakota Industrial Commission. The views and opinions of authors expressed herein do not necessarily state or reflect those of the North Dakota Industrial Commission.

WATER DEMAND AND RECYCLING POTENTIAL AT NORTH DAKOTA POWER PLANTS RETROFITTED WITH CARBON DIOXIDE RECOVERY AND GEOLOGIC SEQUESTRATION

ABSTRACT

With the increasing likelihood that some power plants in North Dakota will be retrofitted with carbon dioxide recovery (CDR), the Energy & Environmental Research Center (EERC) conducted a study to estimate how water demand and wastewater production at these plants would be impacted by CDR retrofitting. The study also collected data about related CDR process water streams and evaluated them as alternative sources of cooling water makeup using both conventional cooling towers and the EERC's water-minimizing hygroscopic cooling. By applying configuration-specific factors to the power plants in North Dakota, water demand was estimated to increase 15% to 20% for derated CDR and 60%–70% for maintaining the plant's full-power output. Key exceptions to these trends were plants that use once-through cooling; for these plants, CDR water consumption was highly dependent on the continued use of their once-through condensers. It was further estimated that the water demand increase for derated CDR could, in theory, be met by improvements to plant water use efficiency, specifically by using plant blowdown for cooling within a hygroscopic cooling tower. Full-power CDR water demands could not be met with improved water use efficiency alone, and a new water supply would be needed. Produced water from geologic CO_2 sequestration in the Inyan Kara Formation shows promise as a possible source of cooling water makeup, but actual testing for this purpose is needed. If Inyan Kara water could be used for plant makeup, it was estimated that it could provide a substantial fraction of the plant's makeup water needs (50%–70%) at an extraction rate that might be relevant for managing reservoir pressure and CO_2 plume spread.

TABLE OF CONTENTS

LIST OF FIGURES

LIST OF TABLES

WATER DEMAND AND RECYCLING POTENTIAL AT NORTH DAKOTA POWER PLANTS RETROFITTED WITH CARBON DIOXIDE RECOVERY AND GEOLOGIC SEQUESTRATION

INTRODUCTION

The Energy & Environmental Research Center (EERC) continues to investigate technology for improving the water use efficiency at coal-fired power plants (1, 2), especially for plant cooling, which is typically the dominant need for water. With the increasing likelihood that some power plants in North Dakota will be retrofitted with carbon dioxide recovery (CDR), the EERC conducted a study to estimate how water demand and wastewater production at these plants would be impacted by CDR retrofitting. The study also collected data about related CDR process water streams and evaluated them as alternative sources of cooling water makeup using both conventional cooling towers and the EERC's water-minimizing hygroscopic cooling.

BACKGROUND

North Dakota Power Plants

There are currently five major power plants in North Dakota that are fueled by lignite mined in-state, and each plant has a unique configuration that impacts its water needs as shown in Table 1. All of the plants in North Dakota are water-cooled and, for these plants, steam condenser cooling is the dominant plant water use. For example, up to 90% of a plant's water consumption can be used for wet recirculating cooling tower makeup (3). North Dakota has plants that use once-through cooling and wet recirculating systems with cooling towers. While significantly more water is withdrawn for once-through cooling than wet recirculating on a normalized basis, nearly all once-through water is returned to the source. On the other hand, water withdrawals for a wet recirculating system are lower on a normalized basis, but much of that water is consumed through evaporation and is not returned to the source. Heated water released by once-through cooling systems can have a negative impact on the environment, and the operation of these systems is strictly regulated. Given the potential environmental impacts of once-through cooling, wet recirculating systems have been identified as a preferred power plant cooling technology and would likely be the design choice for new plants or cooling upgrades to existing plants. Air cooling would also be an option but would likely be considered cost-prohibitive in North Dakota because of the reasonable availability of makeup water.

Table 1. North Dakota Lignite Power Plants

Plant	Net Generating Capacity, MWe	Generating Units	FGD* System Type	Condenser Cooling System
Antelope Valley Station	900	2	Dry	Wet recirculating
Coal Creek Station	1100	2	Wet	Wet recirculating
Coyote Station	420	1	Dry	Wet recirculating
Leland Olds Station	669	2	Wet	Once-through
Milton R. Young Station	705	2	Wet	Once-through

* Flue gas desulfurization.

The second largest water user at a coal-fired power plant is typically for environmental control, specifically FGD. As with cooling, the two most common FGD system types are represented in North Dakota, i.e., wet and dry. Despite their names, both FGD systems consume water in making the SO_2 absorption solution, but in dry FGD, the solution is completely evaporated during contact with the flue gas, while wet systems saturate the flue gas and continually recirculate the absorption solution. Because they take less water to operate, dry FGD systems consume less water than wet systems, and they do not produce a liquid blowdown stream. The remaining power plant water uses generally constitute less than 3% of overall plant needs and are not considered in detail in this analysis.

CDR Retrofitting

The addition of CDR to an existing power plant introduces several new water demands and sources of wastewater as diagrammed in Figure 1. Assuming an aqueous amine-based CDR process, the absorption system itself will require water for CO_2 solvent makeup but will generally be a net water producer from the significant quantity of water condensed by cooling and condensing moisture in the flue gas stream (3, 4). As with the power cycle, the dominant CDR water use is for process cooling, which is likely to employ wet recirculating cooling towers. Major CDR cooling loads are for cooling the lean CO_2 solvent after regeneration and providing interstage cooling during CO_2 compression.

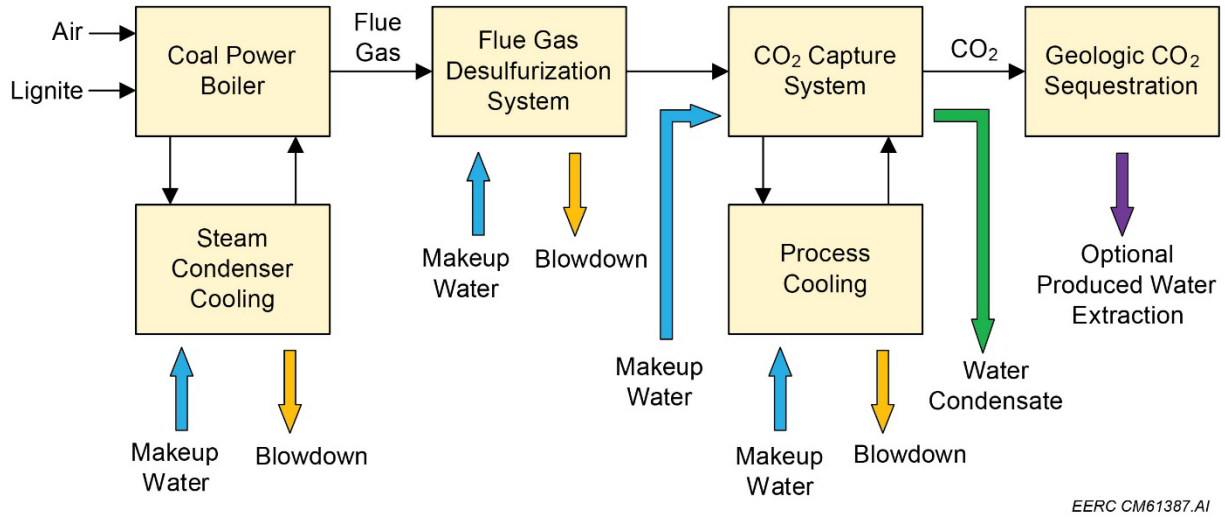

Figure 1. Simplified power plant water and wastewater flow diagram with CDR retrofitting.

A final water stream noted in Figure 1 is produced water associated with the geologic sequestration of CO_2 in a deep saline aquifer. While it is not necessary to extract formation water as it is displaced by injected CO_2, operational benefits of active reservoir management have been hypothesized (5, 6). For example, both a lower rate of reservoir pressure buildup and reduced spreading extent of CO_2 in the formation have been identified. The former benefit of lower pressure can impact operating costs for CO_2 compression, while the latter effect could potentially reduce

the aerial extent needed for a given quantity of CO_2 storage. A simplified schematic of CO_2 plume management is shown in Figure 2, whereby a produced water extraction well is used to draw injected CO_2 to a preferred location in the reservoir. Of course, the benefits of plume management can only be realized if there is a cost-effective disposition for the produced water, and cooling makeup water has been identified as an obvious synergy with fossil power production (7).

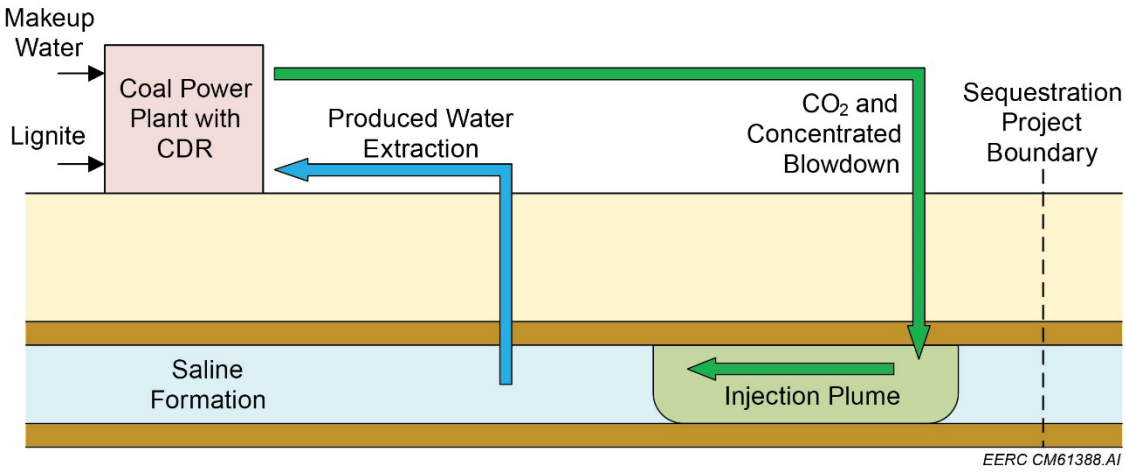

Figure 2. Notional concept for using power plant waste heat to concentrate the brine extracted for CO_2 plume management.

Cooling Tower Water Recycling

For power plants that use cooling towers, makeup water needs are significant, and the waste heat these towers dissipate could be used to concentrate plant blowdown and the potential produced water from CO_2 sequestration. However, the amount of water recycling and concentration that can be done by conventional cooling towers is limited by water quality and is typically expressed in terms of the operating cycles of concentration (COC). For instance, a COC of 5 implies that roughly 80% of the makeup water is evaporated to provide cooling, and the remaining 20% leaves the tower as concentrated blowdown wastewater. In general, the COC goes down as makeup water quality degrades, although water treatment and additives can be used under certain circumstances to increase COC. Conventional cooling tower water treatment is commonly based on precipitation water softening for scaling species removal in combination with the use of additives to extend saturation limits, reduce corrosion potential, and control microbiological growth.

The EERC is developing hygroscopic cooling technology to optimize the use of makeup water and to extend the range of water quality that can be recycled for evaporative cooling (1). The technology is based on the hygroscopic properties of chloride brine that is used as the evaporative working fluid inside a closed-loop cooling tower. Hygroscopic cooling maximizes water use by concentrating makeup water past the saturation level of sparingly soluble species such as $CaCO_3$ and $CaSO_4$. Instead of controlling these species with makeup water treatment, they (and other species) are actively forced to precipitate within the hygroscopic tower on seed nuclei

and are removed from the system as a solid waste that can be landfilled. In effect, the online precipitation of minerals with hygroscopic cooling is an alternative to conventional cooling tower water treatment; it results in higher COC values and the ability to use poor-quality makeup water that could not feasibly be used in a conventional tower. Hygroscopic cooling was field-tested at Coal Creek Station in North Dakota during the summer of 2021 (Figure 3), and some of the plant water quality data from that project are referenced in this analysis.

Figure 3. Hygroscopic cooling pilot system during testing at Coal Creek Station.

Analysis Approach

Water demand estimates after CDR retrofitting were largely based on cost and performance baselines published by the U.S. Department of Energy's National Energy Technology Laboratory (NETL) (3, 4), one of which (4) specifically included cases based on using North Dakota lignite as the fuel source. Results from these studies were adapted to the specific features of North Dakota's power plants, and the three plant configurations diagrammed in Figure 4 were modeled for each North Dakota plant. The baseline without CDR represents current-day water use, while derated CDR and full-power CDR cover two possible options for adding 90% CDR to an existing facility. Under the derated scenario, thermal energy needed to regenerate the CO_2 solvent comes from steam extracted from the plant's boiler and parasitic power is taken from the plant's electrical

output; both factors result in a decrease of approximately 30% in the plant's net generation capacity. Full-power CDR allows the plant to maintain its electric output by generating additional CDR energy using natural gas. Full-power CDR produces additional CO_2 emissions from natural gas consumption, but these emissions were assumed to not undergo CDR. As a result, both CDR cases consumed the same quantity of coal and captured the same quantity of CO_2.

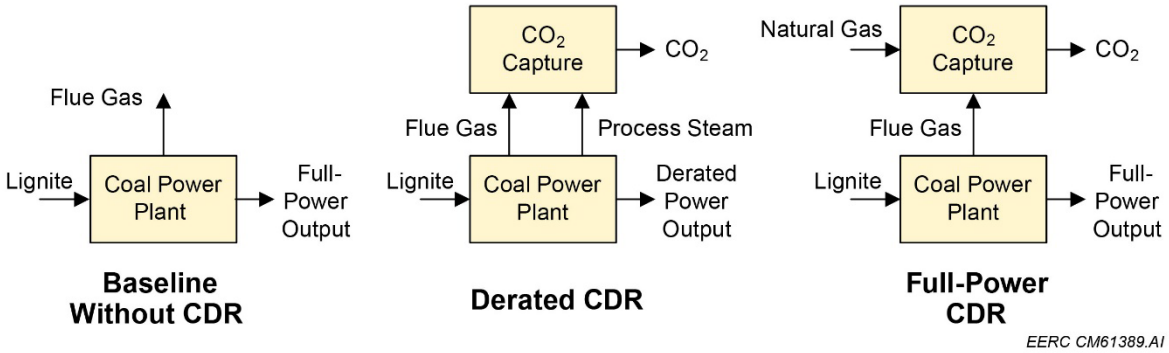

Figure 4. Evaluated configurations for the water impact study.

With respect to water use estimation, some modifications to the NETL baseline modeling were required to be more representative of the plants in North Dakota. Key adjustments to the NETL methodology included the following:

- The NETL North Dakota lignite case study (4) assumed a hybrid cooling system where steam condenser cooling was split equally between a water-cooled condenser and an air-cooled condenser. Since no North Dakota plants have this configuration, makeup cooling water estimates from the NETL study were doubled to account for a single wet recirculating or once-through cooling system.

- The COC assumption for the wet recirculating cooling tower was increased from 6 to 10 for this analysis. A COC of 10 implies that roughly 90% of the incoming makeup water was evaporated for cooling, while the remaining 10% was disposed of as blowdown. Actual COC values were not determined for each plant.

- Only a dry FGD system was included in the NETL lignite study (4). To estimate wet FGD water consumption and wastewater blowdown, values from a companion CDR cost and performance study for bituminous coal plants were referenced (3).

- Internal recycle values from the NETL study were not included in this analysis, except for the CDR condensate collection. These other recycle stream values were not used because they could not be confirmed from the process flow sheets, and they were relatively small in magnitude.

RESULTS

CDR Water Demand and Blowdown

Water use estimates for each North Dakota power plant were prepared using the common set of water intensity factors shown in Table 2 and applied to the specific configuration of each plant presented in Table 1. All intensity factors were normalized by the net electrical output of the baseline plant. The zero-value factors for once-through cooling makeup were based on the fact that virtually no water is consumed by these systems when operated as designed, which was assumed to be the case with no CDR and full-power CDR. However, under the derated CDR scenario, it was assumed that modifying the plant's steam cycle to provide CDR-process heat would lead to the construction of a new cooling system based on wet recirculating cooling towers.

Table 2. Power Plant Water Consumption Factors[a] in gpm/net MWe

	No CDR	Derated CDR	Full-Power CDR
Condenser Cooling Makeup, Wet Recirculating[b]	7.77	3.76	7.77
Condenser Cooling Makeup, Once-Through	0	NA[c]	0
Dry FGD Makeup	0.50	0.50	0.50
Wet FGD Makeup	0.94	0.94	0.94
Wet FGD Blowdown	0.08	0.08	0.08
CDR System Makeup	NA	0.05	0.05
CDR Process Cooling Makeup	NA	6.68	6.68
CDR Water Condensate	NA	1.87	1.87
Total Cooling Blowdown[d]	0.78	1.04	1.45

[a] Values normalized by the net electric output of the baseline plant.
[b] Assumes 10 COC in the cooling tower.
[c] Assumes the once-through condenser could not be reused in a derated scenario.
[d] Combines blowdown from condenser and CDR-process cooling.

Results for all scenarios at all plants are presented graphically in Figure 5 and the numerical values are summarized in Table 3. In each data set, net CDR cooling makeup values were based on the assumption that CDR condensate was used to directly offset cooling makeup water needs. Trends at the majority of plants show a moderate increase in water demand from the addition of derated CDR, but a more significant step increase in water demand with full-power CDR. The exceptions to this trend are Leland Olds and Milton R. Young Stations, both of which use once-through cooling. Counterintuitively, those results suggest that what should be the most water intensive scenario, i.e., full-power CDR, was actually less intensive than derated CDR. Again, these results stem directly from the assumption regarding the continued use of the once-through condenser under the full-power CDR scenario but not under derated CDR.

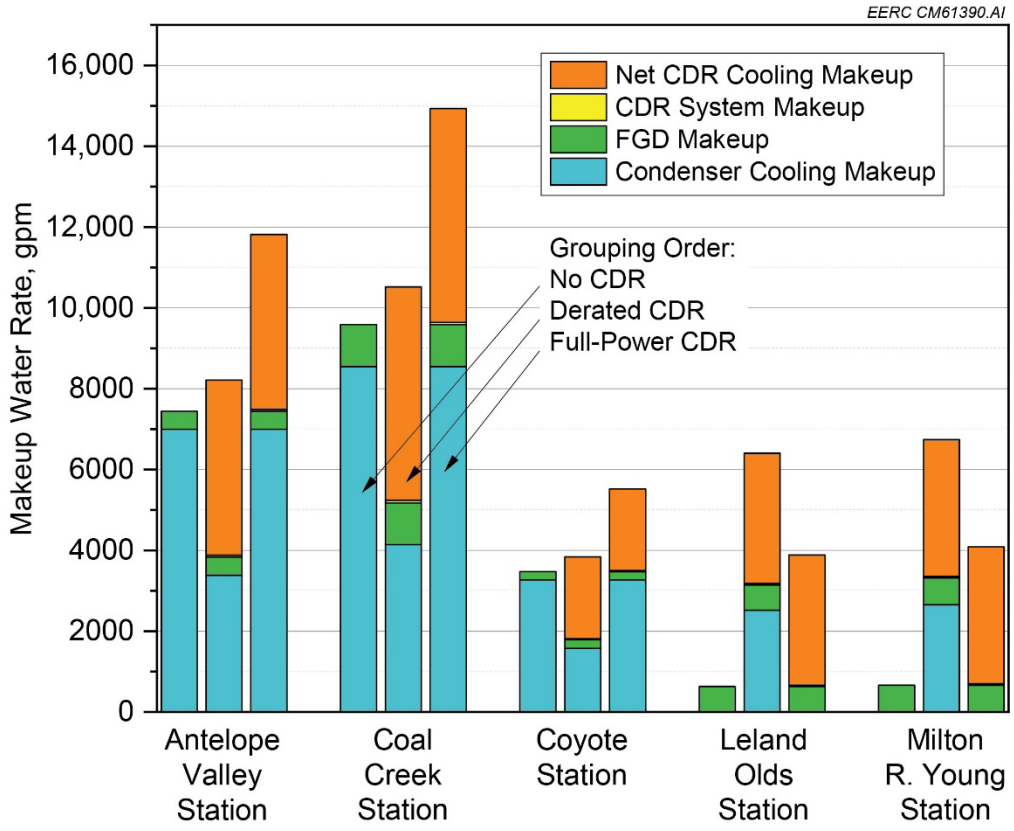

Figure 5. Breakdown of makeup water rates with and without CDR retrofitting.

For the plants that use wet recirculating cooling, the modest increase in water demand from the addition of derated CDR was because the added cooling requirements of CDR were considerably offset by reductions in steam condenser cooling. This offsetting phenomena would also likely extend to equipment utilization as well since any tower capacity no longer used for condenser cooling could be applied to the CDR process. In contrast, full-power CDR would likely require the construction of entirely new CDR cooling capacity.

Total plant blowdown estimates are plotted in Figure 6. These aggregate values include the applicable blowdown values from the FGD system, condenser cooling, and CDR process cooling. Blowdown trends generally increase in accordance with the makeup water trends in Figure 5. However, the incremental increase in blowdown from the addition of derated CDR appears larger than the corresponding increase in makeup water. Ultimately, this effect is because the CDR cooling makeup consumption in Figure 5 is a net value, which is lower than the actual consumption because of a contribution from condensate collection. However, blowdown rates were unaffected by internal water recycling, and they are instead proportional to the actual amount of water consumed for cooling.

Table 3. Water Consumption and Blowdown Values

	Antelope Valley Station	Coal Creek Station	Coyote Station	Leland Olds Station	Milton R. Young Station
No CDR Baseline, gpm					
FGD Consumption	448	1036	209	630	664
Condenser Cooling	6996	8551	3265	0	0
Total Makeup	7445	9587	3474	630	664
Total Blowdown	700	949	326	57	60
Derated CDR, gpm					
FGD Consumption	448	1036	209	630	664
Condenser Cooling	3389	4142	1581	2519	2655
CDR Makeup	48	59	22	36	38
CDR Cooling	6010	7346	2805	4468	4708
CDR Condensate	1684	2059	786	1252	1319
Net CDR Cooling	4326	5287	2019	3216	3389
Total Makeup	8211	10524	3832	6400	6745
Total Blowdown	940	1242	439	756	796
Full-Power CDR, gpm					
FGD Consumption	448	1036	209	630	664
Condenser Cooling	6996	8551	3265	0	0
CDR Makeup	48	59	22	36	38
CDR Cooling	6010	7346	2805	4468	4708
CDR Condensate	1684	2059	786	1252	1319
Net CDR Cooling	4326	5287	2019	3216	3389
Total Makeup	11819	14933	5515	3881	4090
Total Blowdown	1301	1683	607	1024	1079

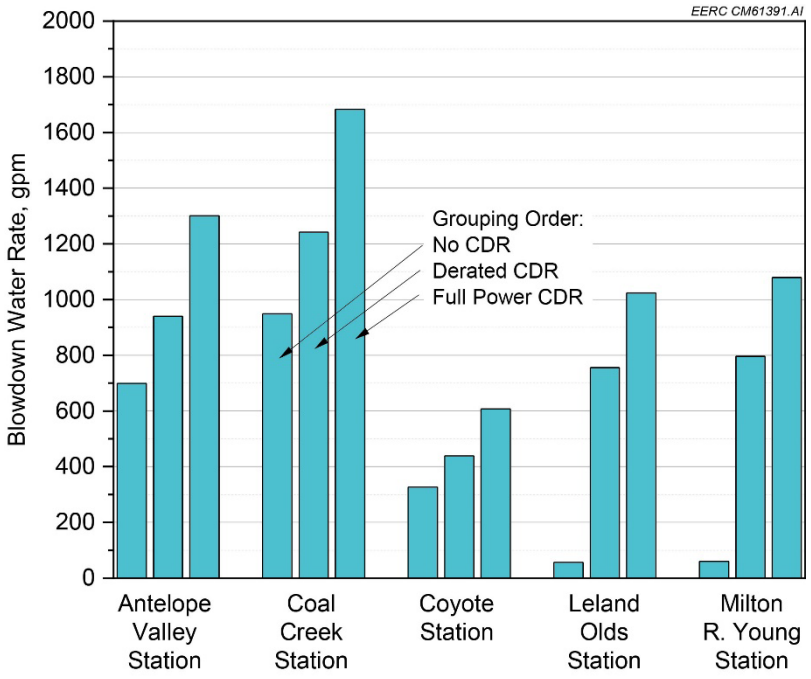

Figure 6. Total blowdown wastewater estimates for each plant.

Alternative Cooling Water Makeup

Various water sources related to CDR were examined and analyzed, in certain cases, for their potential to offset the increase in water demand associated with CDR retrofitting. These sources included condensate from a CDR system (which was already assumed to be recycled in the results of Figure 5), coal plant blowdown streams, and produced water that could possibly be extracted during geologic CO_2 sequestration. A comparison of major ion compositions and elements regulated under the Resource Conservation and Recovery Act (RCRA) for the selected water sources is provided in Table 4.

Table 4. Comparison of Alternative Makeup Water Sources

		Blowdown Streams		CO_2 Sequestration Formation Waters		
	CDR Condensate	Cooling Tower	Plant-Wide	Inyan Kara	Broom Creek	Deadwood
Major Species, mg/L						
Na	4.5	898	1680	1190	16900	90650
Ca	3.3	712	734	13.95	2015	8345
Mg	1.7	313	1190	1	401.5	1250
Cl	1.7	227	440	450	26700	154000
HCO_3	11.6	75	239	697	83.7	32.8
SO_4	11.1	4200	8800	1325	3065	507
TDS, mg/L	29.5	6920	14800	3365	49350	256500
RCRA Elements, µg/L						
As	<10	0.0346	0.108	<5	<5	<5
Ba	34.5	0.5	0.31	81	187.5	2965
Cd	<5	<0.01	<0.01	<2	<2	<2
Cr	<5	<0.05	<0.05	<10	<40	<40
Pb	<5	<0.005	<0.005	<5	<5	93
Hg	<0.05	<0.0001	<0.0001	<0.1	<0.1	<0.3
Se	<10	0.014	0.017	<5	87.8	<5
Ag	<5	<0.05	<0.05	<5	<5	<5

The CDR condensate results in Table 4 are from the average of two samples collected during slipstream CO_2 capture system testing at Coal Creek Station in the winter of 2020–2021, but analysis of these samples was conducted afterward as part of this study. The results in Table 4 confirm that CDR condensate is high quality and would easily be recycled as cooling tower makeup or makeup for other plant processes. For example, the total dissolved solids (TDS) of the condensate appear lower than typical makeup water from the Missouri River, which can be approximately 500 mg/L TDS. The relatively high quality of CDR condensate may make it a preferred water source for plant uses that require significant pretreatment, like boiler feedwater makeup. For the determination of CDR water demands, CDR condensate was assumed to be a direct offset for cooling water makeup.

Two representative plant blowdown streams were included in the analysis, and similar to the CDR condensate samples, the blowdown samples were also collected at Coal Creek Station under a separate project that field-tested the EERC's hygroscopic cooling technology. The blowdown

samples included cooling tower blowdown and the plant-wide blowdown that is ultimately disposed of on-site as part of Coal Creek's zero liquid discharge mandate.

The cooling towers at Coal Creek Station operate with a relatively high COC of 15, which is reflected in the elevated TDS level for this blowdown sample. The plant-wide blowdown sample was collected at a point before being injected into the plant's on-site disposal well. Its composition reflects other plant water uses such as wet FGD (e.g., resulting in increased sulfates and Mg) and further concentration in the plant's evaporation ponds.

The final set of samples represent produced water from several saline aquifers in North Dakota that have been identified as potential CO_2 sequestration targets. Samples were collected by the EERC from test wells in western North Dakota under separate projects. As shown in Table 5, in order of increasing formation depth, the samples came from the Inyan Kara, Broom Creek, and Deadwood Formations. All of the formation waters have Na as the dominant cation, but the major anion shifts from SO_4 to Cl between the Inyan Kara to Deadwood. Similarly, TDS increases with formation depth such that the Deadwood Formation likely has no potential for use as cooling tower makeup.

These produced water samples are intended to illustrate the conditions that can exist in North Dakota. However, the presence and suitability of these formations for sequestration does vary across the state, and site-specific conditions, including produced water composition, will need to be evaluated for each individual CO_2 sequestration project.

Table 5. Representative Sequestration Formation Conditions

	Representative Sampling Conditions			Fluid Density at Reservoir Conditions, lb/ft^3 (kg/m^3)	
Formation	Depth, ft (m)	Temperature, °F (°C)	Pressure, psi (MPa)	Formation Water	Injected CO_2
Inyan Kara	4000 (1200)	125° (51°)	1600 (11.4)	61.7 (990)	31.9 (512)
Broom Creek	5000 (1500)	137° (59°)	2500 (17.0)	63.6 (1020)	42.2 (676)
Deadwood	10,000 (3100)	182° (84°)	4600 (31.8)	72.6 (1164)	46.7 (749)

Comparisons among the water sources are presented in the form of Stiff composition diagrams in Figures 7 and 8. In general, the plant blowdown streams are typified by a relatively balanced mix of sulfate compounds, which likely reflects the impact of H_2SO_4 water treatment and FGD operation on water composition. Both formation waters that could have reuse potential, i.e., those from the Inyan Kara and Broom Creek Formations, have Na as the dominant cation, but the Inyan Kara water has a relatively balanced mix of anions, while the deeper Broom Creek approaches NaCl brine.

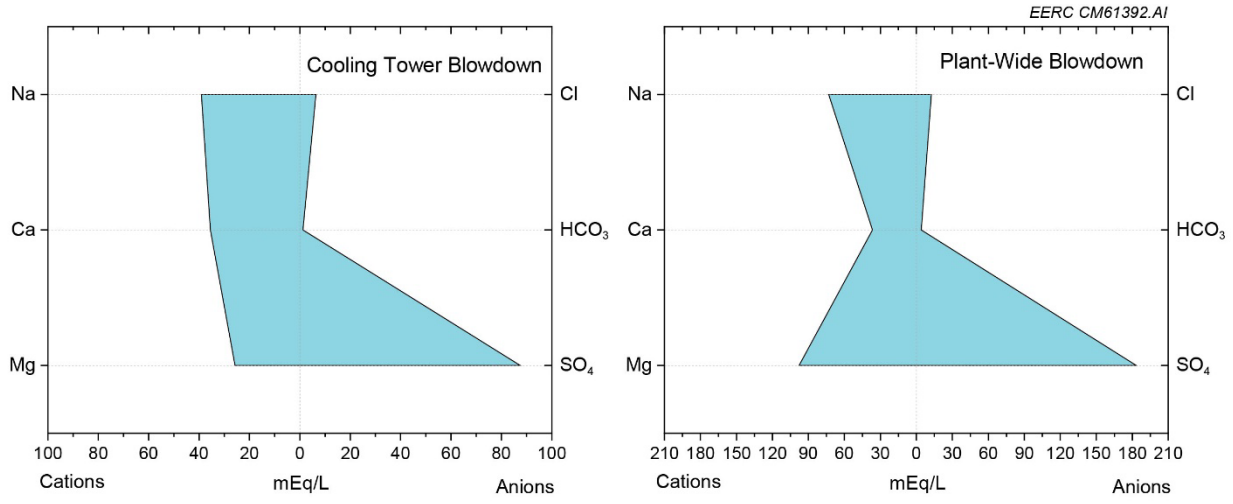

Figure 7. Stiff composition diagrams for plant blowdown water sources.

Cooling Water Makeup Potential

According to the summary results of Figure 5, cooling is still predicted to be the dominant driver of makeup water needs for power plants retrofitted with CDR. To evaluate the use of alternative water sources for cooling makeup, estimates of the maximum possible COC for the water sources in Figures 7 and 8 were made for both conventional cooling towers and a hygroscopic tower. Conventional cooling COC limits were determined using PHREEQC, a geochemical reaction modeling program, to predict the saturation limit of common scaling species as water was numerically evaporated from the starting composition.

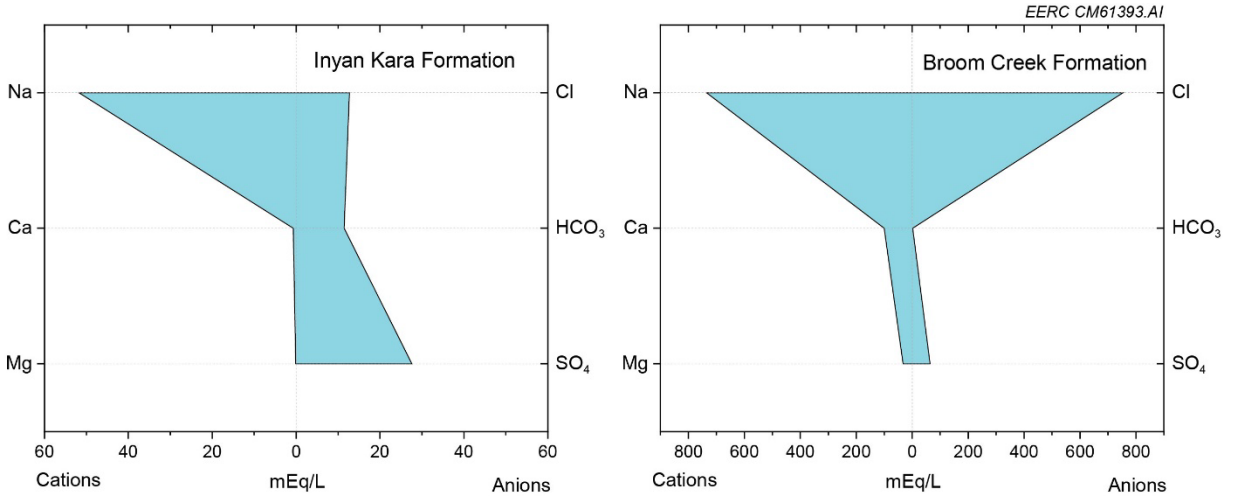

Figure 8. Stiff composition diagrams for the two useable formation water samples.

COC limits for hygroscopic cooling were determined by assuming a final TDS target of 200,000 mg/L, which was derived from field test observations. At this TDS level, the brine working fluid is primarily composed of subsaturated Mg and Na chlorides. The hygroscopic cooling concept can extend to the point of precipitating even these most soluble chloride species to approach zero liquid discharge. However, at such extreme concentration levels, cooling efficiency is impacted, which makes it more difficult to achieve beneficial cooling.

Cooling water use estimates are presented in Table 6 for conventional cooling tower technology and in Table 7 for hygroscopic cooling. With respect to the conventional tower, only the Inyan Kara Formation water is predicted to have a meaningful recycling potential with a 6.3 COC value. This conclusion simply confirms what was known about the blowdown samples, i.e., that they were already concentrated to the point of economically feasible reuse. Additionally, calcium sulfate was identified as the limiting species for these samples, which is consistent with the fact that it is less soluble relative to the sodium and magnesium sulfate species that were also present in the blowdown waters. In contrast, the formation waters were limited by calcium carbonate, which could possibly be reduced through softening, but that option was not modeled since the predicted TDS levels at calcite saturation were already considered high for use with conventional cooling equipment. Deadwood Formation water had no recycling potential as cooling tower makeup.

Table 6. Estimated Makeup Water Potential Using a Conventional Tower

	Estimated COC Limit	Blowdown TDS, mg/L	Volume Reduction, Blowdown:Makeup	Limiting Species
Conventional CT Blowdown	1.5	10,300	0.67	Gypsum, $CaSO_4$, $2H_2O$
Plant-Wide Blowdown	1.3	19,500	0.76	Gypsum, $CaSO_4$, $2H_2O$
Inyan Kara Formation	6.3	21,000	0.16	Calcite, $CaCO_3$
Broom Creek Formation	1.4	67,600	0.73	Calcite, $CaCO_3$
Deadwood Formation	Not useable	NA*	NA	Calcite, $CaCO_3$

* Not applicable.

Table 7. Estimated Makeup Water Potential Using a Hygroscopic Tower

	Estimated COC Limit	Blowdown TDS, mg/L	Volume Reduction, Blowdown:Makeup	Limiting Species
Conventional CT Blowdown	28.9	200,000	0.03	TDS/chloride
Plant-Wide Blowdown	13.5	200,000	0.07	TDS/chloride
Inyan Kara Formation	59.4	200,000	0.02	TDS/chloride
Broom Creek Formation	4.1	200,000	0.25	TDS/chloride
Deadwood Formation	Not useable	NA*	NA	TDS/chloride

* Not applicable.

Significantly higher water use was predicted for hygroscopic cooling according to the results in Table 7. Of course, this observation does not apply to Deadwood Formation water, which was not useable even with the hygroscopic system. Broom Creek Formation water had the lowest evaporation potential with hygroscopic cooling, but its starting volume was still estimated to be reduced by 75%. Hygroscopic cooling has not been tested with formation-produced water, but it has been tested with the blowdown streams included in Table 7 with generally positive results.

Produced-Water Extraction

In order to provide an example of the quantity of produced water that could be extracted and concentrated by a coal power plant, estimates were made assuming the Inyan Kara Formation as the sequestration target and a 1:1 volume extraction of formation fluid per unit volume of injected CO_2 and concentrated blowdown. Fluid density values presented in Table 5 were used to calculate the extraction estimates for both CDR retrofitting scenarios. Cooling utilization of the Inyan Kara water was based on the calculated COC for a conventional cooling tower in Table 6 since the COC of 6.3 was more conservative than the near 60 COC value estimated for hygroscopic cooling.

Produced-water results are presented in Tables 8 and 9 for the derated CDR and full-power CDR scenarios, respectively. The summary values for these calculations are the makeup contribution values, which indicate the percentage of makeup water required by the plant that can be fulfilled by the useable water fraction of the Inyan Kara water. For derated CDR, these makeup contributions fell between 71%–74% for all plants and were 53%–54% for full-power CDR at plants with wet recirculating cooling. These results suggest that there is sufficient waste heat capacity produced at the plant to concentrate the quantity of produced fluid that would initially be expected to be extracted from the reservoir for pressure management.

Table 8. Produced Water Recycling Estimates for the Derated CDR Scenario

	Antelope Valley Station	Coal Creek Station	Coyote Station	Leland Olds Station	Milton R. Young Station
Derated Net Capacity, MWe	612	749	286	455	480
CO_2 Captured, tonne/hr	735	898	343	546	576
Total Plant Makeup Water Requirement, gpm (tonne/hr)	8211 (1863)	10,524 (2388)	3832 (870)	6400 (1453)	6745 (1531)
Blowdown Water, gpm (tonne/hr)	940 (215)	1242 (284)	439 (100)	756 (173)	796 (182)
1:1 Extracted Inyan Kara Brine, gpm (tonne/hr)	7199 (1634)	8893 (2018)	3360 (762)	5408 (1227)	5699 (1293)
Useable Brine Water, gpm (tonne/hr)	6047 (1372)	7470 (1695)	2822 (640)	4543 (1031)	4788 (1087)
Total Plant Makeup Contribution	**74%**	**71%**	**74%**	**71%**	**71%**

Table 9. Produced-Water Recycling Estimates for the Full-Power CDR Scenario

	Antelope Valley Station	Coal Creek Station	Coyote Station	Leland Olds Station	Milton R. Young Station
Net Capacity, MWe	900	1100	420	669	705
CO_2 Captured, tonne/hr	735	898	343	546	576
Total Plant Makeup Water Requirement, gpm (tonne/hr)	11,819 (2682)	14,933 (3389)	5515 (1252)	3881 (881)	4090 (928)
Blowdown Water, gpm (tonne/hr)	1301 (297)	1683 (385)	607 (139)	1024 (234)	1079 (247)
1:1 Extracted Inyan Kara Brine, gpm (tonne/hr)	7560 (1716)	9334 (2118)	3528 (801)	5677 (1288)	5982 (1358)
Useable Brine Water, gpm (tonne/hr)	6350 (1441)	7840 (1779)	2964 (673)	4768 (1082)	5025 (1140)
Total Plant Makeup Contribution	**54%**	**53%**	**54%**	**123%**	**123%**

The remaining plant scenarios, i.e., plants with full-power CDR and once-through cooling, show a makeup balance greater than 100%, which suggests that there is insufficient waste heat for these cases to fully evaporate the produced fluid at a 1:1 extraction ratio. Of course, these plants were estimated to produce the same relative magnitude of waste heat as the others, but the difference was that the heat was carried away by the once-through cooling system, which does not consume makeup water.

DISCUSSION

By applying configuration-specific factors to the plants in North Dakota, water demand was estimated to increase 15% to 20% for derated CDR, and 60%–70% for maintaining the plant's full electrical output. These increases with full-power CDR water demand are smaller than analogous values in the NETL lignite study (4), which estimated water consumption would increase approximately 150% compared to a no-CDR baseline. This difference is largely due to differences in the baseline plant configuration assumed in the NETL study versus the actual configurations of North Dakota's power plants. The NETL study assumed a hybrid cooling system for the steam condenser (50% wet evaporative and 50% dry air-cooled), but none of the North Dakota plants have hybrid cooling and, as a result, their starting water consumption values were higher than the baseline configuration modeled by NETL.

The results show that the modest increases in water demand for derated CDR might be met by improvements to plant water use efficiency, specifically by recycling plant blowdown for cooling. However, advanced water use technologies like hygroscopic cooling would be required to make productive use of plant blowdown since these waters will have already been concentrated to the maximum feasible extent using conventional cooling towers and treatment methods. If the blowdown water rates tabulated in Table 3 were used for cooling at the hygroscopic COC for plant-wide blowdown (i.e., a COC of 13.5), then all of the derated CDR water increase could be met without sourcing a new water supply for the three plants that use wet recirculating cooling.

On the other hand, the magnitude of increased water demand for full-power CDR suggests that improved water use efficiency cannot solely meet the demand, and a new water supply would be needed for this scenario. While it would likely require new infrastructure investment, obtaining additional water is not expected to be a limiting factor for North Dakota's power plants given their proximity to the Missouri River.

Wastewater disposal is also projected to increase with CDR retrofitting, which would require permit modification to increase liquid discharge or, perhaps more likely, require investment in zero liquid discharge treatment capacity. The state's two largest power stations (Antelope Valley and Coal Creek Stations) are already zero liquid discharge facilities, and it is possible that CDR retrofitting would result in similar liquid discharge restrictions. Here again, concentrating blowdown to the maximum feasible extent with a technology like hygroscopic cooling may prove worthwhile since it could reduce the volume of liquid ultimately needing disposal.

One final consideration with respect to plant water needs and CDR is the possibility of using produced water from geologic CO_2 sequestration for power plant cooling. The results show that this water source could be substantial, approximately 50%–70% of plant needs, assuming Inyan Kara Formation water quality. The benefits of this approach need to be analyzed in more detail, but they appear to be associated with the injection reservoir and may include a reduced rate of reservoir pressure buildup and some ability to manage the subsurface CO_2 plume.

CONCLUSIONS

- By applying configuration-specific factors to the power plants in North Dakota, water demand was estimated to increase 15% to 20% for derated CDR and 60%–70% for maintaining the plant's full-power output. Key exceptions to these trends were plants that use once-through cooling, i.e., Milton R. Young and Leland Olds Stations. For these plants, CDR water consumption was highly dependent on the continued use of their once-through condensers.

- It was further estimated that the water demand increase for derated CDR could, in theory, be met by improvements to plant water use efficiency, specifically by using plant blowdown for cooling within a hygroscopic cooling tower.

- Full-power CDR water demands could not be met with improved water use efficiency alone, and it is likely that a new water supply would be needed to meet added demand.

- Produced water from the Inyan Kara Formation shows promise as a possible source of cooling water makeup, but actual testing for this purpose is needed. If Inyan Kara water could be used for plant makeup, it was estimated that it could provide a substantial fraction of the plant's makeup water needs (50%–70%) at an extraction rate that might be relevant for managing reservoir pressure and CO_2 plume spread.

REFERENCES

1. Martin, C.L. Wastewater Recycling Using a Hygroscopic Cooling System. 2020 Virtual Review for DE-FE0031810; U.S. Department of Energy National Energy Technology Laboratory, November 2020. https://www.netl.doe.gov/sites/default/files/netl-file/20WTVPR_Martin.pdf (accessed Jan 2021).

2. Martin, C.L. Heat Dissipation Systems with Hygroscopic Working Fluid. U.S. Patent 10,260,761, April 16, 2019.

3. James III, R.E.; Kearins, D.; Turner, M.; Woods, M.; Kuehn, N.; Zoelle, A. *Cost and Performance Baseline for Fossil Energy Plants Volume 1: Bituminous Coal and Natural Gas to Electricity*; Report NETL-PUB-22638; U.S. Department of Energy National Energy Technology Laboratory, September 2019.

4. U.S. Department of Energy National Energy Technology Laboratory. *Cost and Performance Baseline for Fossil Energy Plants Volume 3b: Low Rank Coal to Electricity: Combustion Cases*; Report DOE/NETL-2011/1463; U.S. Department of Energy National Energy Technology Laboratory, March 2011.

5. Buscheck, T.A.; Sun, Y.; Chen, M.; Hao, Y.; Wolery, T.J.; Bourcier, W.L.; Court, B.; Celia, M.A.; Friedmann, J.; Aines, R.D. 2012. Active CO_2 Reservoir Management for Carbon Storage: Analysis of Operational Strategies to Relieve Pressure Buildup and Improve Injectivity. *International Journal of Greenhouse Gas Control* **2012**, *6*, 230–245.

6. Roach, J.D.; Heath, J.E.; Kobos, P.H.; Klise, G.T. System-Level Benefits of Extracting and Treating Saline Water from Geologic Formations During National-Scale Carbon Capture and Storage. *International Journal of Greenhouse Gas Control* **2014**, *25*, 186–197.

7. Klise, G.T.; Roach, J.D.; Kobos, P.H.; Heath, J.E.; Gutierrez, K.A. The Cost of Meeting Increased Cooling-Water Demands for CO_2 Capture and Storage Utilizing Non-Traditional Water from Geologic Saline Formations. *Hydrogeology Journal* **2013**, *21*, 587–604.